IMPLEMENTATION OF CDMA2000 SYSTEM FOR UWA COMMUNICATION USING SIMULINK

Thesis submitted in partial fulfillment of the requirement for
The award of the degree of

MASTER of ENGINEERING (M.E.)
In
ELECTRONICS AND COMMUNICATION ENGINEERING

Submitted By

RICHA SINGLA
Roll No. 80661018

Under the guidance of

Dr. RAJESH KHANNA
Associate Professor
ECED, TU

DEPARTMENT OF ELECTRONICS AND COMMUNICATION ENGINEERING, THAPAR UNIVERSITY,
(Formerly as Thapar Institute of Engineering and Technology)
Patiala-147001, Punjab, INDIA

June 2008

CERTIFICATE

I, Richa Singla hereby declare that this report entitled ***"Implementation of CDMA2000 System for UWA Communication using SIMULINK"*** *is an authentic record of my own work carried out towards the partial fulfillment for the award of degree of M. E. (Master of Engineering) at Thapar University, (formerly as Thapar Institute of Engineering & Technology), Patiala under the guidance of Dr. Rajesh Khanna, Associate Prof., ECED, during January to June 2008.*

The matter presented in this report has not been submitted in any other University or Institute for the award of any degree.

(Richa Singla)

Dated: _____ Signature of student

This is certified that the above statement made by the student is correct to the best of my knowledge and belief.

(Dr. Rajesh Khanna)
Associate Prof., ECED
Date: _____

Countersigned By:

(Dr. A. K. Chatterjee)
Head of Department, ECED
Thapar University, Patiala
Date: _____

(Dr. R.K. Sharma)
Dean, Academic Affairs
Thapar University, Patiala
Date: _____

ACKNOWLEDGEMENT

A thesis cannot be completed without the help of many people who contribute directly or indirectly through their constructive criticism in the evolution and preparation of this work. A special debt of gratitude is owed to my thesis supervisor, Dr. Rajesh Khanna (Associate Professor, E.C.E.D.) for their gracious efforts and keen pursuit which has remained as a valuable asset for the successful fulfillment of my thesis. Their dynamism and diligent enthusiasm have been highly instrumental in keeping my spirits high. Their flawless & forthright suggestions blended with an innate intelligent application have crowned my task with success.

I would also like to offer my sincere thanks to all faculty, teaching and non-teaching, of Electronics & Communication Engineering Department (ECED), and staff of central library, TU, Patiala for their assistance.

I am also thankful to the authors whose works I have consulted and quoted in this work. I would also like to thank my elder brother Mr. Anurag Jindal (Employee, Freescale) for his deep discussion on some topic in this report. Last, but not the least, very special thanks to my parents and my friends for their constant encouragement and best wishes. Their patience and understanding without which this study would not have been in this present form, is greatly appreciated.

RICHA SINGLA

ABSTRACT

Underwater communication finds applications in oceanographic data collection, pollution monitoring, offshore exploration, disaster prevention, assisted navigation, tactical surveillance, and mine reconnaissance. The enabling technology for these applications is acoustic wireless networking. A major challenge for the deployment of UW-ASNs is the development of a Multiple Access technique and modulation technique tailored for the underwater environment and this is what my thesis is all about.

The title of my thesis is “Implementation of CDMA2000 System for UWA communication using SIMULINK”. In this, designing of underwater system is done by using CDMA2000 technology for multiple access. The underwater CDMA2000 system is designed using MATLAB SIMULINK Tools. It consists of various sections which perform different functions. Firstly, on the transmitter side, there are two major blocks named encoder and transmitter block which include error correction, security and spreading techniques. Transmitted signal is affected by rayleigh fading channel and on the receiver end, there are again two major blocks receiver block and decoder. These blocks include delay compensation, channel compensation, Signal to noise ratio optimizing, despreading and error correction techniques. All these major blocks are subdivided into various functional blocks which perform these operations.

The aim of the thesis is to design a system which is capable of efficient transmission as underwater communication is effected by many factors. The main focus of this system is to estimate the delay in the channel and to apply proper channel estimation. For this, proper techniques are used in the design. Along with that CDMA2000 system itself provide many advantages like robustness to frequency-selective fading, compensates for the effect of multipath by exploiting Rake filters at the receiver, multiple access capability, protection against multipath interference, privacy, interference rejection.

The performance of the system is evaluated by various calculations and comparisons. Major performance determining factors are bit error rate of Underwater CDMA2000 system after the receiver section as well of the complete system which comes out to be 0.0236 after receiver section on the receiver side and 0.002909 of complete system , checking the synchronization between the signal at transmitter and receiver side by making use of delay estimation technique and by comparing the signal at different level of implementation, verifying the effect of the channel on the signal after applying compensation techniques by comparing the signal without including channel in the system with the signal retrieved from the system after including channel and after applying channel compensation techniques and comparing the signals taken before and after channel compensation.

Table of Contents

LIST OF TABLES

LIST OF FIGURES

LIST OF ABBREVIATIONS

2G	Second-Generation
3G	Third-Generation
ADC	Analog-To-Digital Conversion
AUV	Autonomous Underwater Vehicle
AWGN	Additive White Gaussian Noise
CDMA	Code Division Multiple Access
CRC	Cyclic Redundancy Check
CSMA	Carrier Sense Multiple Access
CS	Carrier Sensing
DFE	Decision Feedback Equalizers
DPSK	Differential Phase Shift Keying
DSSS	Direct Sequence Spread Spectrum
FAMA	Floor Acquisition Multiple Access
FDMA	Frequency Division Multiple Access
FSK	Frequency Shift Keying
FHSS	Frequency Hopping Spread Spectrum
GPS	Global Positioning System
ISI	Inter Symbol Interference
ITU	International Telecommunication Union
LC	Long Code
LFSR	Linear Feedback Shift Register
LPI	Low Probability of Interception
MAI	Multiple Access Interference
MATLAB	Matrix Laboratory
MIMO	Multiple Inputs Multiple Outputs
MLS	Maximal Length Sequence
OFDM	Orthogonal Frequency Division Multiplexing
OVSF	Orthogonal Variable Spreading Factor

PCG	Power Control Group
PCSCh	Power Control Subchannel
PN	Pseudo Noise
PSK	Phase Shift Keying
QAM	Quadrature Amplitude Modulation
QOF	Quasi Orthogonal Function
QoS	Quality of Service
RTS/CTS	Request To Send/ Clear To Send
RTT	Round Trip Time
SDMA	Space Division Multiple Access
SDV	Delivery Vehicle
SF	Spreading Factor
SNR	Signal-to- Noise Ratio
STS	Space Time spreading
TD	Transmit Diversity
TDMA	Time Division Multiple Access
UUV	Unmanned Underwater Vehicle
UW-A	UnderWater-Acoustic
WCDMA	Wide Code Division Multiple Access
WLL	Wireless Local Loop

CHAPTER 1
INTRODUCTION

1.2 Need of Underwater Acoustic Network

During the last few decades, the growing interest in the conditions and resources of the oceans has driven many researchers to investigate the reliability of the underwater acoustic (UWA) channel as a communication medium. This channel is one of the most complex and hostile environments to be encountered for the transmission of data. Underwater sensor networks are envisioned to enable applications for oceanographic data collection, pollution monitoring, offshore exploration, disaster prevention, seismic monitoring, equipment monitoring, assisted navigation and tactical surveillance applications. Multiple Unmanned or Autonomous Underwater Vehicles (UUVs, AUVs), equipped with underwater sensors, will also find application in exploration of natural undersea resources and gathering of scientific data in collaborative monitoring missions. To make these applications viable, there is a need to enable underwater communications among underwater devices. Underwater sensor nodes and vehicles must possess self-configuration capabilities, i.e., they must be able to coordinate their operation by exchanging configuration, location and movement information, and to relay monitored data to an onshore station [3].

Wireless underwater acoustic networking is the enabling technology for these applications. Underwater Acoustic Sensor Networks (UW-ASNs) consist of a variable number of sensors and vehicles that are deployed to perform collaborative monitoring tasks over a given volume of mater. To achieve this objective, sensors and vehicles self-organize in an autonomous network, which can adapt to the characteristics of the ocean environment.

The above described features enable a broad range of applications for underwater acoustic networks:

- **Ocean Sampling Networks**. Networks of sensors and AUVs, such as the Odysseyclass AUVs, can perform synoptic, cooperative adaptive sampling of the 3D coastal ocean environment.

- **Environmental Monitoring.** UW-ASN can perform pollution monitoring (chemical, biological, and nuclear). For example, it may be possible to detail the chemical slurry of antibiotics, estrogen-type hormones and insecticides to monitor streams, rivers, lakes, and ocean bays (*water quality in-situ analysis*) [2]. In addition, UWASNs can perform ocean current and wind monitoring, and biological monitoring such as tracking of fish or micro-organisms. Also, UW-ASNs can improve weather forecast , detect climate change, and understand and predict the effect of human activities on marine ecosystems.
- **Undersea Explorations.** Underwater sensor networks can help detecting underwater oilfields or reservoirs, determine routes for laying undersea cables, and assist in exploration for valuable minerals.
- **Disaster Prevention.** Sensor networks that measure seismic activity from remote locations can provide *tsunami* warnings to coastal areas [3], or study the effects of submarine earthquakes (*seaquakes*).
- **Seismic Monitoring.** Frequent seismic monitoring is of great importance in oil extraction from underwater fields to asses' field performance. Underwater sensor networks would allow reservoir management approaches.
- **Equipment Monitoring.** Sensor networks would enable remote control and temporary monitoring of expensive equipment immediately after the deployment, to assess deployment failures in the initial operation or to detect problems.
- **Assisted Navigation.** Sensors can be used to identify hazards on the seabed, locate dangerous rocks or shoals in shallow waters, mooring positions, submerged wrecks, and to perform bathymetry profiling.
- **Distributed Tactical Surveillance**. AUVs and fixed underwater sensors can collaboratively monitor areas for surveillance, reconnaissance, targeting, and intrusion detection systems. A 3D underwater sensor network is used for a tactical surveillance system that is able to detect and classify submarines, Small Delivery Vehicles (SDVs) and divers based on the sensed data from mechanical, adiation, magnetic, and acoustic microsensors. With respect to traditional radar/sonar systems, underwater sensor networks can reach a higher accuracy, and enable detection and

classification of low signature targets by also combining measures from different types of sensors.

- **Mine Reconnaissance**. The simultaneous operation of multiple AUVs with acoustic and optical sensors can be used to perform rapid environmental assessment and detect mine-like objects[1].

1.2 Factor effecting Underwater Acoustic Communication

The factors that influence acoustic communications are

1. **High delay and delay variance**
   - The propagation speed in the UW-A channel is five orders of magnitude lower than in the radio channel. This large propagation delay can reduce the throughput of the system considerably.
   - The high delay variance is even more harmful for efficient protocol design, as it prevents from accurately estimating the Round Trip Time (RTT), which is the key parameter for many common communication protocols.

2. **Doppler spread**
   - The Doppler frequency spread can be significant in UW-A channels [5], causing a degradation in the performance of digital communications: transmissions at a high data rate cause many adjacent symbols to interfere at the receiver, requiring sophisticated signal processing to deal with the generated ISI.
   - The Doppler spreading generates a simple frequency translation, which is relatively easy for a receiver to compensate for; and a continuous spreading of frequencies, which constitutes a non-shifted signal, which is more difficult to compensate for.
   - If a channel has a Doppler spread with bandwidth B and a signal has symbol duration T, then there are approximately BT uncorrelated samples of its complex envelope. When BT is much less than unity, the channel is said to be underspread and the effects of the Doppler fading can be ignored, while, if greater than unity, it is said to be *overspread* [6].

3. Path loss

- *Attenuation.* Is mainly provoked by absorption caused by the conversion of acoustic energy into heat. The attenuation is also caused by scattering and reverberation (on rough ocean surface and bottom), refraction, and dispersion (due to the displacement of the reflection point caused by wind on the surface). Water depth plays a key role in determining the attenuation.
- *Geometric Spreading*. This refers to the spreading of sound energy as a result of the expansion of the wavefronts. It increases with the propagation distance and is independent of frequency. There are two common kinds of geometric spreading: *spherical* (omni-directional point source), which characterizes deep water communications, and *cylindrical* (horizontal radiation only), which characterizes shallow water communications.

4. **Noise**

- *Man made noise.* This is mainly caused by machinery noise (pumps, reduction gears, power plants), and shipping activity (hull fouling, animal life on hull, cavitation), especially in areas encumbered with heavy vessel traffic.
- *Ambient Noise.* Is related to hydrodynamics (movement of water including tides, current, storms, wind, and rain), and to seismic and biological phenomena.

  In [7], boat noise and snapping shrimps have been found to be the primary sources of noise in shallow water by means of measurement experiments on the ocean bottom.

5. **Multi-path**

- Multi-path propagation may be responsible for severe degradation of the acoustic communication signal, since it generates Inter Symbol Interference (ISI).
- The multi-path geometry depends on the link configuration. Vertical channels are characterized by little time dispersion, whereas horizontal channels may have extremely long multi-path spreads.
- The extent of the spreading is a strong function of depth and the distance between transmitter and receiver.

To overcome these effects, different types of modulation and multiple access techniques are used which are discussed in successive sections.

1.3 Underwater Modulation Techniques

Various types of modulation techniques are used for underwater acoustic communication. The use of a modulation technique depends on the application for which it is used and the environment it is operated.

The detail of all modulating techniques are discussed beneath.

Frequency Shift Keying (FSK) modulation, since it relies on energy detection and thus does not require phase tracking, which is a very difficult task mainly because of the Doppler-spread in the UW-A channel. In FSK modulation schemes developed for underwater, the multi-path effects are suppressed by inserting time guards between successive pulses to ensure that the reverberation, caused by the rough ocean surface and bottom, vanishes before each subsequent pulse is received. Dynamic frequency guards can also be used between frequency tones to adapt the communication to the Doppler spreading of the channel.

Although non-coherent modulation schemes are characterized by high power efficiency, their low bandwidth efficiency makes them unsuitable for high data rate multi-user networks. Hence, coherent modulation techniques have been developed for long-range, high-throughput systems. fully coherent modulation techniques, such as Phase Shift Keying (PSK) and Quadrature Amplitude Modulation (QAM), are used more frequently because of the availability of powerful digital processing. Channel equalization techniques are exploited to leverage the effect of the Inter Symbol Interference (ISI), instead of trying to avoid or suppress it. Decision Feedback Equalizers (DFE) tracks the complex, relatively slowly varying channel response and thus provide high throughput when the channel is slowly varying[4].

Differential Phase Shift Keying (DPSK) serves as an intermediate solution between incoherent and fully coherent systems in terms of bandwidth efficiency. DPSK encodes information relative to the previous symbol rather than to an arbitrary fixed reference in the signal phase and may be referred to as a partially coherent modulation. While this strategy substantially alleviates carrier phase-tracking requirements, the penalty is an increased error probability over PSK at an equivalent data rate[8].

Another promising solution for underwater communications is the Orthogonal Frequency Division Multiplexing (OFDM) spread spectrum technique, which is particularly efficient when noise is spread over a large portion of the available bandwidth. OFDM is frequently referred to as multi-carrier modulation because it transmits signals over multiple sub-carriers simultaneously. In particular, sub-carriers which experience higher Signal-to-Noise Ratio (SNR), are allotted with a higher number of bits, whereas less bits are allotted to sub-carriers experiencing attenuation which requires channel estimation. Since the symbol duration for each individual carrier increases, OFDM systems perform robustly in severe multi-path environments, and achieve a high spectral efficiency[4].

1.4 Underwater Multiple Access Techniques

Underwater multiple access techniques poses additional challenges because of the peculiarities of the underwater channel, in particular limited bandwidth, and high and variable delay.

- **Frequency Division Multiple Access (FDMA)** is not suitable for UW-ASNs due to the narrow bandwidth in UW-A channels and the vulnerability of limited band systems to fading and multi-path.
- **Time Division Multiple Access (TDMA)** shows a limited bandwidth efficiency because of the long time guards required in the UW-A channel. In fact, long time guards must be designed to account for the large propagation delay and delay variance of the underwater channel, to minimize packet collisions from adjacent time slots. Moreover, the variable delay makes it very challenging to realize a precise synchronization, with a common timing reference, which is required for TDMA.
- **Carrier Sense Multiple Access (CSMA)** prevents collisions with the ongoing transmission at the transmitter side. To prevent collisions at the receiver side, however, it is necessary to add a guard time between transmissions dimensioned according to the maximum propagation delay in the network. This makes the protocol dramatically inefficient for UW-ASNs. The use of contention-based techniques that rely on handshaking mechanisms such as RTS/CTS in shared medium access is impractical in underwater, for the following reasons:

❖ large delays in the propagation of RTS/CTS control packets lead to low throughput;

- due to the high propagation delay of UW-A channels, when carrier sense is used, as in 802.11, it is more likely that the channel be sensed idle while a transmission is ongoing since the signal may not have reached the receiver yet;
- the high variability of delay in handshaking packets makes it impractical to predict the start and finish time of the transmissions of other stations. Thus, collisions are highly likely to occur.

Moreover, the additional challenges in underwater channels such as variable and high propagation delays, and very limited available bandwidth, further complicate the medium access problem in underwater environments[8].

- **Code Division Multiple Access (CDMA)** is quite robust to frequency selective fading caused by underwater multi-paths, since it distinguishes simultaneous signals transmitted by multiple devices by means of pseudo-noise codes that are used for spreading the user signal over the entire available band. This allows exploiting the time diversity in the UW-A channel by leveraging Rake filters [9] at the receiver. These filters are designed to match the pulse spreading, the pulse shape, and the channel impulse response, so as to compensate for the effect of multi-path. CDMA allows reducing the number of packet retransmissions, which results in decreased battery consumption and increased network throughput. Two code-division spread-spectrum access techniques are compared in shallow water, namely Direct Sequence Spread Spectrum (DSSS) and Frequency Hopping Spread Spectrum (FHSS). Although FHSS is more prone to the Doppler shift effect, since the transmission takes place in narrow bands, this scheme is more robust to Multiple Access Interference (MAI) than DSSS. Furthermore, although FHSS is shown to lead to a higher bit error rate than DHSS, it results in simple receivers and provides robustness to the near-far problem, thus potentially simplifying the power control functionality. One of the most attractive access techniques in the recent underwater literature combines multi carrier transmission with the DSSS CDMA [5], as it may offer higher spectral efficiency than its single carrier counterpart and increase the flexibility to support integrated high data rate applications with different quality of service requirements. The main idea is to spread each data symbol in the frequency domain by transmitting all the chips of a spread symbol at the same time into a large number of narrow sub channels. This way, high data rate can be supported by increasing

the duration of each symbol, which drastically reduces ISI. In conclusion, although the high delay spread that characterizes the horizontal link in underwater channels makes it difficult to maintain synchronization among the stations, especially when orthogonal code techniques are used [9], CDMA is a promising multiple access technique for underwater acoustic networks, particularly in shallow water where multi-paths and Doppler-spreading play a key role in the communication performance. In [6], a protocol is proposed for networks with AUVs. The proposed scheme is based on organizing the network in multiple clusters, each composed of adjacent vehicles. Inside each cluster, TDMA is used with long band guards, to overcome the effect of propagation delay in underwater. In this case, TDMA is not highly inefficient since vehicles in the same cluster are close to one another. Hence, the effect of propagation delay is limited. Interference among different clusters is avoided by assigning different spreading codes to different clusters[10].

As clear from the above detail that CDMA system is best for underwater communication, so i am dealing with CDMA system for underwater communication in my thesis.

1.5 Objective of Thesis

The title of my thesis is “Implementation of CDMA2000 System for UWA Communication using SIMULINK”. In this, I have designed CDMA2000 system for underwater communication using MATLAB SIMULINK Tools. It consists of various sections which perform different functions. Firstly, on the transmitter side, there are two major blocks named encoder and transmitter. Then there is a rayleigh fading channel and on the receiver end, there are two major blocks receiver and decoder. All these major blocks are subdivided into various functional blocks. Detail of all these blocks and sub-bocks is covered in chapter 4 with the output of all the blocks. The major challenges and the final objectives of my thesis are discussed as follows.

A major challenge for the deployment of UW-ASNs is the development of a Multiple Access technique tailored for the underwater environment. In particular, an underwater multiple access technique should provide high network throughput, variable delay estimation, channel compensation and low energy consumption, in face of the harsh

characteristics of the underwater propagation medium, while guaranteeing fairness among competing nodes.

The major objective of my thesis are

- To calculate the bit error rate of Underwater CDMA2000 system after the receiver section as well of the complete system considering the maximum probability of error that may occur.
- To check the synchronization between the signal at transmitter and receiver side by making use of delay estimation on the receiver side accurately.
- To verify the effect of the channel on the signal after applying compensation techniques.
- To compare the signals taken before and after channel compensation verifying that channel estimation technique is implemented correctly.
- Add power control technique so that power can be controlled for further transmission.

To achieve these objectives, I prefer to go for CDMA2000 system. Code Division Multiple Access (CDMA)2000 is the most promising physical layer and multiple access technique for UW-ASNs. The reasons for choosing it are explained below by applying direct sequence spread-spectrum techniques.

- **Variable Delay Estimator**:- As underwater channel add variable delay to the transmitted signal, so a section is added which calculates the delay for each frame of the transmitted signal. Then delay the locally generated PN and walsh code by the same delay to bring the received signal and the locally generated signals in synchronization and signal can be retrieved easily.
- **Channel Estimation**:-Channel estimation is done in rake receiver section which compensate for the effect of channel on the signal.
- CDMA is robust to frequency-selective fading,
- CDMA compensates for the effect of multipath by exploiting Rake filters at the receiver,
- **Multiple Access Capability** -- If multiple users transmit a spread-spectrum signal at the same time, the receiver will still be able to distinguish between the users provided each user has a unique code that has a sufficiently low cross-correlation

with the other codes. Correlating the received signal with a code signal from a certain user will then only despread the signal of this user, while the other spread-spectrum signals will remain spread over a large bandwidth. Thus, within the information bandwidth the power of the desired user will be larger than the interfering power provided there are not too many interferers, and the desired signal can be extracted. At the receiver only the signal of required user data is "despread" and the data recovered.

- **Protection Against Multipath Interference** -- In a radio channel there is not just one path between a transmitter and receiver. Due to reflections (and refractions) a signal will be received from a number of different paths. The signals of the different paths are all copies of the same transmitted signal but with different amplitudes, phases, delays, and arrival angles. Adding these signals at the receiver will be constructive at some of the frequencies and destructive at others. In the time domain, this results in a dispersed signal. Spread-spectrum modulation can combat this multipath interference; however, the way in which this is achieved depends very much on the type of modulation used.
- **Privacy** -- The transmitted signal can only be despread and the data recovered if the code is known to the receiver.
- **Interference Rejection** -- Cross-correlating the code signal with a narrowband signal will spread the power of the narrowband signal thereby reducing the interfering power in the information bandwidth. The spread-spectrum signal (s) receives a narrowband interference (i). At the receiver the SS signal is "despread" while the interference signal is spread, making it appear as background noise compared to the despread signal.
- **Anti-Jamming Capability, Especially Narrowband Jamming** -- This is more or less the same as interference rejection except the interference is now willfully inflicted on the system. It is this property, together with the next one, that makes spread-spectrum modulation attractive for military applications.
- **Low Probability of Interception (LPI)** -- Because of its low power density, the spread-spectrum signal is difficult to detect and intercept by a hostile listener.

Thus,UWCDMA2000 manages to simultaneously achieve the three objectives in deep water communications, which are not severely affected by multipath. In shallow water communications, which may be heavily affected by multipath, it dynamically finds the optimal trade-off among these objectives.

CHAPTER 2

LITERATURE SURVEY

2.1 History

The underwater and general ocean environment is one which poses somewhat of a predicament for any kind of engineering undertaking. This quandary is further amplified when the undertaking is of an electronic nature. This is perhaps one of the reasons why the underwater communications applications are a niche market which has been vastly overlooked over recent times. Perhaps another reason for this situation would be the obvious limitations of this market, being only restricted to commercial and recreational divers as users. As a result of this limitation, applications to date that have been developed for this purpose have been extremely costly and targeted primarily at professional commercial divers and the military.

Unfortunately, the transmission of radio waves underwater is extremely limited. The reason for this being that water appears to have the effect of "shorting out" radio wave signals. Unlike in air, RF transmissions are severely impeded when traveling through water creating an effect similar to placing a C.B. radio antenna down flat on the hood of a car instead of vertical, and trying to transmit a radio signal. The metal car hood shorts out the radio signal. Another possibility examined was the use of acoustic the nominal value for speed of sound in seawater is nominally 1500 m/s at about 13 degrees centigrade. At salinity level of 35 parts per thousand, depth 0 meters and temperature 0 degrees, speed of sound is 1449.3 m/s. Speed of sound in air is nominally 344m/s at 25 degrees, this speed drops to 334 at 0 degrees. The temperature dependency is second order given that other parameters are constant. A prime example of its effectiveness is in nature as it is used by dolphins and whales, as well as several other species of marine life to communicate over vast distance as well as in navigation. Another advantage of the use of sound waves is that they are unaffected by murky or turbid water, transmission is equally good in fresh or salt water[6].

Underwater acoustic communications are mainly influenced by path loss, noise, multi-path, Doppler spread, and high and variable propagation delay. All these factors determine the temporal and spatial variability of the acoustic channel, and make the

available bandwidth of the UnderWater Acoustic channel (UW-A) limited and dramatically dependent on both range and frequency. Long-range systems that operate over several tens of kilometers may have a bandwidth of only a few kHz, while a short-range system operating over several tens of meters may have more than a hundred kHz of bandwidth. In both cases these factors lead to low bit rate [11], in the order of tens of kbit/s for existing devices.

Underwater acoustic communication links can be classified according to their range as very long, long, medium, short, and very short links [11]. Table 1.1 shows typical bandwidths of the underwater channel for different ranges. Acoustic links are also roughly classified as vertical and horizontal, according to the direction of the sound ray with respect to the ocean bottom. Their propagation characteristics differ considerably, especially with respect to time dispersion, multi-path spreads, and delay variance. Shallow water refers to water with depth lower than 100m, while deep water is used for deeper oceans.

Table 2.1 *Available Bandwidth for different ranges in UW channel [11]*

	Range[Km]	**Bandwidth[KHz]**
Very Long	1000	<1
Long	10-100	2-5
Medium	1-10	10
Short	0.1-1	20-50
Very Short	<0.1	>100

2.2 Communication Architectures

In this section, the communication architectures of underwater acoustic sensor networks are described.The network topology is in general a crucial factor in determining the energy consumption, the capacity, and the reliability of a network. Hence, the network topology should be carefully engineered and post-deployment topology optimization should be performed, when possible[16].

Underwater monitoring missions can be extremely expensive because of the high cost of underwater devices. Hence, it is important that the deployed network be highly reliable, so as to avoid failure of monitoring missions due to failure of single or multiple devices.

For example, it is crucial to avoid designing the network topology with single points of failure, which could compromise the overall functioning of the network. The network capacity is also influenced by the network topology. Since the capacity of the underwater channel is severely limited, it is very important to organize the network topology in such a way that no communication bottleneck is introduced [15].

2.2.1 Two-dimensional Underwater Sensor Networks

Reference architecture for two-dimensional underwater networks is shown in Fig.2.1. A group of sensor nodes are anchored to the bottom of the ocean with deep ocean anchors. Underwater sensor nodes are interconnected to one or more underwater gateways (uwgateways) by means of wireless acoustic links. Uw-gateways, as shown in Fig. 2.1, are network devices in charge of relaying data from the ocean bottom network to a surface station.To achieve this objective, uw-gateways are equipped with two acoustic transceivers, namely a vertical and a horizontal transceiver.

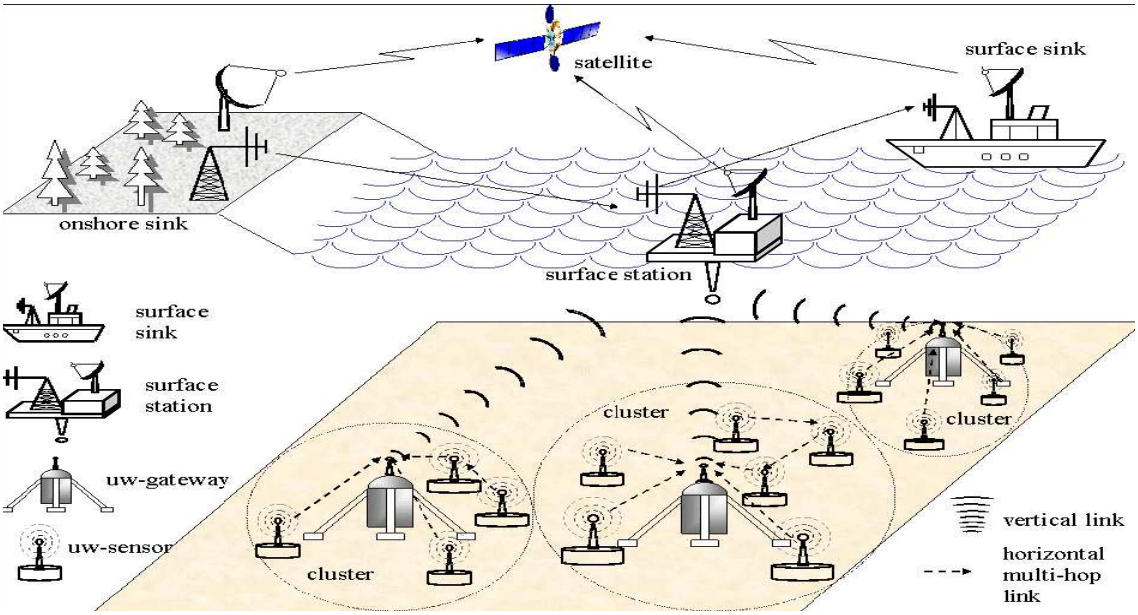

***Figure* 2.1** *Architecture for 2D underwater sensor networks[13]*

The horizontal transceiver is used by the uw-gateway to communicate with the sensor nodes to:

i) send commands and configuration data to the sensors (uw-gateway to sensors);

ii) collect monitored data (sensors to uw-gateway). The vertical link is used by the uw- ateways to relay data to a surface station.

In deep water applications, vertical transceivers must be long range transceivers as the ocean can be as deep as 10km. The surface station is equipped with an acoustic transceiver that is able to handle multiple parallel communications with the deployed uw-gateways. It is also endowed with a long range RF and/or satellite transmitter to communicate with the onshore sink (os-sink) and/or to a surface sink (s-sink). Sensors can be connected to uw-gateways via direct links or through multi-hop paths. In the former case, each sensor directly sends the gathered data to the selected uw-gateway. However, in UW-ASNs, the power necessary to transmit may decay with powers greater than two of the distance [18], and the uw-gateway may be far from the sensor node. Consequently, although direct link connection is the simplest way to network sensors, it may not be the most energy efficient solution. Furthermore, direct links are very likely to reduce the network throughput because of increased acoustic interference caused by the high transmission power[15].

2.2.2 Three-dimensional Underwater Sensor Networks

Three dimensional underwater networks are used to detect and observe phenomena that can not be adequately observed by means of ocean bottom sensor nodes, i.e., to perform cooperative sampling of the 3D ocean environment. In three-dimensional underwater networks, sensor nodes float at different depths to observe a given phenomenon. One possible solution would be to attach each uw-sensor node to a surface buoy, by means of wires whose length can be regulated so as to adjust the depth of each sensor node [15].

However, although this solution allows easy and quick deployment of the sensor network, multiple floating buoys may obstruct ships navigating on the surface, or they can be easily detected and deactivated by enemies in military settings.

For these reasons, a different approach can be to anchor sensor devices to the bottom of the ocean. In this architecture, depicted in Fig. 2.2, each sensor is anchored to the ocean bottom and equipped with a floating buoy that can be inflated by a pump. The buoy pushes the sensor towards the ocean surface. The depth of the sensor can then be regulated by adjusting the length of the wire that connects the sensor to the anchor, by means of an electronically controlled engine that resides on the sensor.

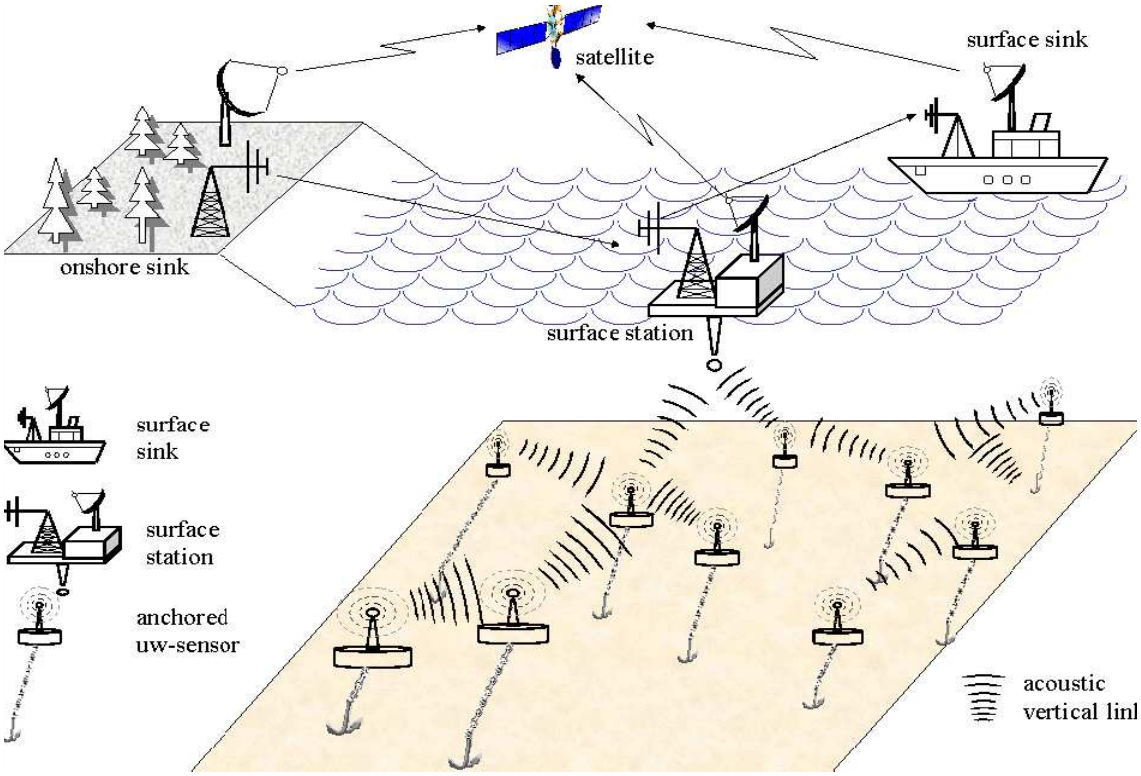

Figure* 2.2: *Architecture for 3D underwater sensor networks[13]

2.2.3 Sensor Networks with Autonomous Underwater Vehicles

AUVs can function without tethers, cables, or remote control, and therefore they have a multitude of applications in oceanography, environmental monitoring, and underwater resource study. Previous experimental work has shown the feasibility of relatively inexpensive AUV submarines equipped with multiple underwater sensors that can reach any depth in the ocean. Hence, they can be used to enhance the capabilities of underwater sensor networks in many ways. Figure 2.3 shows reference architecture for 3D underwater sensor networks with AUVs[14].

The integration and enhancement of fixed sensor networks with AUVs is an almost unexplored research area that requires new network coordination algorithms such as:

- **Adaptive sampling.** This includes control strategies to command the mobile vehicles to places where their data will be most useful. This approach is also known as adaptive sampling and has been proposed in pioneering monitoring missions. For example, the density of sensor nodes can be adaptively increased in

a given area when a higher sampling rate is needed for a given monitored phenomenon.

- **Self-Configuration.** This includes control procedures to automatically detect connectivity holes caused by node failures or channel impairment and request the intervention of an AUV. Furthermore, AUVs can either be used for installation and maintenance of the sensor network infrastructure or to deploy new sensors. They can also be used as temporary relay nodes to restore connectivity. One of

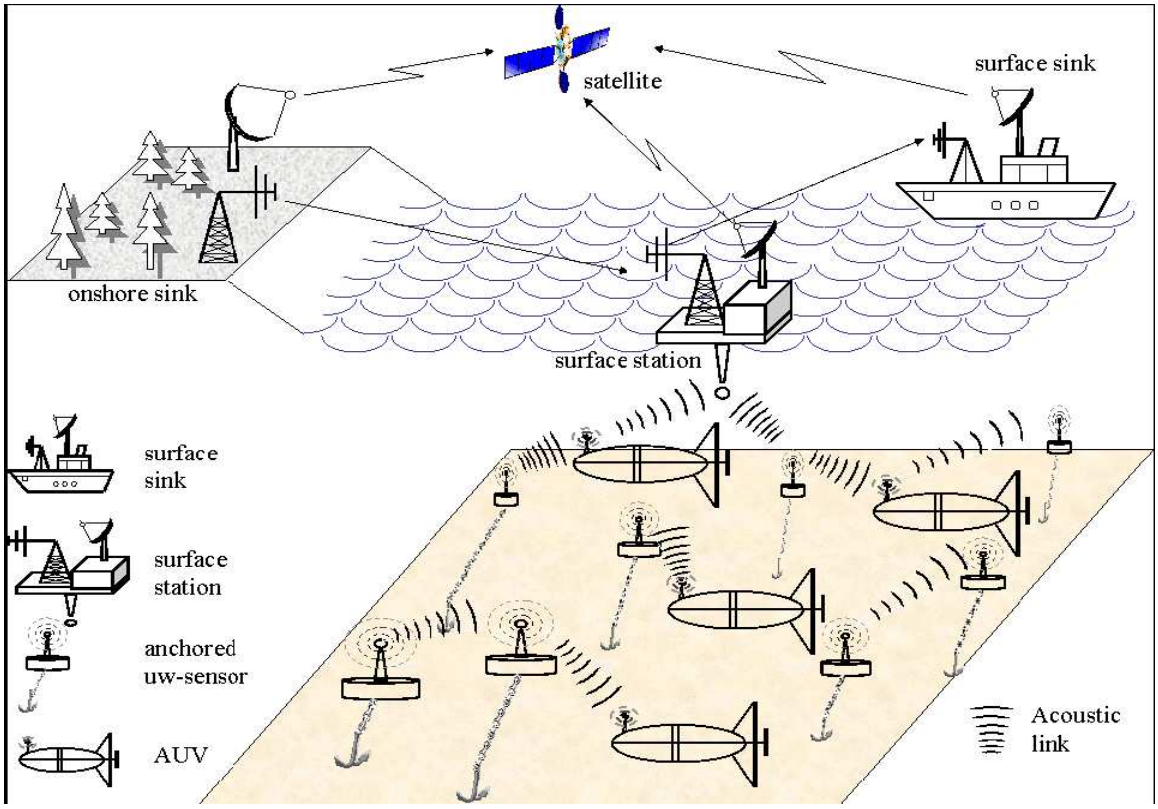

Figure2.3: *Architecture for 3D underwater sensor networks with AUVs[13]*

the design objectives of AUVs is to make them rely on local intelligence, and be less dependent on communications from online shores [13].

In general, control strategies are needed for autonomous coordination, obstacle avoidance, and steering strategies. Solar energy systems allow increasing the lifetime of AUVs, i.e., it is not necessary to recover and recharge the vehicle on a daily basis. Hence, solar powered AUVs can acquire continuous information for periods of time of the order of months [14].

Several types of AUVs exist as experimental platforms for underwater experiments. Some of them resemble small-scale submarines. Others are simpler devices that do not encompass such sophisticated capabilities. For example, drifters and gliders are oceanographic instruments often used in underwater explorations. Drifter underwater vehicles drift with local current and have the ability to move vertically through the water column, and are used for taking measurements at preset depths [17]. Underwater gliders [12] are battery powered autonomous underwater vehicles that use hydraulic pumps to vary their volume by a few hundred cubic centimeters to generate the buoyancy changes that power their forward gliding. When they emerge on the surface, Global Positioning System (GPS) is used to locate the vehicle. This information can be relayed to the onshore station while operators can interact by sending control information to the gliders. These long durations are possible because gliders move very slowly, typically 25 cm/s. The proposed framework allows preserving the symmetry of the group of gliders. The group is constrained to maintain a uniform distribution as needed, but is free to spin and possibly wiggle with current.

Table 2.2: *Evolution of modulation technique[18]*

TYPE	YEAR	RATE[kbps]	BANDWIDTH[kHz]	RANGE[km]
FSK	1984	1.2	5	3s
PSK	1989	500	125	0.06d
FSK	1991	1.25	10	2d
PSK	1993	0.3-0.5	0.3-1	200d-90d
PSK	1994	0.02	20	0.9s
FSK	1997	0.6-2.4	5	10d-5s
DPSK	1997	20	10	1d
PSK	1998	1.67-6.7	2-10	4d-2s
16-QAM	2001	40	10	0.3s

The subscripts d and s stand for deep and shallow water

With respect to Table 2.2, it is worth noticing that early phase-coherent systems achieved higher bandwidth efficiencies (bit rate/occupied bandwidth) than their incoherent

counterparts, but they did not outperform incoherent modulation schemes yet. In fact, coherent systems had lower performance than incoherent systems for long-haul transmissions on horizontal channels until ISI compensation via decision-feedback equalizers for optimal channel estimation was implemented [18].

2.3 CDMA Evolution

The wireless communications era was born in the 1970s. This system supports a variable number of users in 1.25MHz wide channels using direct sequence spread spectrum. While the analog AMPS system requires that the signal be at least 18dB above the co-channel interference to provide acceptable call quality, CDMA systems can operate at much larger interference levels because of their inherent interference resistance properties. The ability of CDMA to operate with a much smaller signal-to-noise ratio (SNR) than conventional narrowband FM techniques allows CDMA systems to use the same set of frequencies in every cell, which provides a large improvement in capacity.

CDMA is a spread spectrum technology, which means that it spreads the information contained in a particular signal of interest over a much greater bandwidth than the original signal. The codes are shared by both the mobile station and the base station, and are called pseudo-random code sequences. Since each user is separated by a unique code, all users can share the same frequency band (range of radio spectrum).

CDMA uses unique spreading codes to spread the baseband data before transmission. The signal is transmitted in a channel, which is below noise level. The receiver then uses a correlator to despread the wanted signal, which is passed through a narrow bandpass filter. Unwanted signals will not be despread and will not pass through the filter. Codes take the form of a carefully designed one/zero sequence produced at a much higher rate than that of the baseband data. The rate of a spreading code is referred to as chip rate rather than bit rate. CDMA (Code-Division Multiple Access) refers to any of several protocols used in so-called second-generation (2G) and third-generation (3G) wireless communications. As the term implies, CDMA is a form of multiplexing, which allows numerous signals to occupy a single transmission channel, optimizing the use of available bandwidth. CDMA employs analog-to-digital conversion (ADC) in combination with spread spectrum technology. Audio input is first digitized into binary elements. The

frequency of the transmitted signal is then made to vary according to a defined pattern (code), so it can be intercepted only by a receiver whose frequency response is programmed with the same code, so it follows exactly along with the transmitter frequency. There are trillions of possible frequency-sequencing codes, which enhance privacy and makes cloning difficult[19].

The original CDMA standard, also known as CDMA One and still common in cellular telephones in the U.S., offers a transmission speed of only up to 14.4 Kbps in its single channel form and up to 115 Kbps in an eight-channel form. CDMA2000 and wideband CDMA deliver data many times faster than the conventional 2G technology system 3G CDMA2000 standard was created to support IS-95 evolution.

Table 2.3 *Emerging 3G Data Communication Standards.[20]*

Technology	**Channel BW**	**Duplex**	**Infrastructure change required**	**Requires new spectrum**	**Requires new handsets**
W-CDMA	5 MHz	FDD	Completely new base station	Yes	Yes
CDMA 2000 1xRTT	1.25 MHz	FDD	New software in backbone and new channel cards at base station	No	Yes
CDMA 2000 1xEV	1.25 MHz	FDD	Software and digital card upgrade	No	Yes
CDMA 2000 3xRTT	3.75 MHz	FDD	Backbone modifications and new channel cards at base station	May be	Yes

2.4 Underwater CDMA literature survey

There has been intensive research on multiple access protocols for ad hoc and wireless terrestrial sensor networks in the last decade. However, due to the different nature of the underwater environment and applications, existing terrestrial multiple access protocol solutions are unsuitable for this environment. In fact, channel access control in UW-ASNs poses additional challenges due to the peculiarities of the underwater channel, in particular limited bandwidth, very high and variable propagation delays, high bit error rates, temporary losses of connectivity, channel asymmetry, and heavy multipath and fading phenomena. For a thorough discussion on the reasons why several multiple access techniques widely employed in terrestrial sensor networks such as TDMA, FDMA, and CSMA, are not suitable for the underwater environment[20]. Since CDMA is the most promising physical layer and multiple access technique for UW-ASNs. In fact, CDMA is i) robust to frequency-selective fading, ii) compensates for the effect of multipath by exploiting Rake filters [21] at the receiver, and iii) allows receivers to distinguish among signals simultaneously transmitted by multiple devices. For these reasons, CDMA increases channel reuse and reduces packet retransmissions, which results in decreased energy consumption and increased network throughput. In [23], two spread-spectrum physical layer techniques, namely Direct Sequence Spread Spectrum (DSSS) and Frequency Hopping Spread Spectrum (FHSS), are compared for shallow water communications. While in DSSS data is spread to minimize the mutual interference, in FHSS different simultaneous communications use different hopping sequences and transmit on different frequency bands. Interestingly, [23] shows that in the underwater environment FHSS leads to a higher bit error rate than DSSS. Another attractive access technique combines DSSS CDMA with multi-carrier transmissions [24], which may offer higher spectral efficiency than its single-carrier counterpart. This way, high data rate can be 124 supported by increasing the duration of each symbol, which reduces Inter Symbol Interference (ISI). However, multi-carrier transmissions may not be suitable for low-end sensors because of their high complexity. Therefore, i focus on single-carrier CDMA to keep the complexity of resource-limited sensor transceivers low. Remarkably, the above papers [23][24] merely consider CDMA from a physical layer perspective, i.e., they analyze the suitability of different forms of CDMA-based transmission techniques with

respect to the challenges raised by the underwater channel. Even they contribution is to develop a dynamic multiple access protocol for UW-ASNs that efficiently shares the scarce underwater channel bandwidth by fully leveraging the CDMA medium access properties. In [22], a solution for underwater networks with AUVs was devised. The scheme is based on organizing the network in multiple clusters, each composed of adjacent vehicles.

Interference among different clusters is minimized by assigning orthogonal spreading codes to different clusters. Inside each cluster, TDMA is used with long band guards to overcome the effect of the propagation delay. Since vehicles in the same cluster are assumed to be close to one another, the negative effect of the very high underwater propagation delay is limited. The proposed solution, however, assumes a clustered network architecture and proximity among nodes within the same cluster, while we seek a more general and flexible solution suitable for different network sizes and architectures.

In [16], Slotted FAMA, a protocol based on a channel access discipline called Floor Acquisition Multiple Access (FAMA) is proposed. It combines both carrier sensing (CS) and a dialogue between the source and receiver prior to data transmission. During the initial dialogue, control packets are exchanged between the source node and the intended destination node to avoid multiple transmissions at the same time. Time slotting eliminates the asynchronous nature of the protocol and the need for long control packets, thus providing energy savings. However, guard times should be inserted in the time slot to account for any system clock drift. In addition, because of the high underwater acoustic propagation delay, the handshaking mechanism may lead to low system throughput, and the CS scheme may sense the channel idle while a transmission is still taking place, thus causing packet collisions.

In [23], the impact of the large propagation delay on the throughput of selected classical multiple access protocols and their variants is analyzed, and PCAP, Propagation-delay-tolerant Collision Avoidance Protocol, is introduced. Its objective is to fix the time spent on setting up links for data frames, and to avoid collisions by scheduling the activity of sensors.

Although PCAP offers higher throughput than widely used conventional protocols for wireless networks, it does not provide a flexible solution for applications with heterogeneous requirements.

A distributed CSMA-based energy-efficient multiple access protocol for the underwater environment was recently proposed in [20]. Its objective is to save energy based on sleep periods with low duty cycles. The solution is tied to the assumption that nodes follow sleep periods, and is aimed at efficiently organizing the sleep schedules.

I m interested in implementing a complete CDMA2000 system for underwater communication because it has additional features as compared to CDMA-one. Along with this I m also aiming at the point of proper recovery of signal by adding some features to CDMA2000 system such as delay estimation and channel estimation technique. In addition to it CDMA2000 system has in itself many features like rake receiver which helps in maximizing signal to noise ratio, low interference , privacy and many other features which are helpful in designing a better underwater communication system.

CHAPTER 3

CDMA2000 SYSTEM

3.1 Introduction to Spread Spectrum System

Third Generation (3G) is the term used for CDMA2000 system to describe the latest generation of communication services which provide advanced communications quality and high-speed data connectivity The International Telecommunication Union (ITU), working with industry standards bodies from around the world, has defined the technical requirements and standards as well as the use of spectrum for 3G systems under the IMT-2000 (International Mobile Telecommunications-2000) program.

Five radio interface modes for IMT-2000 standards (Recommendation 1457). Three of the five approved standards (CDMA2000® , TD-SCDMA, WCDMA) are based on CDMA. CDMA2000 is also known by its ITU name, IMT-2000 CDMA Multi-Carrier (MC).

CDMA2000 builds on the inherent advantages of CDMA technologies and introduces other enhancements, such as Orthogonal Frequency Division Multiplexing (OFDM and OFDMA), advanced control and signaling mechanisms, improved interference management techniques, end-to-end Quality of Service (QoS), and new antenna techniques such as Multiple Inputs Multiple Outputs (MIMO) and Space Division Multiple Access (SDMA) to increase data throughput rates and quality of service, while significantly improving network capacity and reducing delivery cost[25].

Key features of CDMA2000 are:

- **Leading performance:** CDMA2000 performance in terms of data-speeds, voice capacity and latencies continue to outperform in commercial deployments other comparable technologies
- **Efficient use of spectrum:** CDMA2000 technologies offer the highest voice capacity and data throughput using the least amount of spectrum, lowering the cost of delivery for operators and delivering superior customer experience for the end users
- **Support for advanced mobile services:** CDMA2000 1xEV-DO enables the delivery of a broad range of advanced services, such as high-performance VoIP,

push-to-talk, video telephony, multimedia messaging, multicasting and multi-playing online gaming with richly rendered 3D graphics

- All-IP – CDMA2000 technologies are compatible with IP and ready to support network convergence. Today, CDMA2000 operators that have deployed IP-based services enjoy more flexibility and higher bandwidth efficiencies, which translate into greater control and significant cost savings
- **Devices selection:** CDMA2000 offers the broadest selection of devices and has a significant cost advantage compared to other 3G technologies to meet the diverse market needs around the world
- **Seamless evolution path** : CDMA2000 has a solid and long-term evolution path which is built on the principle of backward and forward compatibility, in-band migration, and support of hybrid network configurations
- **Flexibility:** CDMA2000 systems have been designed for urban as well as remote rural areas for fixed wireless, wireless local loop (WLL), limited mobility and full mobilility applications in multiple spectrum bands, including 450 MHz, 800 MHz, 1700 MHz, 1900Mhz and 2100 MHz [26].

CDMA2000 system has two basic characteristics related to frequency spectrum:

- Centre frequency
- Bandwidth.

The bandwidth occupied by a conventional transmission system is directly related to that of the original information waveform and to the carrier modulation scheme. If Amplitude Modulation is used, a bandwidth of twice the size of the baseband signal is required, whereas single side band amplitude modulation and frequency modulation require a transmission bandwidth comparable to the bandwidth of the baseband signal[28]. The FM bandwidth depends on the frequency deviation applied to the carrier and the information signal and is calculated using Carson's rule

$$B_{RF} = 2(\Delta f + f_m) \qquad (3.1)$$

Two the most important characterstics of spread spectrum systems are the following

- Transmission bandwidth much larger than the bandwidth of the baseband data signal.
- Transmitted bandwidth dependent on the rate of the code employed for spreading.

Spread spectrum systems are based on the Hartley-Shannon law that calculates the asymptotic transmission capacity in a channel distributed by Additive White Gaussian Noise(AWGN)

$$C_{Sh} = B \times \log_2 (1+SNR) \qquad (3.2)$$

Where C_{Sh} asymptotic channel transmission capacity in bps

B channel bandwidth in Hz

SNR signal-to-noise ratio.

3.2 Direct Sequence Spread Spectrum CDMA2000 Technique

This is categorized by two of the most widely used methods of direct sequence spread spectrum (DS-SS) and frequency-hopping spread spectrum (FH-SS). In both of these methods, a pseudorandom code sequence is utilized to spread or map the signal information over a wide bandwidth. DS-SS is used in underwater communication, so it is discussed in the following section.

A direct sequence spread spectrum (DS-SS) system spreads the base band data bi directly multiplying the baseband data pulses with the pseudo-noise sequence that is produced by a pseudo-noise code generator. A single pulse or symbol of the PN waveform is called a chip. This system is one of the most widely used direct sequence implementations.

Synchronised data symbols, which may be information bits or binary channel code symbols, are added in modulo-2 fashion to the chips before being phase modulated[26]. A coherent or differencial coherent phase- shift keying(PSK) demodulation may be used in the-receiver.The BPSK modulated data, is spread after multiplication by a *pseudorandom* (PN) sequence with a bandwidth much greater than the information signal. The transmitted signal $x(t)$ can be expressed as

$$X(t) = \sqrt{2p}\, b(t)\, a(t) \exp(jwt) \qquad \ldots\ldots\ldots\ldots\ldots\ldots (3.3)$$

where $a(t)$ is the spreading PN sequence with chips of ±1 of duration and code length of $N = \frac{T_b}{T_c}$. The signal spectrum at various stages of transmission is shown in Figure 3.1 [27].

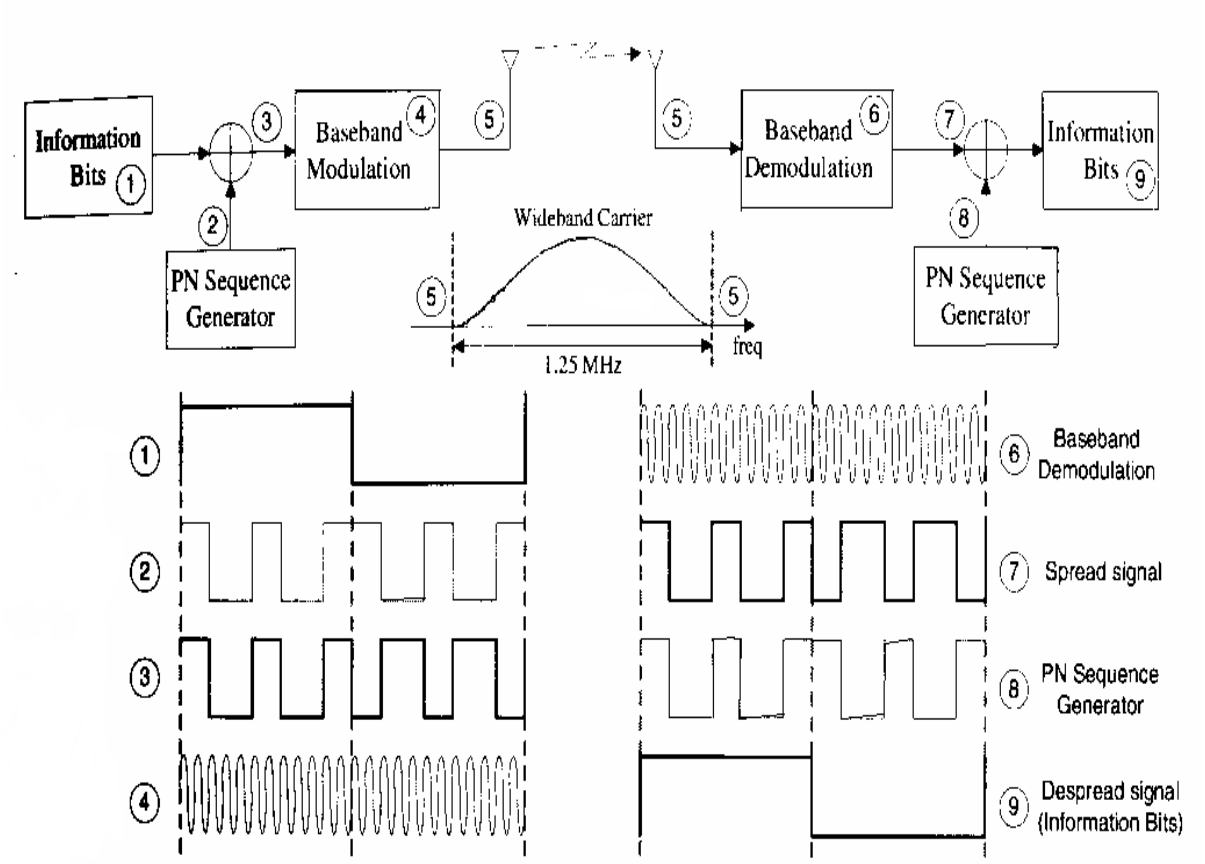

Figure 3.1: *Diagram of a direct sequence system and associated waveform[28]*

As an information signal is multiplied by the PN sequence, its energy is spread over a wide bandwidth while the total signal energy remains constant. If the spreading ratio is large enough, the spread signal appears as very low power noise[26].

The received signal $y(t)$ is expressed as

$$Y(t) = h(t)\ x(t-\delta_d)\ +\ n(t)$$

where $h(t)$ represents the propagation channel impulse response, including multipath fading, shadowing, and path loss; δ_d is the channel propagation delay; and $n(t)$ is zero mean additive white Gaussian noise (AWGN) with a two-sided power spectral density of $N0/2$.

Substituting for $x(t)$ from (1.7) yields:

$$y(t) = h(t)\sqrt{2p}\ b(t-\delta_d)\,a(t-\delta_d)\ \exp[\,jw(t-\delta_d\,] + n(t) \qquad (3.5)$$

The received signal $y(t)$ of (3.5) is multiplied by a delayed replica of the spreading sequence $a(t-\hat{\delta}_d)$, where $\hat{\delta}_d$ is a local estimate of the propagation delay δ_d :

$$\hat{d}(t)=\sqrt{2p}\ h(t)\ b(t-\delta_d)\ a(t-\delta_d)\ a(t-\hat{\delta}_d)\ \exp[(jw(t-\delta_d)]+b(t-\hat{\delta}_d)\ n(t) \qquad (3.6)$$

The despreading of signal $y(t)$ is realized if $\hat{\delta}_d$ can be estimated at the receiver to be equal to δ_d , in which case $a(t-\hat{\delta}_d)a(t-\delta_d) = 1$. Noise power remains unchanged[29].

3.3 Spreading and dispreading of DS CDMA2000 system

Direct sequence CDMA systems do not change the centre frequency over time as hopping systems do. At the modulator output, or exclusive-OR logic circuit, the data has the same transmission rate as the code. In CDMA systems, codes are assigned to each user to allow distinguishing them from each other. To de-spread a given channel, the two cods generated by the transmitter and by the receiver must be synchronized. The de-spreading is done through the multiplication of the received signal by the code associated with the desired channel.

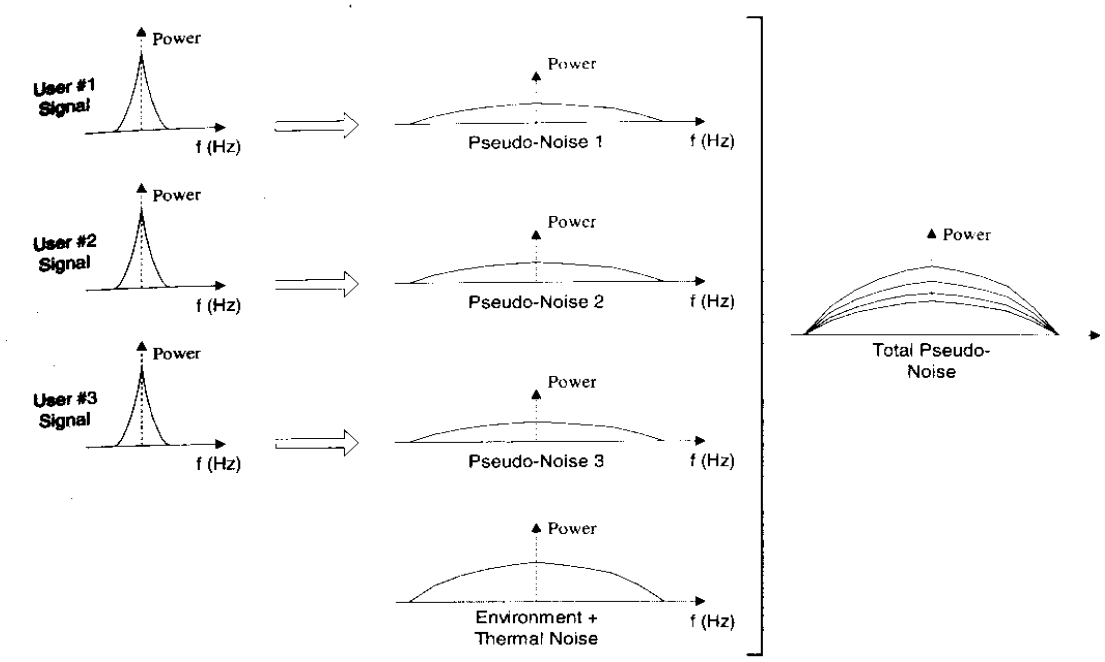

Figure 3.2 *Spectrum spreading in DS-CDMA2000 system[26]*

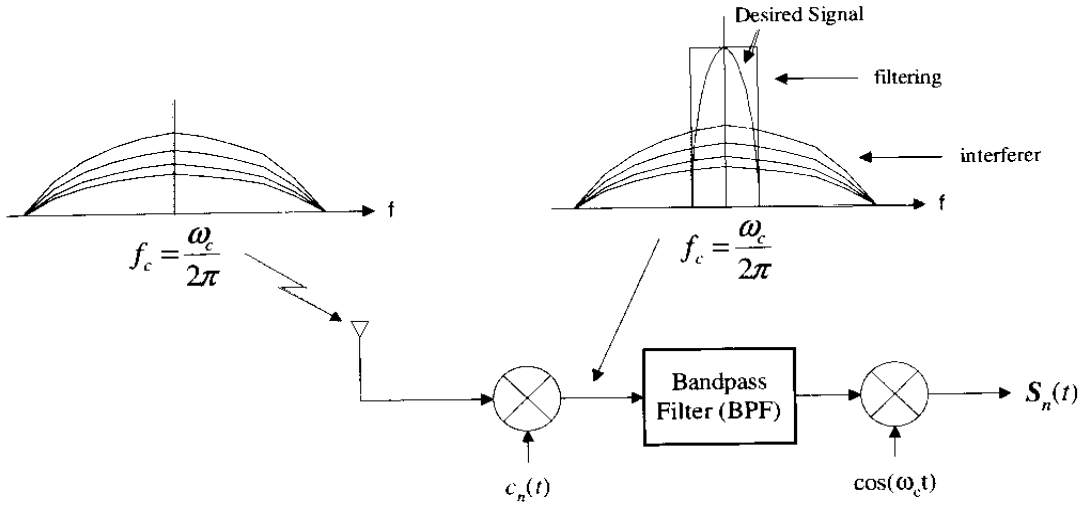

Figure 3.3 *Spectrum de-spreading in DS-CDMA2000 system[26]*

3.4 Walsh codes used in CDMA2000 system

The spreading procedure consists of two separate operations:

- channelization
- scrambling.

Channelization uses orthogonal codes and scrambling uses PN codes. Channelization occurs before scrambling in the transmitter both in the uplink and the downlink. Channelization transforms each data symbol into multiple chips. This ratio (number of chips/symbol) is called the spreading factor (SF). Thus, it is this procedure that actually expands the signal bandwidth. Data symbols on the *I* and *Q* branches are combined with the channelization code. Channelization codes are orthogonal codes (more precisely, orthogonal variable spreading factor [OVSF] codes), meaning that in an ideal environment they don't interfere with each other. However, orthogonality requires that the codes be time synchronized. Therefore, it can be used in the downlink to separate different users within one cell, but in the uplink only to separate the different services of one user. It cannot be used to separate different uplink users in a surface station, as all underwater sensor nodes are unsynchronized in time; thus, their codes cannot be orthogonal (unless the system in question employs the TDD mode with uplink synchronization). Also, orthogonal signals cannot be used as such between surface stations in the downlink because there is only a limited number of orthogonal codes[30].

These codes correspond to the rows of a special square matrix known as the Hadamard matrix. For a set of Walsh codes of length *n,* there consists of *n* rows to form an *n* x *n* Walsh code square matrix. The first row of this matrix contains a string of all zeros with each of the subsequent rows containing different combinations of bit 0's and 1's. Every row is orthogonal and has an equal occurrence for the binary bits. This matrix is defined recursively as follows:

$$W_1 = [0] \qquad\qquad W_{2n} = \begin{bmatrix} W_n & W_n \\ W_n & \overline{W_n} \end{bmatrix}$$

where *n* is a power of 2 indicating the various dimensions of the matrix and *n* $\overline{W}$ denotes the logical NOT operation on all bits in that matrix. The three matrices W2, W4 and W8, show the Walsh function for dimension 2, 4 and 8 respectively.

$$W_2 = \begin{bmatrix} 0 & 0 \\ 0 & 1 \end{bmatrix} \qquad W_4 = \begin{bmatrix} 0 & 0 & 0 & 0 \\ 0 & 1 & 0 & 1 \\ 0 & 0 & 1 & 1 \\ 0 & 1 & 1 & 0 \end{bmatrix} \qquad W_8 = \begin{bmatrix} 0 & 0 & 0 & 0 & 0 & 0 & 0 & 0 \\ 0 & 1 & 0 & 1 & 0 & 1 & 0 & 1 \\ 0 & 0 & 1 & 1 & 0 & 0 & 1 & 1 \\ 0 & 1 & 1 & 0 & 0 & 1 & 1 & 0 \\ 0 & 0 & 0 & 0 & 1 & 1 & 1 & 1 \\ 0 & 1 & 0 & 1 & 1 & 0 & 1 & 0 \\ 0 & 0 & 1 & 1 & 1 & 1 & 0 & 0 \end{bmatrix}$$

Each row in the 64 by 64 Walsh matrix corresponds to a channel number. Channel number 0 is mapped to the first row of the Walsh matrix, which is the all zeros code. This channel is also known as the pilot channel and is used to train and estimate the impulse response of the underwater communication channel[31].

Note that the spreading codes must be time aligned; otherwise, the orthogonality is lost. The downlink transmissions from separate surface stations are not orthogonal. A UE must first identify the right surface station transmission according to the scrambling code, and then from that signal extract its own data using the orthogonal channelization code. Thus, in the real world the downlink environment is never purely orthogonal and interference free. Intracell interference exists because of multipath reflections and intercell interference from asynchronous base stations. From the asynchronous nature of the system follows inter-surface-station nonorthogonality[32].

3.5 PN Codes used in CDMA2000 system

The orthogonal codes alone cannot handle the spreading function in the interface. As explained earlier, they can only be used when the signals applying them are time synchronous. Clearly this is not the case between asynchronous sensor nodes in the uplink direction. If orthogonal spreading codes alone were used in the uplink, then they could easily cancel each other. Moreover, the downlink signals are only orthogonal within one base station. But even in this case, orthogonality is partially lost with channel distortions.

The surface station's orthogonality decreases as we move out toward to the sensor nodes in water. Therefore, something else is needed. To solve these problems, the system employs pseudorandom codes. They are used in the second part of the spreading procedure, which is called the scrambling stage. In the scrambling procedure, the signal, which is already spread to its full bandwidth with an orthogonal spreading code, is further combined (XORed) with a pseudorandom scrambling code. These pseudorandom codes have good autocorrelation properties. There are millions of scrambling codes available in the uplink, so no special code management is needed. Time-synchronization and orthogonal signals would reduce the interference in the uplink direction because fully orthogonal signals do not cause any interference with each other. In the downlink direction, pseudorandom scrambling codes are used to reduce the inter-base-station interference. There are 512 different primary scrambling codes possible in the downlink. The primary scrambling codes are divided into 64 code groups, each consisting of 8 codes. Dividing the 512 possible primary scrambling codes into only 64 small groups of codes can speed up the synchronization procedure[33].

The specifications also define secondary scrambling codes. Each primary scrambling code has a set of 16 secondary scrambling codes. They can be employed while transmitting channels that do not need to be received by everyone in the cell. However, they should be used sparingly because channels transmitted with secondary scrambling codes are not orthogonal to channels that use the primary scrambling code. One possible application could be in sectored cells, where separate sectors do not have to be orthogonal to each other.

PN sequence is also known as Maximal Length Sequence (MLS). The term pseudo-noise is used because these sequences are neither completely deterministic nor truly random. The most common MLS consists of a shift register working according to a specific logic that provides a feedback path, which combines the state of two stages of the shift register. The length of the MLS generated by a Linear Feedback Shift Register (LFSR) circuit is given by the following expression

$$L = 2^N - 1 \text{ chips}$$

Where N is number of shift registers used in the generator circuit.

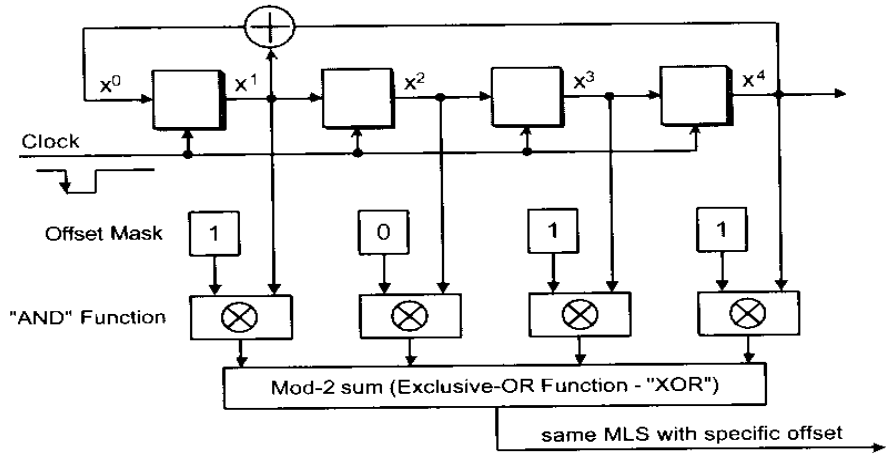

***Figure 3.4** : 4-stage-register MLS generator with offset mask and mod-2 sum[33]*

A polynomial expression can be associated with each set of shift registers. These expressions are primitive, that is, their only roots are '1' and

$P(x) = a_n x^n + a_{n-1} x^{n-1} + a_{n-2} x^{n-2} + a_{n-3} x^{n-3} + a_{n-4} x^{n-4} + \ldots\ldots\ldots\ldots\ldots\ldots + a_2 x^2 + a_1 x + 1$

Where a_n is the existence of feedback path.

3.5.1 Short PN Sequence

CDMA short PN sequences are based on two distinct MLSs generated by a circuit with 15 shift-register stages arranged to produce the following polynomials

PN-I: $P(x) = x^{15} + x^{13} + x^9 + x^8 + x^7 + x^5 + 1$

PN-Q: $P(x) = x^{15} + x^{12} + x^{11} + x^{10} + x^6 + x^5 + x^4 + x^3 + 1$

Each of the circuits generates 32767 chips long sequences ($2^N - 1$), composed of 16384 '1's and 16383 '0's. However, an external circuit inserts an additional chip '0' into each

sequence after reading a set of 14 consecutive 0s, which happens only once on a complete set of 32767 chips[32].

3.5.2 Long PN Sequence

The long code is a 4398046511103 chips long MLS(2^{42} -1) generated by a 42-stage shift-register circuit described by the following polynomial

$$P(x) = x^{42} + x^{35} + x^{33} + x^{31} + x^{27} + x^{26} + x^{25} + x^{22} + x^{21} + x^{19} + x^{18} + x^{17} + x^{16} + x^{10} + x^{7} + x^{6} + x^{5} + x^{3} + x^{2} + x + 1$$

The transmission rate of this sequence is 1.2288Mcps. The starting point of the sequence is the first '1' after all 41 consecutive '0's.

3.6 Quasi-Orthogonal Function

CDMA2000 system allows variable Walsh length, CDMA2000-1X systems use Walsh codes upto length 128 and CDMA2000-3X upto length 256. The limitation on Walshcode length may cause limitationsto the system due to unavailability of walsh codes, especially when dealing with high data rates. Therefore, CDMA2000 standards propose the use of an additional function, referred to as Quasi Orthogonal Function(QOF), to enhance system capacity. The QOFs are specially employed when Transmit Diversity(TD) techniques are used, such as Space Time spreading(STS).

QOFs consists of the multiplication of the walsh codes by a QOF mask, which is a vector of binary symbols. The resulting codes are not fully orthogonal to the original walsh cods, but the masks selected by the standard are optimal in terms of minimizing the correlation(non-orthogonality). QOF has a length of 256 chips, while walsh codes can have variable lengths. This implies that depending on the walsh code, a single QOF may be applied into more than one code sequence.

QOFs are applied to the system in two steps:

- The first is known as QOF_{sign}
- Second is $Walsh_{rot}$.

The QOF_{sign} changes the polarity of the symbols: when the QOF_{sign} chip is '1' the walsh code symbols is inverted: when the QOF_{sign} chip is '0', walsh code symbols remains the same. The QOF set 0 corresponds to the original walsh code vector.

The $Walsh_{rot}$ corresponds to a symbol phase modification, or rotation. Rotation is only enabled when the $Walsh_{rot}$ chip is '1'. To perform the rotation,the QOF multiplies the walsh code vector by 'j' where 'j' is a complex variable that corresponds to a 90 phase rotation. If $Walsh_{rot}$ chip is '0' , the walsh code symbol remain the same[34].

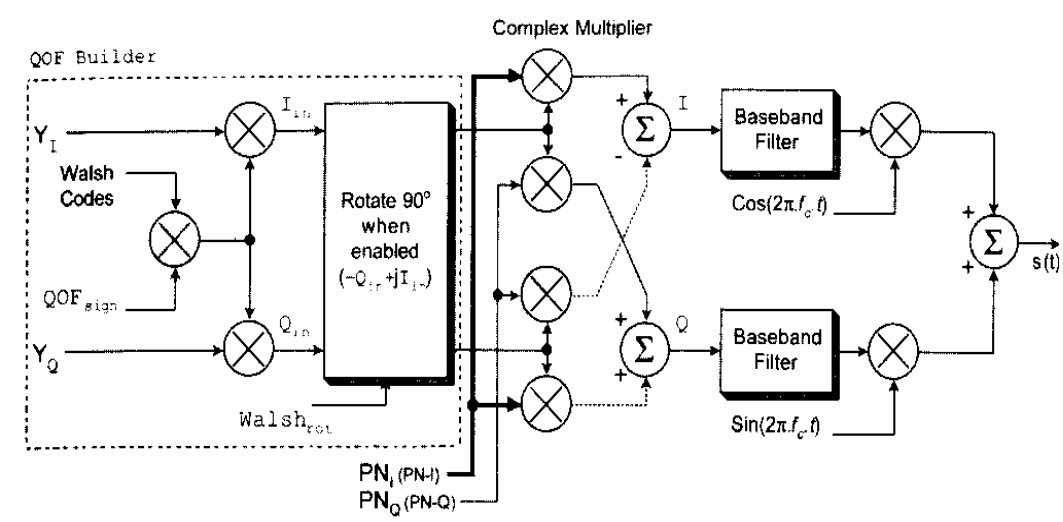

Figure 3.5 *:Quasi-orthogonal function implementation[34]*

CHAPTER 4

IMPLEMENTATION OF UNDERWATER CDMA2000 SYSTEM

In this chapter, implementation of CDMA2000 system for UW communication is done using MATLAB SIMULINK Tools. It consists of various sections which perform different functions. Initially, 172 bits per 20msec data i.e 8600 bps is given as information to the CDMA2000 system. Firstly, it is passed through encoder section that increases its data rate to 384 bits per 20msec i.e. 19.2 Kbps. After that power control are added to the data in transmitter section. Along with this scrambling and spreading operations are performed in this transmitter section. It results in a transmission data rate of 1.2288Mbps. This data is transmitted in the form of frames of 24 bits having duration of 1.042msec. This transmitted data is attenuated by rayleigh fading channel. The distorted data is received at the receiver side. The first section on the receiver side is receiver block. It performs the function of channel compensation, delay estimation, channel diversity compensation, synchronization and optimizes signal to noise ratio. Despreading and descrambling is done on recovered bits. After that the power control bits are extracted from the received signals which are used to adjust the power level of the retransmitted signal. The data rate after receiver section is again 384 bits per 20msec i.e 19.2Kbps. Then decoder section performs function exactly opposite to the functions performed in encoder on the transmitter side. The final data rate retrieved is 172bps same as the data rate of the input data on the transmitter side. The comparison of the data on transmitter and receiver side at various stages of this system will give the bit error rate of that section. In Chapter 5, various graphs are shown to determine the performance of the system.

4.1 DESIGN OF UNDERWATER CDMA2000 SYSTEM

The design of full fledged Underwater CDMA2000 system is shown in figure 4.1. It consists of many sub blocks which are discussed in detail in this chapter.

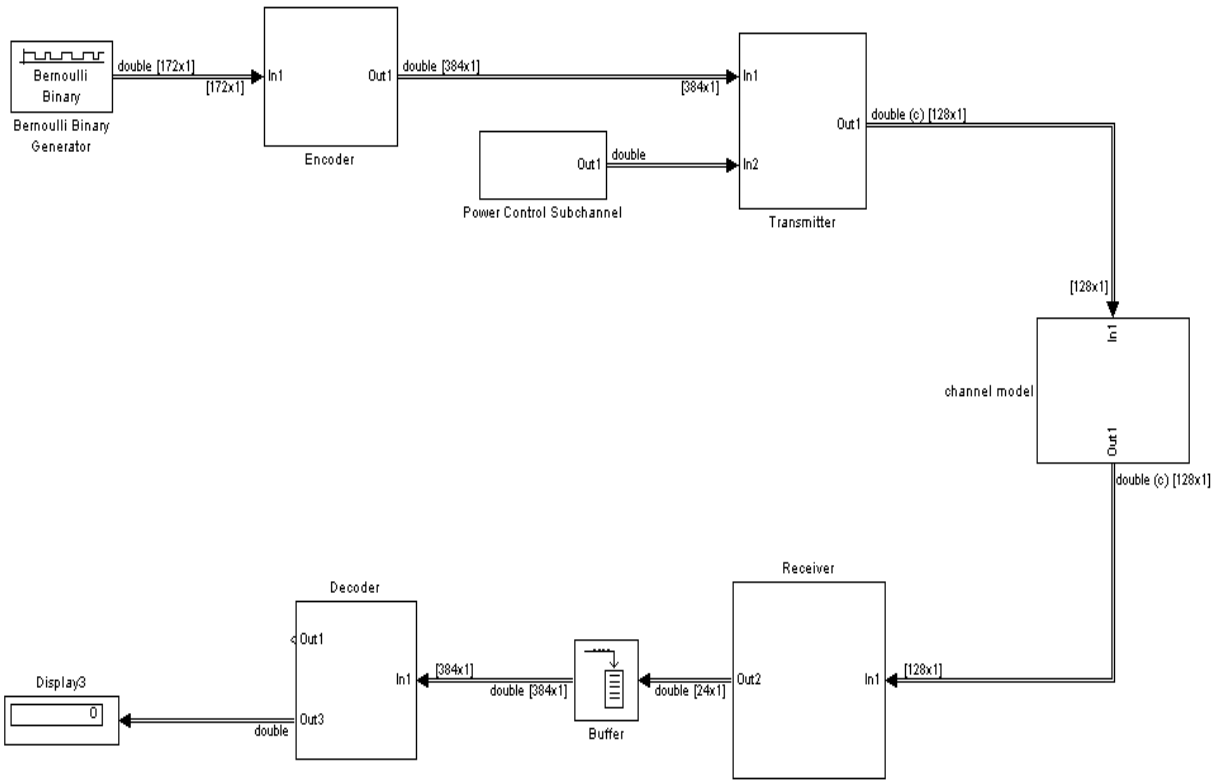

Figure 4.1 *Design of underwater CDMA2000 system*

**All Data rates mentioned in design diagrams are bits per frame*

4.2 BINARY GENERATOR

The source of binary generation is Bernoulli binary generator. The Bernoulli Binary Generator block generates random binary numbers using a Bernoulli distribution. The Bernoulli distribution with parameter p produces zero with probability p and one with probability 1-p. The Bernoulli distribution has mean value 1-p and variance p(1-p). The Probability of a zero parameter specifies p, and can be any real number between zero and one.

Attributes of Output Signal

The output signal can be a frame-based matrix, a sample-based row or column vector, or a sample-based one-dimensional array. These attributes are controlled by the Frame-based outputs, Samples per frame, and Interpret vector parameters as 1-D parameters. See Signal Attribute Parameters for Random Sources in Using the Communications Block set for more details. The number of elements in the Initial seed and Probability of a

zero parameters becomes the number of columns in a frame-based output or the number of elements in a sample-based vector output. Also, the shape (row or column) of the Initial seed and Probability of a zero parameters becomes the shape of a sample-based two-dimensional output signal. Figure 4.2 shows the source block parameters for Bernoulli binary generator [35].

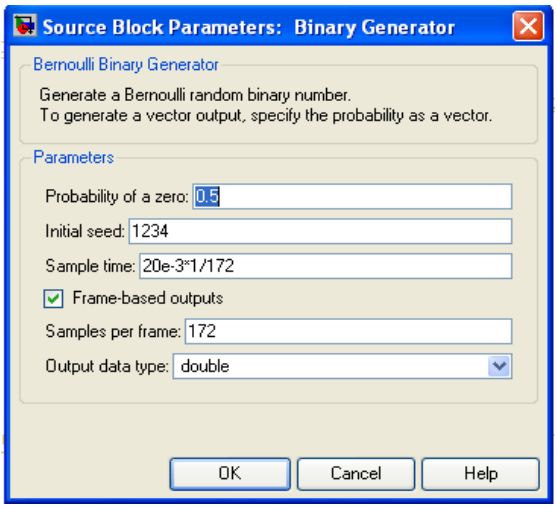

Figure 4.2 *Source block parameters for Bernoulli binary generator*

Output:-It generates a binary sequence at a rate of 172 bits in 20msec in one frame. This means that it is generating a data rate of 8600(172 X 50) bps constituting of total 50 frames.

4.3 ENCODER

The next block is encoder. It performs various operations on the input data for error correction and for reducing bit error rate. Figure 4.3 shows the design of encoder.

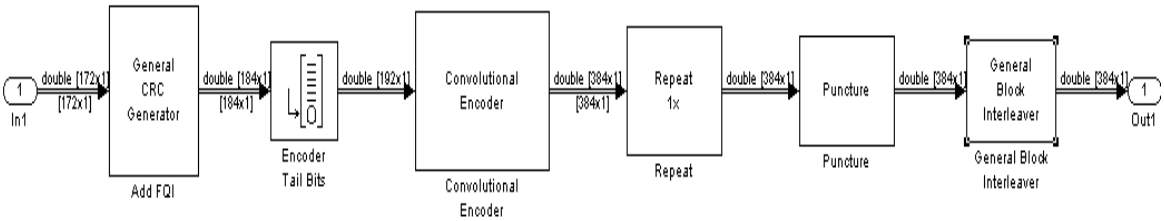

Figure 4.3*: Design of encoder*

4.3.1 Cyclic Redundancy Check

The first function performed in encoder is to add cyclic redundancy check (CRC) bits. The CRC algorithm accepts a binary data frame, corresponding to a polynomial M, and appends a checksum of r bits, corresponding to a polynomial C. The concatenation of the input frame and the checksum then corresponds to the polynomial $T = M*x^r + C$, since multiplying by x^r corresponds to shifting the input frame r bits to the left. The algorithm chooses the checksum C so that T is divisible by a predefined polynomial P of degree r, called the generator polynomial. The algorithm divides T by P, and sets the checksum equal to the binary vector corresponding to the remainder. That is, if T = Q*P + R, where R is a polynomial of degree less than r, the checksum is the binary vector corresponding to R. If necessary, the algorithm pretends zeros to the checksum so that it has length r. The General CRC Generator block which implement the transmission phase of the CRC algorithm, do the following:

- Left shift the input data frame by r bits and divide the corresponding polynomial by P.
- Set the checksum equal to the binary vector of length r, corresponding to the remainder from step 1.
- Append the checksum to the input data frame. The result is the output frame[36].

Example :- Suppose the input frame is [1 1 0 0 1 1 0], corresponding to the polynomial $M = x^6 + x^5 + x^2 + x$, and the generator polynomial is $P = x^3 + x^2 + 1$, of degree r = 3. By polynomial division, $M*x = (x^6 + x^3 + x)*P + x$. The remainder is R = x, so that the checksum is then [0 1 0]'. An extra 0 is added on the left to make the checksum have length 3. The General CRC Generator block generates cyclic redundancy code (CRC) bits for each input data frame and appends them to the frame. The polynomial can be represented in one of these ways:

- As a binary row vector containing the coefficients in descending order of powers. For example, [1 1 0 1] represents the polynomial $x^3 + x^2 + 1$.
- As an integer row vector containing the powers of nonzero terms in the polynomial, in descending order. For example, [3 2 0] represents the polynomial $x^3 + x^2 + 1$.

The initial state of the internal shift register is specified by the Initial states parameter. For example, the default initial state of [0] is expanded to a row vector of all zeros. The

number of checksums that the block calculates for each input frame can be specified by the Checksums per frame parameter. The Checksums per frame value must evenly divide the size of the input frame. If the size of the input frame is m and the degree of the generator polynomial is r, the output frame has size m + k * r[35].

Example:-Suppose the size of the input frame is 10, the degree of the generator polynomial is 3, Initial states are [0], and Checksums per frame is 2. The block divides each input frame into two sub frames of size 5 and appends a checksum of size 3 to each sub frame, as shown below. The initial states are not shown in this example, because an initial state of [0] does not affect the output of the CRC algorithm. The output frame then has size 5 + 3 + 5 + 3 = 16[37].

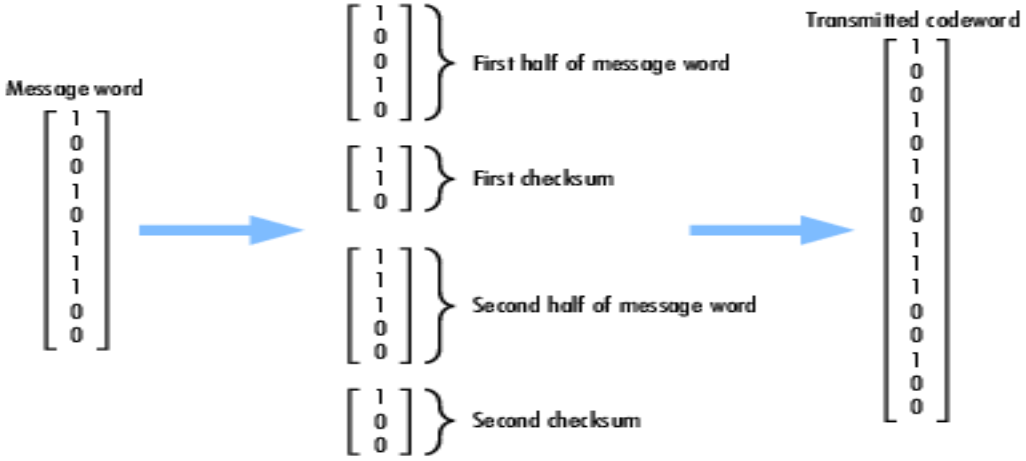

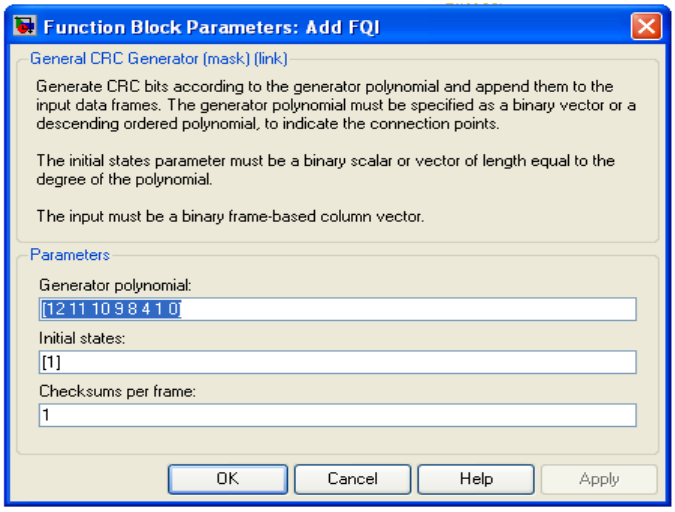

Figure 4.4 *Function block parameters of general CRC generator*

Output:-As the degree of generator polynomial is 12, so 12 bits are append at the end of every frame. The total size of the frame becomes 184(172+12) bits and the total data rate becomes 9200(184 X 50) bps.

4.3.2 Encoder Tail Bit

Encoder tail bits append tail bits at the end of every frame according to the parameters set in the source block parameter.

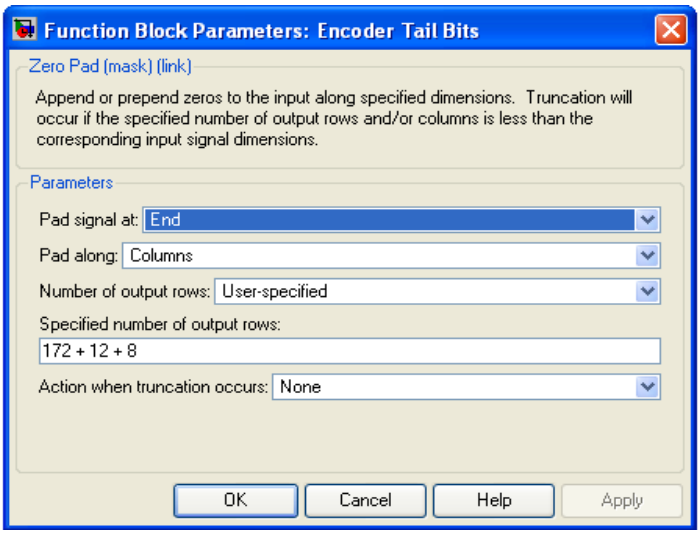

Figure 4.5: *Function block parameters of Encoder tail bits*

***Output*:-** As the row size is set to 192(172+12+8), so total of 8 tail bits are added at the end of every frame. The total data rate now becomes 9600(192 X 50)bps.

4.3.3 Convolutional Encoder

The Convolutional Encoder block encodes a sequence of binary input vectors to produce a sequence of binary output vectors. This block can process multiple symbols at a time. If the encoder takes k input bit streams (that is, can receive 2k possible input symbols), this block's input vector length is L*k for some positive integer L. Similarly, if the encoder produces n output bit streams (that is, can produce 2n possible output symbols), this block's output vector length is L*n.

The input can be a sample-based vector with L = 1, or a frame-based column vector with any positive integer for L. To define the convolutional encoder, use the Trellis structure

parameter. This parameter is a MATLAB structure whose format is described in Trellis Description of a Convolutional Encoder in the Communications Toolbox documentation. This parameter field of the encoder can be specified by using poly2trellis command within the Trellis structure field which uses constraint length, generator polynomials, and possibly feedback connection polynomials. For example, to use an encoder with a constraint length of 7, code generator polynomials of 171 and 133 (in octal numbers), and a feedback connection of 171 (in octal), set the Trellis structure parameter to poly2trellis(7,[171 133],171) [35].

The encoder registers begin in the all-zeros state. A polynomial description of a convolutional encoder has either two or three components, depending on whether the encoder is a feedforward or feedback type [36].

In case of Feedback connection polynomials

Constraint Lengths:- The constraint lengths of the encoder form a vector whose length is the number of inputs in the encoder diagram. The elements of this vector indicate the number of bits stored in each shift register, including the current input bits.

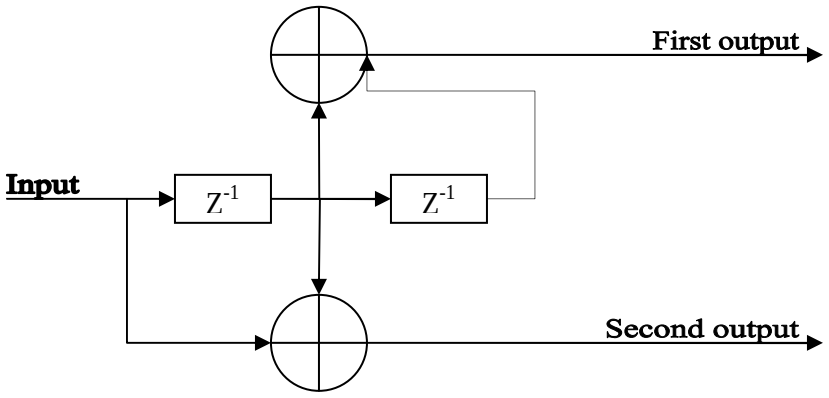

Figure 4.6: *order-3 convolutional encoder[35]*

In the figure above, the constraint length is three. It is a scalar because the encoder has one input stream, and its value is one plus the number of shift registers for that input.

Generator Polynomials:-If the encoder diagram has k inputs and n outputs, then the code generator matrix is a k-by-n matrix. The element in the ith row and jth column indicates how the ith input contributes to the jth output.

In other situations, the (i,j) entry in the matrix can be described as follows:

1. Build a binary number representation by placing a 1 in each spot where a connection line from the shift register feeds into the adder, and a 0 elsewhere. The leftmost spot in the binary number represents the current input, while the rightmost spot represents the oldest input that still remains in the shift register.
2. Convert this binary representation into an octal representation by considering consecutive triplets of bits, starting from the rightmost bit. The rightmost bit in each triplet is the least significant. If the number of bits is not a multiple of three, then place zero bits at the left end as necessary. (For example, interpret 1101010 as 001 101 010 and convert it to 152.)

The binary numbers corresponding to the upper and lower adders in the figure 4.6 are 011 and 110, respectively. These binary numbers are equivalent to the octal numbers 3 and 6, respectively. Thus the generator polynomial matrix is [3 6] [35].

Feedback Connection Polynomials:-In feedback encoder, then a vector of feedback connection polynomials is needed. The length of this vector is the number of inputs in the encoder diagram. The elements of this vector indicate the feedback connection for each input, using an octal format. First build a binary number representation as in step 1 above. Then convert the binary representation into an octal representation as in step 2 above. If the encoder has a feedback configuration and is also systematic, then the code generator and feedback connection parameters corresponding to the systematic bits must have the same values [35].

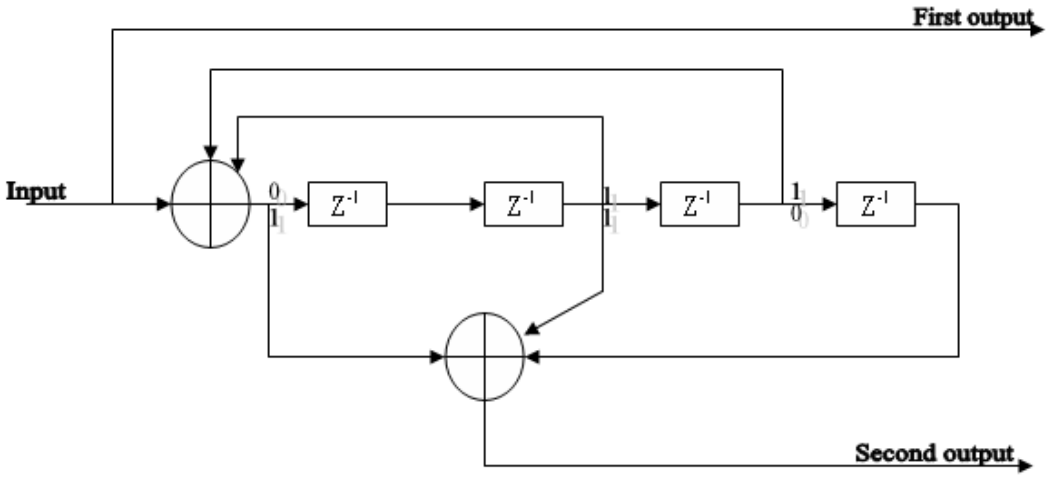

Figure 4.7: *Order-5 convolutional encoder[35]*

In the figure 4.7, this encoder has a constraint length of 5, a generator polynomial matrix of [22 21], and a feedback connection polynomial of 22.The first generator polynomial matches the feedback connection polynomial because the first output corresponds to the

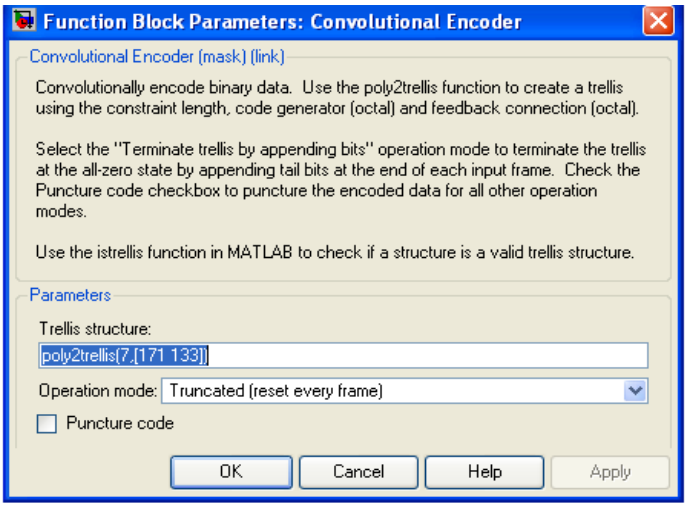

***Figure 4.8**: Function block parameters of convolutional encoder*

systematic bits. The feedback polynomial is represented by the binary vector [1 0 1 1 0], corresponding to the upper row of binary digits in the diagram. These digits indicate connections from the outputs of the registers to the adder. Note that the initial 1 corresponds to the input bit. The octal representation of the binary number 10110 is 22. The second generator polynomial is represented by the binary vector [1 0 1 0 1], corresponding to the lower row of binary digits in the diagram. The octal number corresponding to the binary number 10101 is 21 [37].

Output:- The convolutional encoder is of order 7 and has two feedback paths having feedback connection polynomials 171 and 133, so it has output having rate double that of the input rate. As the input data rate is 192 bits per frame, so output rate of convolutional encoder is 384(192 X 2) bits per frame. The total data rate is 19200 bps(9600 X 2).

4.3.4 Repeat Block

The Repeat block upsamples each channel of the M_i-by-N input to a rate L times higher than the input sample rate by repeating each consecutive input sample L times.

Output:- As the repetition count is 1 so the output is same as that of the input maintaining its input frame rate i.e. number of frame of output should be same as that of input which is 50 in count.

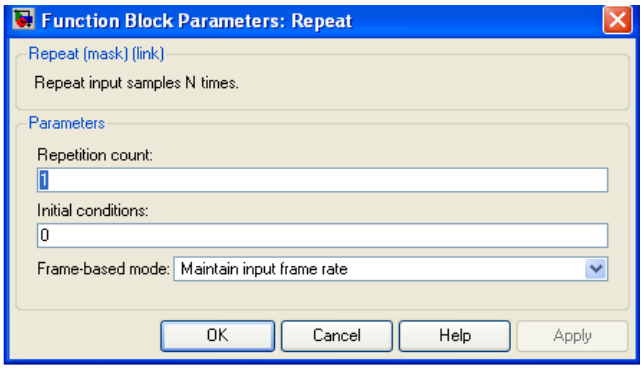

***Figure 4.9**: Function block parameters of repeat*

4.3.5 Puncture

The Puncture block creates an output vector by removing selected elements of the input vector and preserving others. The input can be a real or complex vector of length K. The block determines which elements to remove or preserve by using the binary Puncture vector parameter:

- If Puncture vector(k) = 0, then the kth element of the input vector does not become part of the output vector.
- If Puncture vector(k) = 1, then the kth element of the input vector is preserved in the output vector.

Here, k is between 1 and K. The preserved elements appear in the output vector in the same order in which they appear in the input vector.

If the Puncture vector parameter is the six-element vector [1; 0; 1; 1; 1; 0], then the block:

- Removes the second and sixth elements from the group of six input elements.
- Sends the first, third, fourth, and fifth elements to the output vector [35].

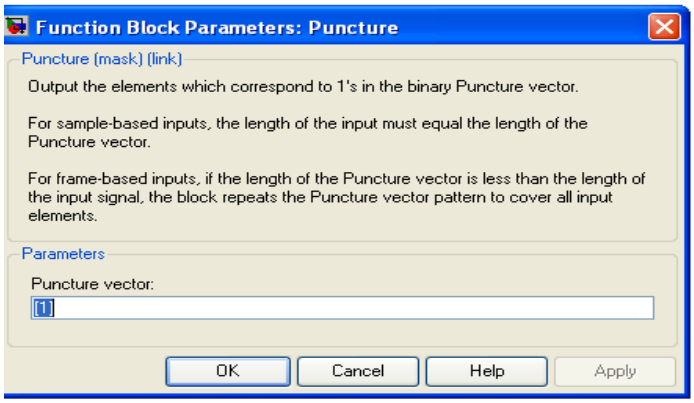

***Figure 4.10:** Function Block Parameters of puncture*

Output:-As puncture vector is set to 1 so no removal of bits is done, so output is same as that of the input.

4.3.6 Interleaver

The General Block Interleaver block rearranges the elements of its input vector without repeating or omitting any elements. The interleaving is intended to improve reliability of coded transmitted signals, rearranging the bit transmission order. In case of burst errors during transmission, this avoids error that damage many consecutive bits, which could affect detection and de-coding capabilities. The advantage of this process is spreading of burst error, which can be caused by fading, for example. With interleaving, errors are spread throughout several blocks and also within a single block, providing more efficiency in error detection and correction [36].

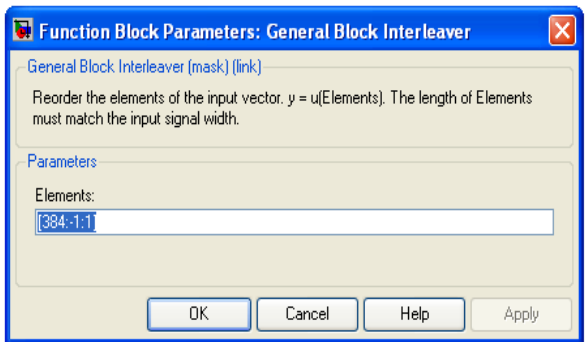

Figure 4.11: *Function block parameters of general block interleaver*

Output:-The element set in function block reverse the order of occurrence of the bits in the frame. So, the final output data rate of the encoder is 384 bits per frame or 19200 bps.

4.4 POWER CONTROL SUBCHANNEL

This block generates the power control bits. The power control sub-channel is transmitted every 1.25 ms in the forward traffic channel (800 bps). This sub-channel carries commands for the sensor node to increase or decrease transmission power on the reverse channel. One bit'0' transmitted by PCSCh indicates that the sensor node underwater needs to increase its transmission power, whereas a bit'1' indicates that the underwater sensor node needs to reduce the power. During the 1.25 ms period between the PCSChs transmission, the surface station or surface sinks estimates the level received in the

reverse traffic channel. The surface stations use this information to determine the power control bit,'0' or '1' , to be transmitted in the PCSCh assigned to each underwater sensor node. This process consists of closed loop power control scheme [40].

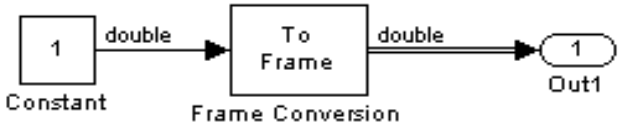

Figure 4.12: *Design of power control subchannel*

It consists of a power control bit generation source which generates bits at a rate 800 bps as shown in source block parameters in figure 4.13. The ouput is converted into frame by passing it through frame conversion block as shown in figure 4.12.

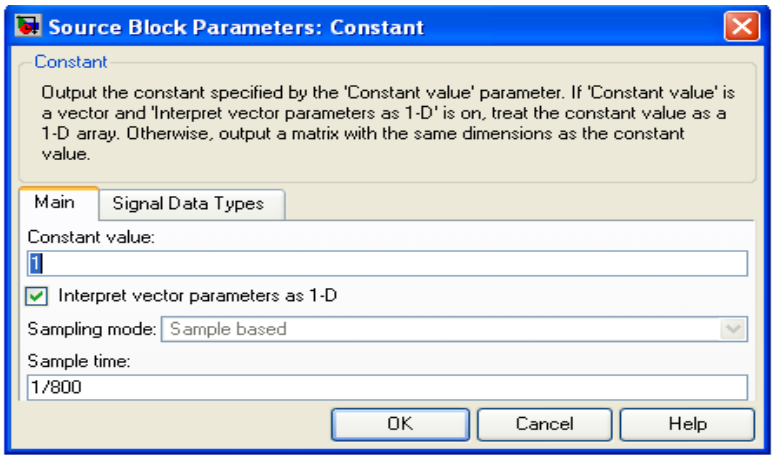

Figure 4.13: *Source block parameters for constant data source for power control subchannel.*

Output:- This block generate power control bits in form of a frame at 800 bps rate[37].

4.5 TRANSMITTER SECTION

Transmission section has two input

- First input is the output of the encoder having data rate 384 bits per frame(19200 bps)
- Second input is power control subchannel having data rate 800 bps

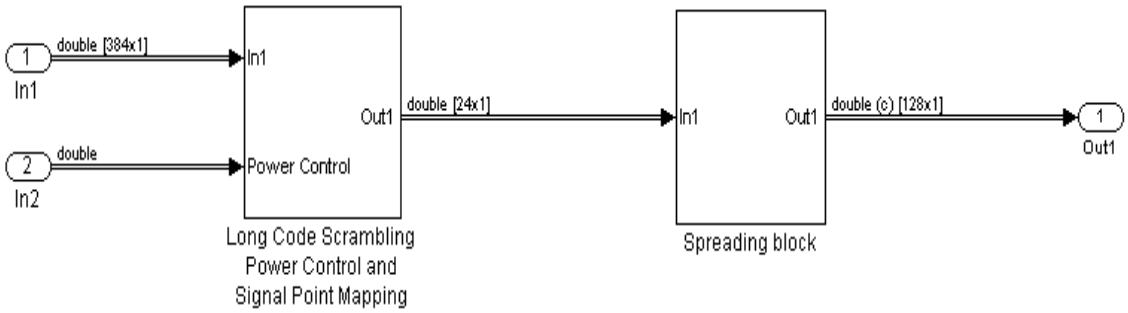

Figure 4.14: *design of transmitter section*

4.5.1 Long Code Scrambling and Power Control Mapping

In this section, long code scrambling is done. Along with this power bits are inserted in transmitted data. Figure 4.15 shows the design of this section.

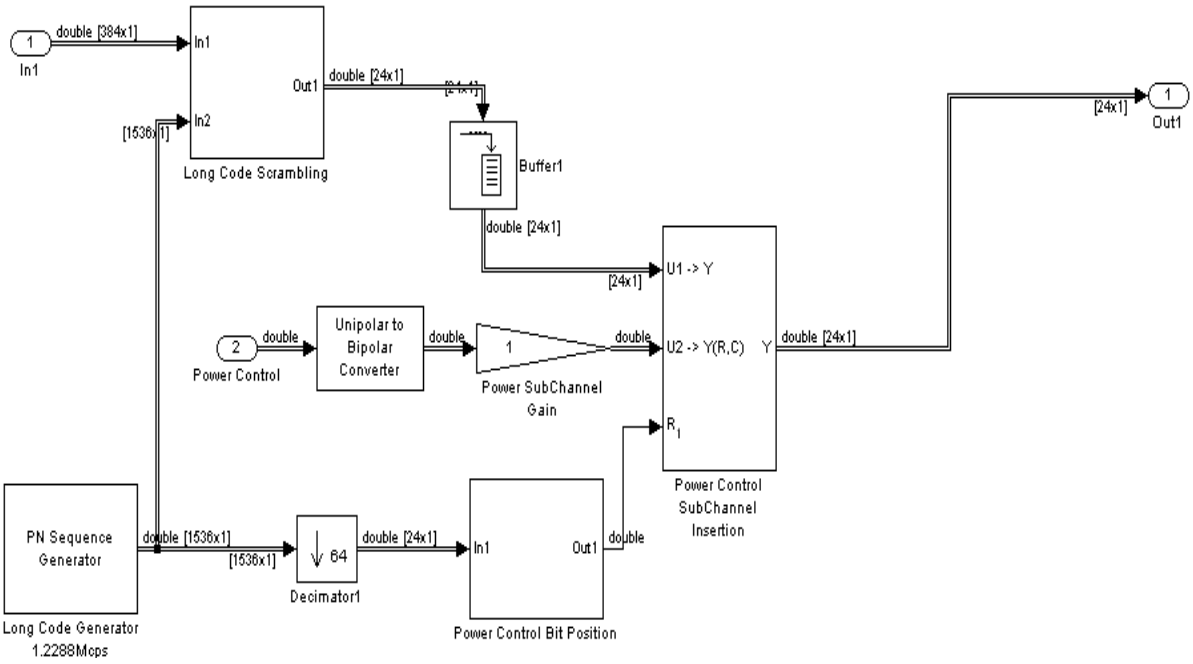

Figure 4.15: *Design of Long code scrambling and power control mapping*

4.5.1.1 Long code sequence generator

The PN Sequence Generator block generates a sequence of pseudorandom binary numbers. A pseudonoise sequence can be used in a pseudorandom scrambler and descrambler. It can also be used in a direct-sequence spread-spectrum system.

The PN Sequence Generator block uses a shift register to generate sequences, as shown in figure 4.16.

All r registers in the generator update their values at each time step according to the value of the incoming arrow to the shift register. The adders perform addition modulo 2. The shift register is described by the Generator Polynomial parameter, which is a primitive binary polynomial in z, $g_r z^r + g_{r-1} z^{r-1} + g_{r-2} z^{r-2} + ... + g_0$. The coefficient g_k is 1 if there is a connection from the kth register, as labeled in the preceding diagram, to the adder. The leading term g_r and the constant term g_0 of the Generator Polynomial parameter must be 1 because the polynomial must be primitive.

Generator polynomial parameter can be specified using either of these formats:

- A vector that lists the coefficients of the polynomial in descending order of powers. The first and last entries must be 1. Note that the length of this vector is one more than the degree of the generator polynomial.
- A vector containing the exponents of z for the nonzero terms of the polynomial in descending order of powers. The last entry must be 0 [38].

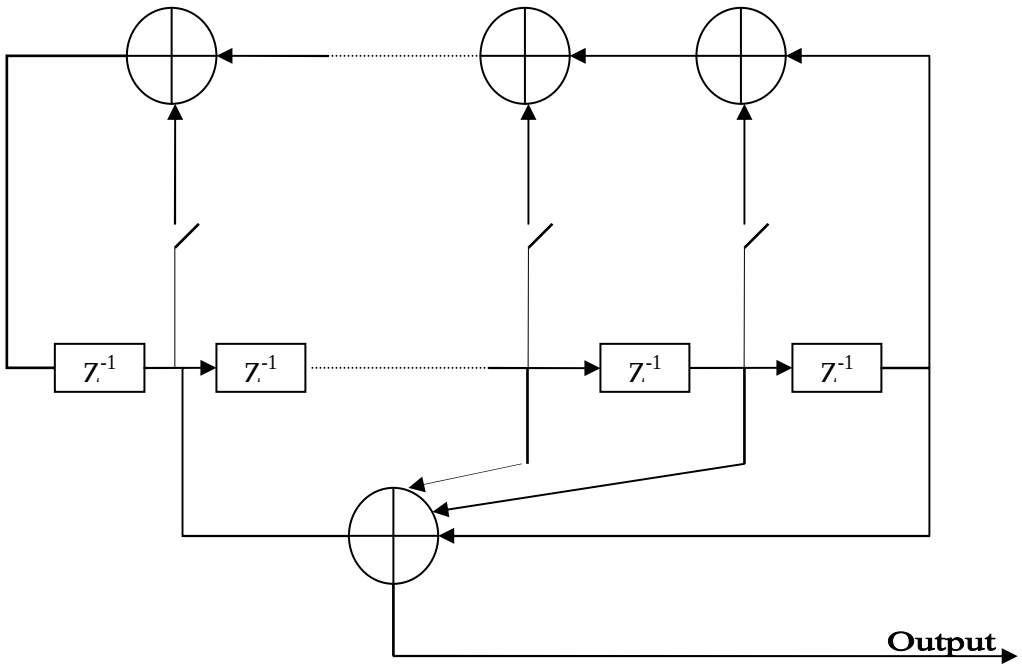

Figure 4.16: *Long code generator[38]*

For example, [1 0 0 0 0 0 1 0 1] and [8 2 0] represent the same polynomial, $p(z) = z^8 + z^2 + 1$.The Initial states parameter is a vector specifying the initial values of the registers.

The Initial states parameter must satisfy these criteria:

- All elements of the Initial state vector must be binary numbers.
- The length of the Initial state vector must equal the degree of the generator polynomial.

For example, the following table indicates two sets of parameter values that correspond to a generator polynomial of $p(z) = z^8 + z^2 + 1$ [40].

***Table 4.1**: Possible format for parameters[40]*

Quantity	Example 1	Example 2
Generator polynomial	`g1 = [1 0 0 0 0 0 1 0 1]`	`g2 = [8 2 0]`
Degree of generator polynomial	8, which is `length(g1)-1`	8
Initial states	`[1 0 0 0 0 0 0 10]`	`[1 0 0 0 0 0 0 10]`

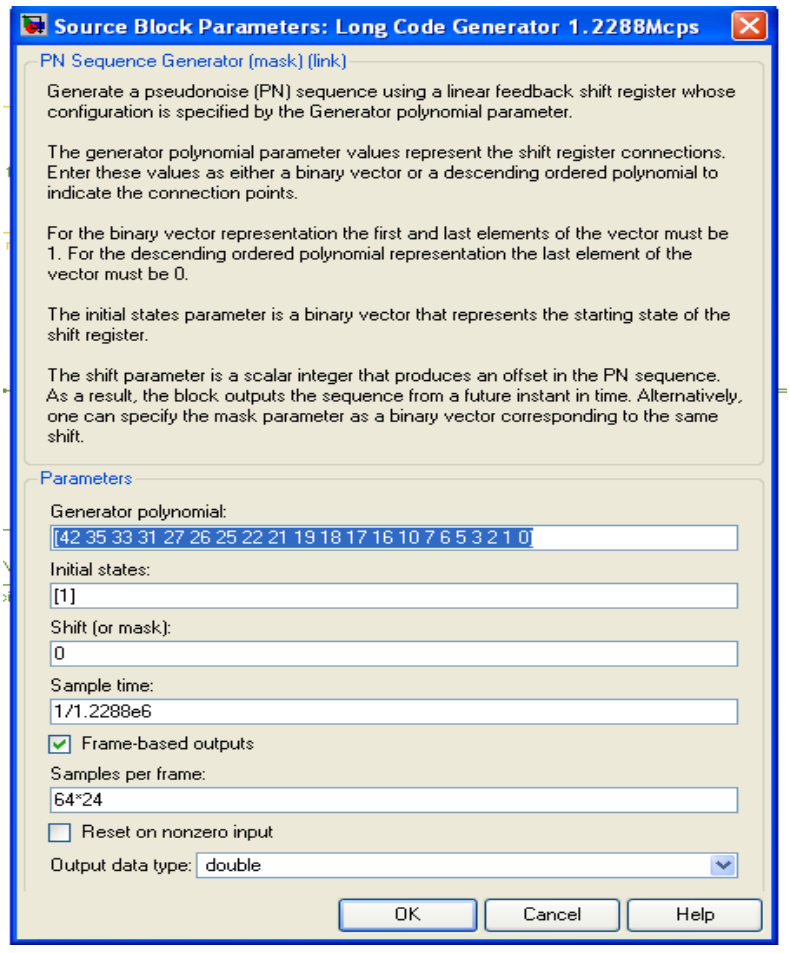

***Figure 1.17:** Source block parameters for long code generator*

The Shift parameter shifts the starting point of the output sequence. With the default setting for this parameter, the only connection is along the arrow labeled m_0, which corresponds to a shift of 0.

The parameter can be specified in either of two ways:

- An integer representing the length of the shift
- A binary vector, called the mask vector, whose length is equal to the degree of the generator polynomial [39].

Output:- As shown in Source block parameters, a 42-stage Long code generator is used and it generates a Pseudo noise sequence at a rate of 1.228800 Mbps. The output data is in form of frame with 64 X 24 samples per frame and 0 shifts.

4.5.1.2 Long code scrambling

Long code scrambling consists of modulo-2 addition(exclusive 'OR' circuit) of the input data and a binary value determined by the long code generator after decimation(one decimated LC chip out of every 64 chips).The scrambling process provide encryption and security of data. This is because by masking the PN sequence by different values, different codes can be generated, which can be used to identify a specific underwater sensor node as each underwater sensor node has its own code with a specified mask.

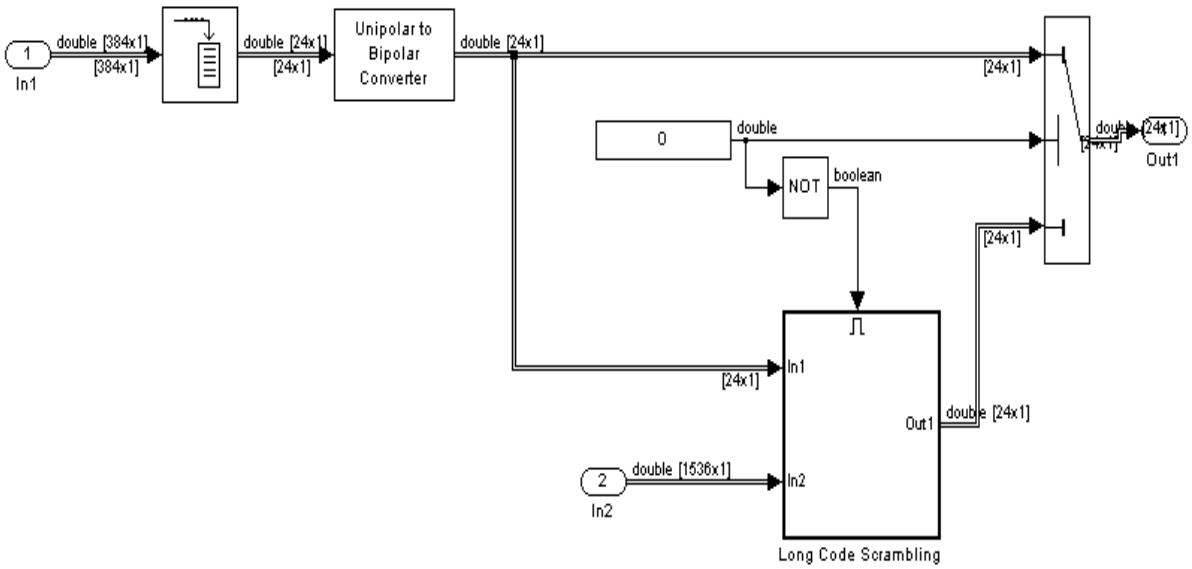

Figure 4.18: *Design of long code scrambling*

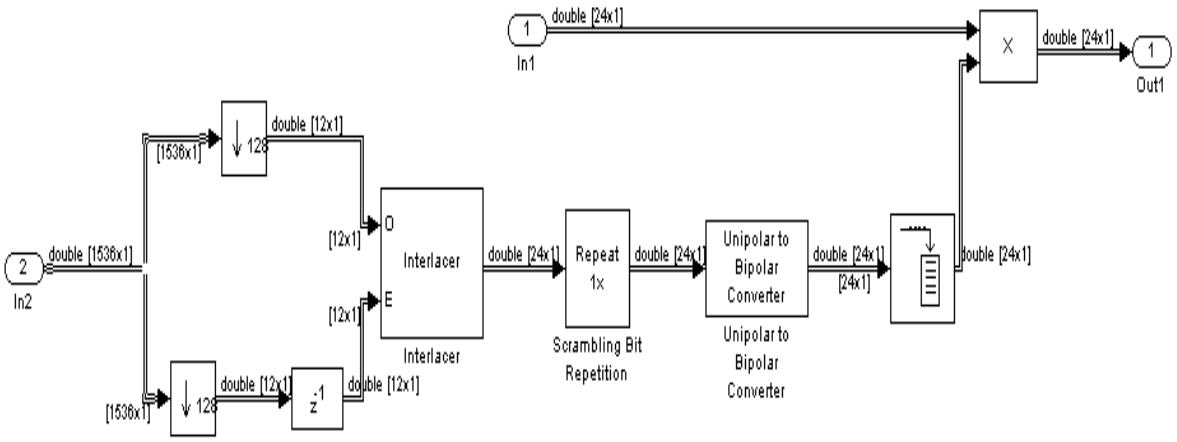

Figure 4.19: *Design of Long code scrambling1*

4.5.1.2.1 Operation of long code scrambling1

In Long code scrambling1 , first PN sequence is decimated by 128 bits resulting in output of rate 9600bps(12 bits per frame). This output is applied over two paths and interlaced with one path having one chip delay. The Interlacer block accepts two inputs that have the same vector size, complexity, and sample time. It produces one output vector by alternating elements from the first input (labeled O for odd) and from the second input (labeled E for even). As a result, the output vector size is twice that of either input. The output vector has the same complexity and sample time of the inputs. This results in an output of rate 19200bps (24 bits per frame). Each frame is of duration 1.25ms (24/19200).

The output of interlacer is passed through a unipolar to bipolar conversion block with negative polarity as shown in figure 4.20. In negative polarity, '0' bit is converted to 1

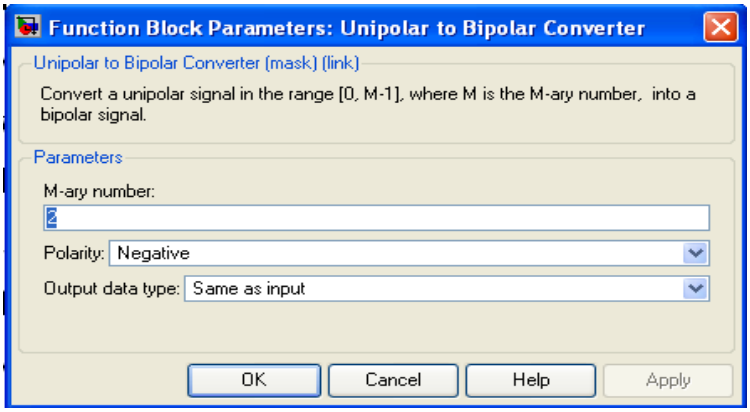

Figure 4.20: *Function block parameters of unipolar and bipolar converter*

and ‘1’ bit is converted to -1. This is done to carry out the modulo-2 addition of the data. Finally the data is passed through a buffer which generate a frame of size 24 bits. This data constitute the PN code sequence which is used to scramble the data input.

4.5.1.2.2 Operation performed by long code scrambling block

In this block, data input is framed into 24 bit frame and then unipolar to bipolar conversion is done to carry out modulo-2 addition of data with PN sequence in Long code scrambling1 block. After this the input data or the scrambled data is being mapped to the output by using a switch. If enable input of switch is 1, then input data without any scrambling is transferred to output; otherwise output is scrambled data[42].

Output:- Output data can be scrambled data or data without scrambling, depending upon enable signal , having a data rate of 24 bits per frame i.e. a frame of 1.25ms duration. Total data rate is 19200bps.

4.5.1.3 Power control bit position

The insertion position of the power control bits within its power control group(PCG)of 1.25ms is not fixed and needs to be defined in a frame-by-frame basis in a process called power control bit randomization. In this section, PN sequence is used to determine the position where power bit is inserted in 24 bit frame.

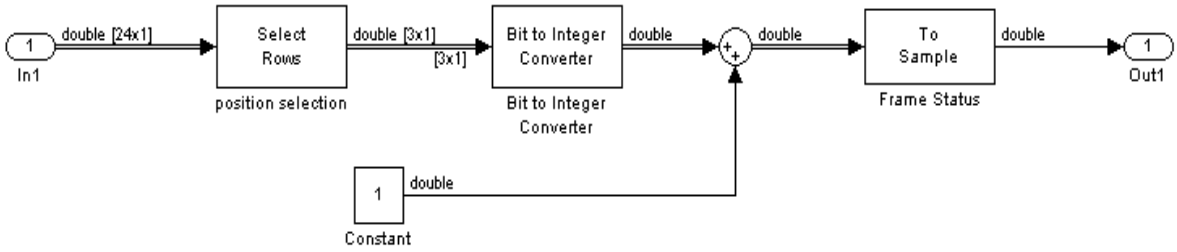

Figure 4.21*: Design of power control bit position block*

Operation: - After decimating the Long code sequence by 64, the system generates a sequence with Pseudo-random behavior at a rate of 19.2 kbps. At every 1.25 ms, this sequence provides 24 chips used for describing the position of the power bit. The last 3 chips of the decimated PN sequence, corresponding to the PCG immediately before the one being processed, determine the position of the power control bit[35].

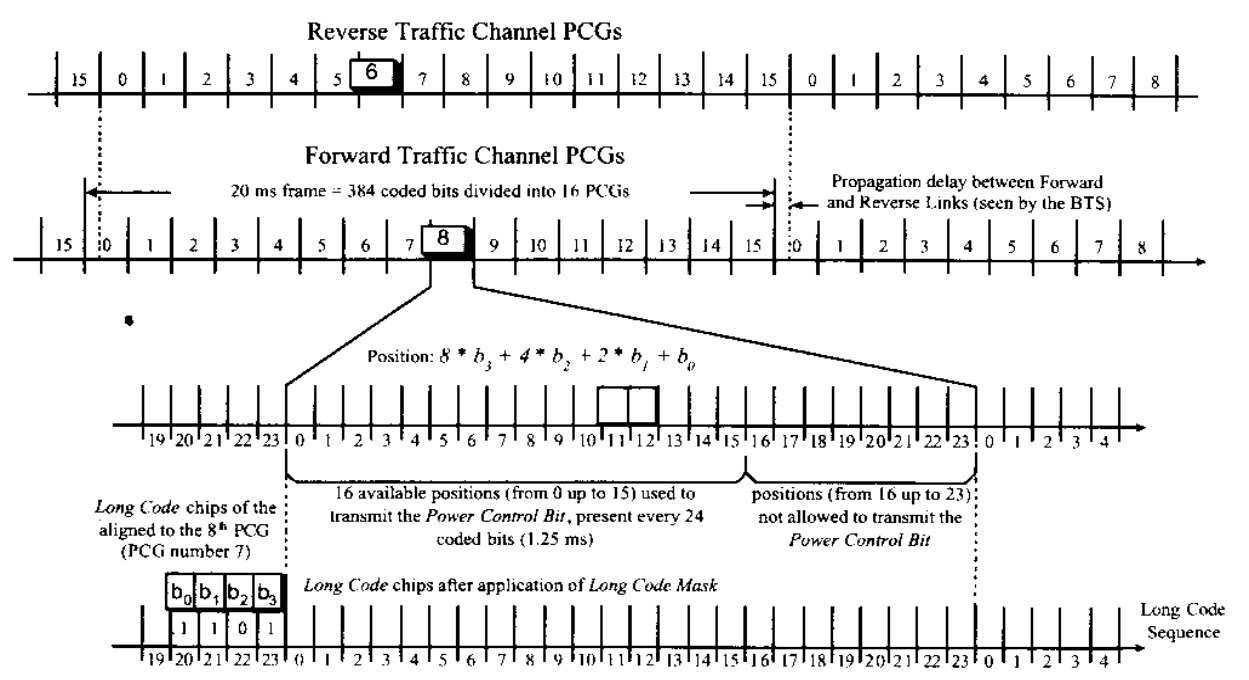

Figure 4.22: *Power estimation and power control bit randomization process[34]*

In Figure 4.22, the scrambling bits b_{23}, b_{22},b_{21},b_{20} are '1011' or 11 in decimal notation. In this case, the power control bit is inserted in position 11, replacing data symbols 11 and 12 in power control group 8 [34].

After selecting rows, binary data is converted into decimal notation by using binary to integer converter. After this 1 is added to the integer so as to start the power bit position from 1 instead of 0. Then it is passed through the frame converter block set to sample format.

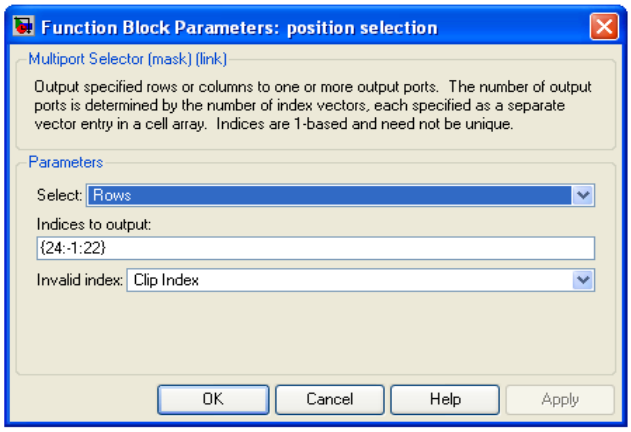

Figure 4.23*: Function block parameters for position selection*

Output:- This block generate the position where the power control bit is placed in the frame of 1.25 ms. The rate of generation of power bit position is 800 bps.

4.5.1.4 Power control subchannel insertion

It is basically an assigning block operating in matrix mode. In this, output is assigned the Value of U2 when row and column at the enable input line occurs; otherwise output is assigned the value of U1.

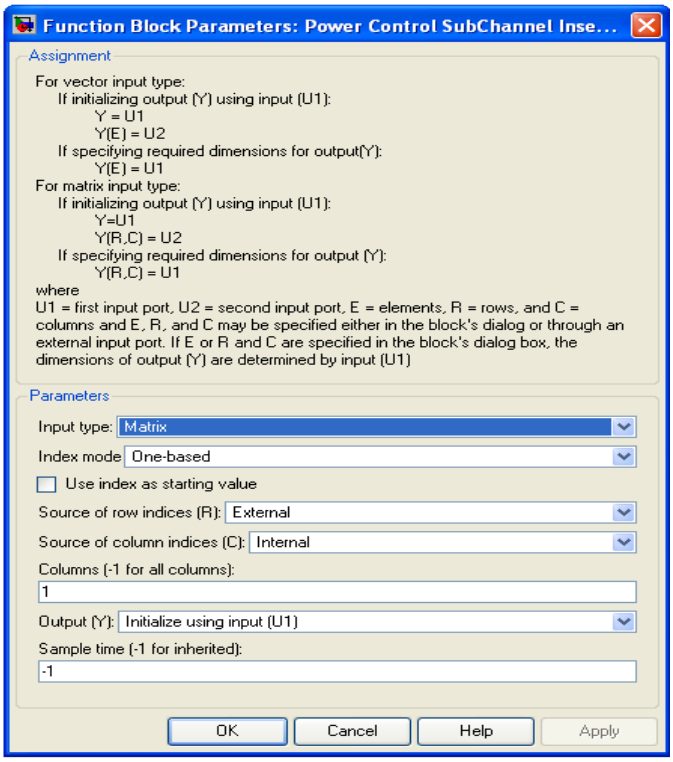

Figure 4.24: *Function block parameters of power control subchannel insertion block*

Operation:- At U1 input data at the rate 24 bits per frame of duration 1.25 ms is applied, at U2 power control subchannel is applied at the rate 1 bit during 1.25 ms duration and output of power control bit position is applied at enable input line. Column selection is made default to 1 and row is selected by power bit control bit position output. On reaching the selected row, output bit is replaced by power control subchannel else output is same as data input [41].

Output:- Output is data bits with power bit insertion having data rate 24 bits per frame of duration of 1.25 ms.

4.5.2 Spreading Block

In this block data is spread by Quasi orthogonal function using walsh code and PN sequence. Figure 4.25 shows the block diagram of Qausi orthogonal function. Figure 4.26 shows the design of spreading block.

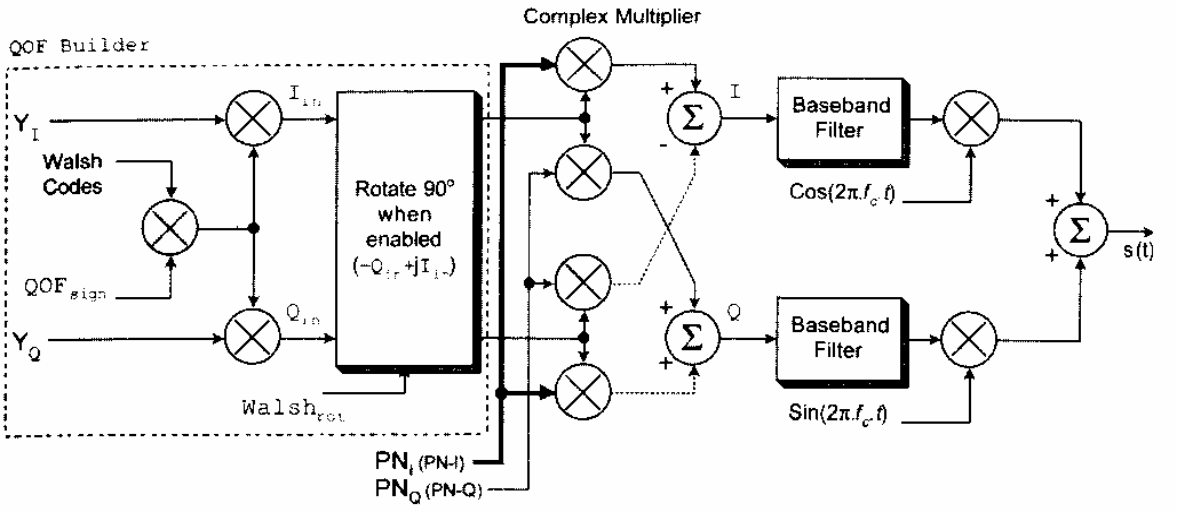

Figure 4.25 *:Quasi-orthogonal function implementation[34]*

Operation:-

I-Q mapping

Output of Long code scrambling and power control mapping block is passed through a buffer of size 2 bits. The two adjacent bits are mapped into I-Q format i.e. data is modulated orthogonally. This results in data rate half of the input data rate i.e. 9600 bps (19200/2). Each frame of 1 symbol is repeated 128 times resulting in data rate 1.228800 Mbps (9600 X 128). Then it is passed through a buffer of size 128 to generate a frame of size 128 symbols of duration 0.1042 ms (128/1228800) [36].

Walsh Code

Walsh code generator generates walsh code at a rate 1.228800 Mbps with 128 bits per frame as specified by source block parameters in Figure 4.27.

QOF mask

QOF mask is set from workspace and then passed through unipolar to bipolar conversion block and buffer of size 128 samples.

PN-I and PN-Q orthogonal mapping

PN-I and PN-Q sequence are generated using Long code generator block by setting the parameters as shown in Figure 4.28 and 4.29 respectively. PN-I and PN-Q undergoes orthogonal modulation and generate the PN sequence for Quadrature Spreading of the data [35].

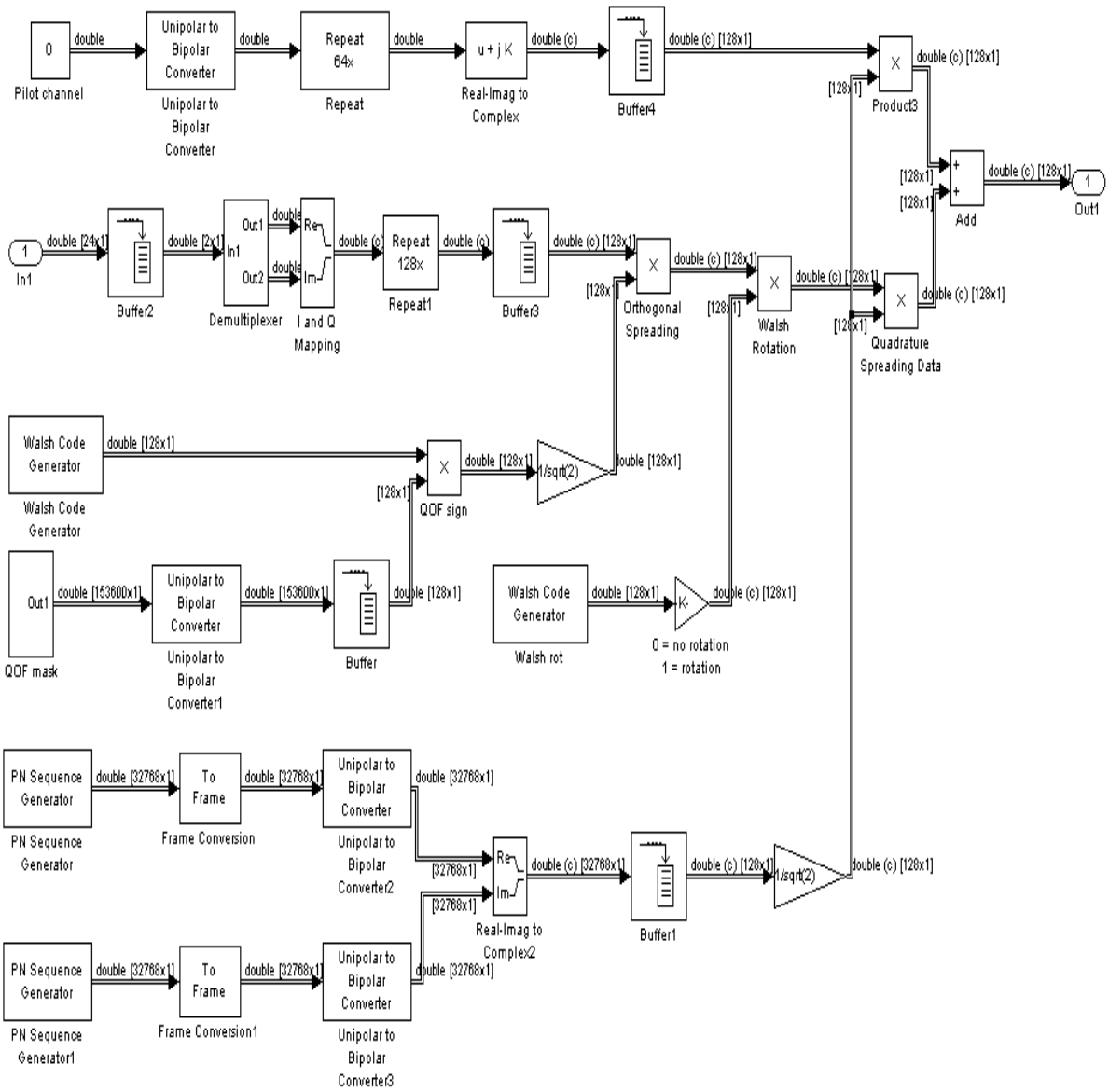

***Figure 4.26**: Design of spreading block*

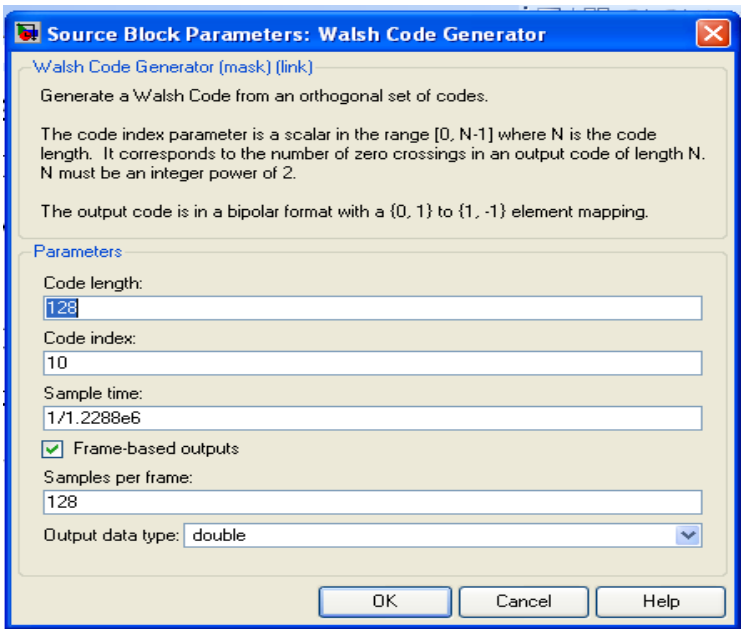

Figure 4.27: *Source block parameters for walsh code generator*

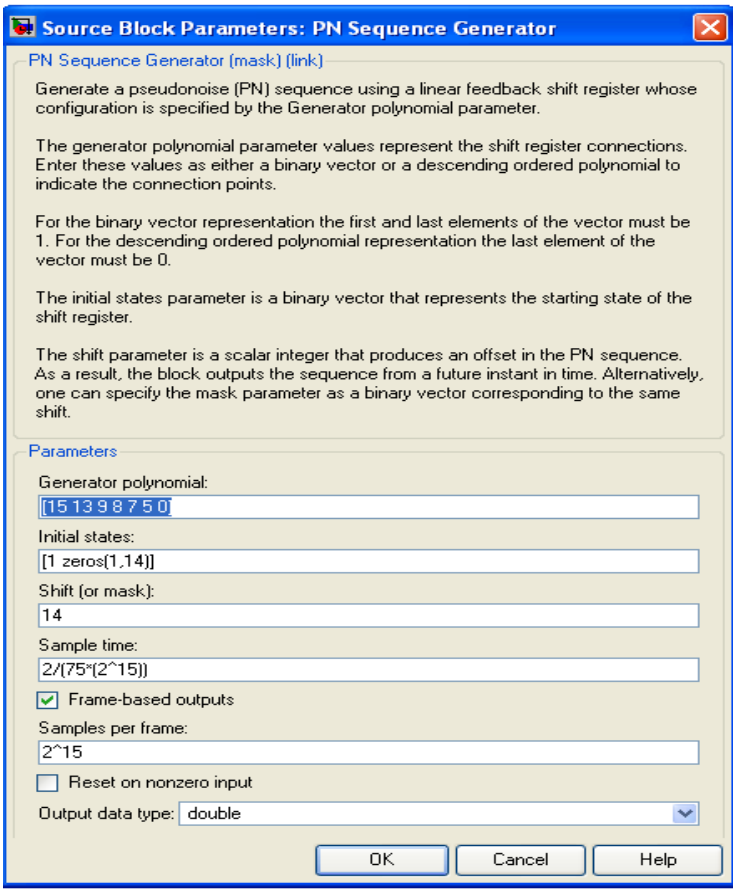

Figure 4.28*: Source block parameters for PN-I generator*

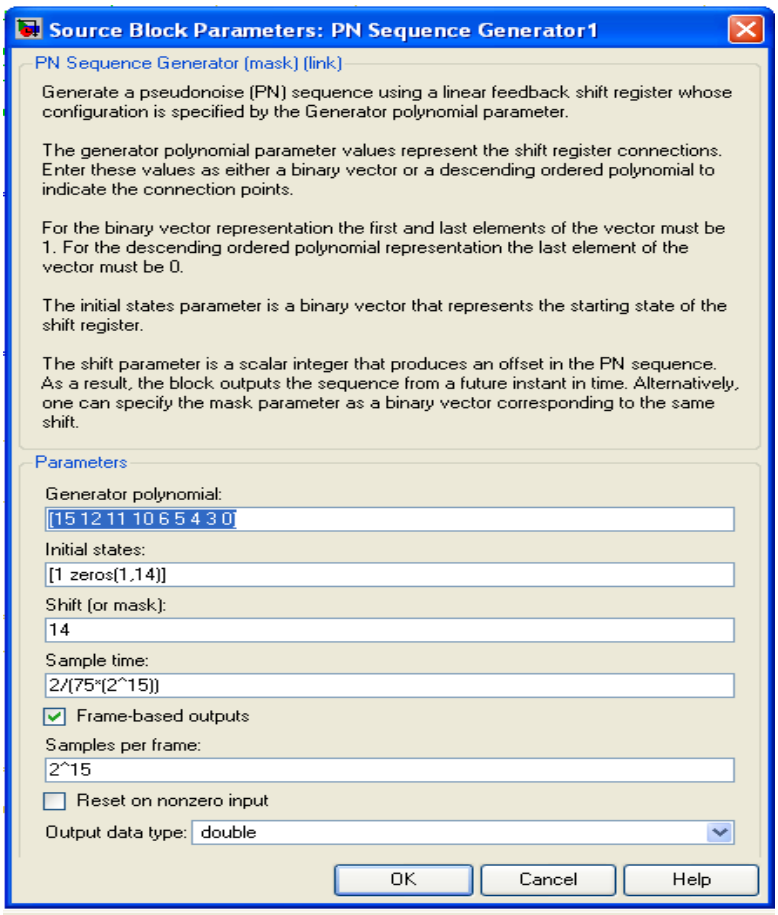

***Figure 4.29**: Source block parameters for PN-Q sequence generator*

Walsh code and QOF mask are multiplied to generate the QOF sign. Then orthogonal spreading is done by multiplying QOF sign with data input. After this Walsh rotation is done by multiplying orthogonal spread data with walsh rot code. Quadrature spreading is done by multiplying walsh rotation data with PN sequence [38].

In addition to Qausi orthogonal spreading, reference pilot channel is added to the output. Reference pilot channel is used at receiver end to estimate the delay in channel and to estimate the channel.

So, the final output of spreading block is

Out = data x PN_seq x walsh + Pilotref. x PN_seq (4.1)

***Output :* -** Spreaded output has a data rate of 1.228800 Mbps. Each frame has a size of 128 having duration of 0.1042 ms(128/1228800).

Out = data x PN_seq x walsh + Pilotref. x PN_seq (4.1)

4.6 CHANNEL MODEL

Channel is considered as slow underwater rayleigh fading channel. Source block parameters for rayleigh fading block are shown in figure 4.30

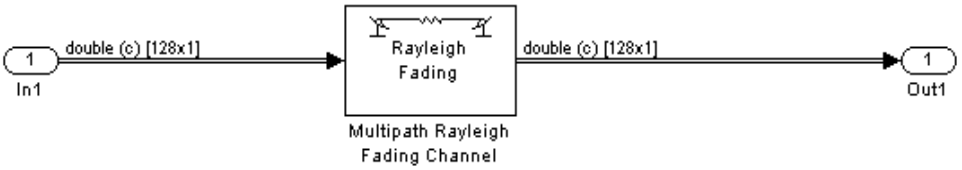

***Figure 4.30**: Design of Channel section*

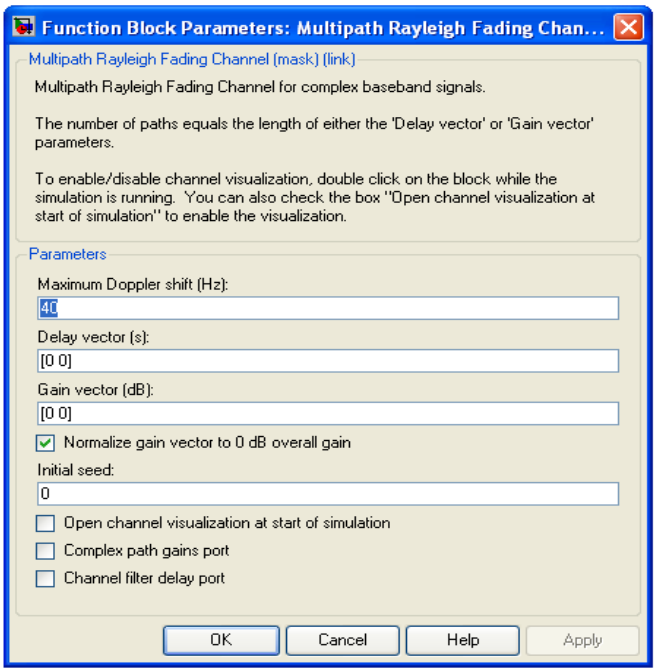

***Figure 4.31:** Source block parameters for rayleigh fading block*

4.7 RECEIVER BLOCK

A CDMA receiver separates the signals by means of a correlator that uses the particular binary sequence to despread the signal and collect the energy of the desired signal. Other users signals, whose spreading codes do not match this sequence, are not despread in bandwidth and, as a result, contribute only to the noise. These signals represent a self-interference generated by the system. The output of the correlator is sent to a narrow-bandwidth filter. The filter allows all of the desired signal's energy to pass through, but reduces the interfering signal's energy by the ratio of the bandwidth before the correlator to the bandwidth after the correlator. This reduction greatly improves the signal-to-

interference ratio of the desired signal. This ratio is also known as the processing gain. The signal-to-noise ratio is determined by the ratio of the desired signal power to the sum of all of the other signal powers. It is enhanced by the processing gain or the ratio of spread bandwidth to baseband data rate [37].

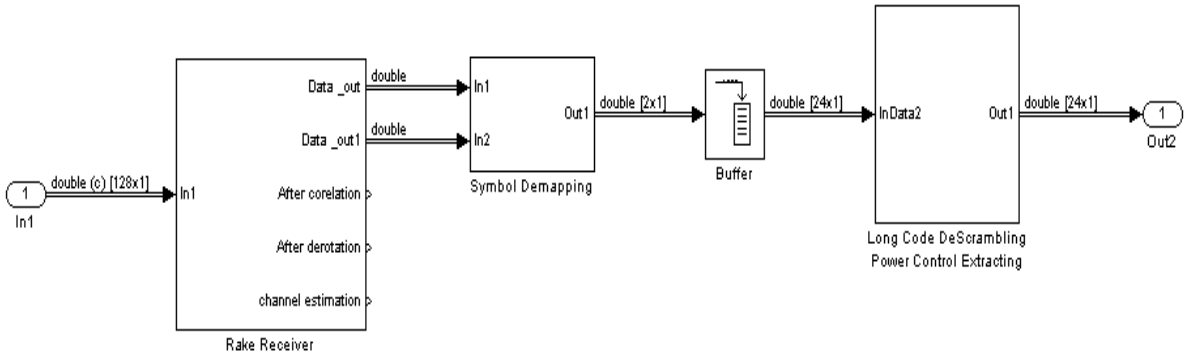

Figure 4.32: *Design of receiver section*

4.7.1 Rake Receiver

This block demolulate the data obtained at the receiver end. The block operates on data using four fingers of a rake receiver and generates the demodulated symbols for each finger. The demodulation process utilizes the channel estimate or pilot signal for each finger to demodulate the symbols for each finger.

Rake receiver is a radio receiver designed to counter the effects of multipath fading. It does this by using several "sub-receivers" each delayed slightly in order to tune in to the individual multipath components. Each component is decoded independently, but at a later stage combined in order to make the most use of the different transmission

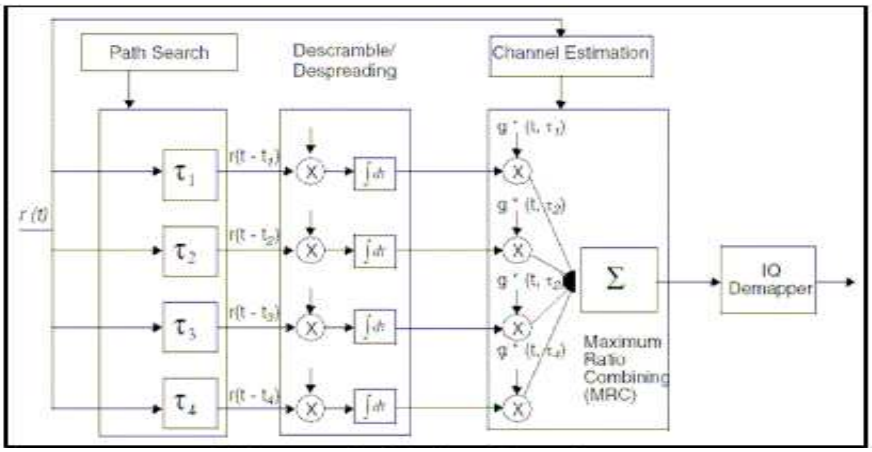

Figure 4.33: *Rake Receiver[33]*

characterstics of each transmission path. This could very well result in higher signal to noise ratio (or E_b/N_0) in a multipath environment than in a "clean" environment.

A receiver technique uses several baseband correlators to individually process several signal multipath components. The correlator out-puts are combined to achieve improved communications reliability and performance[40].

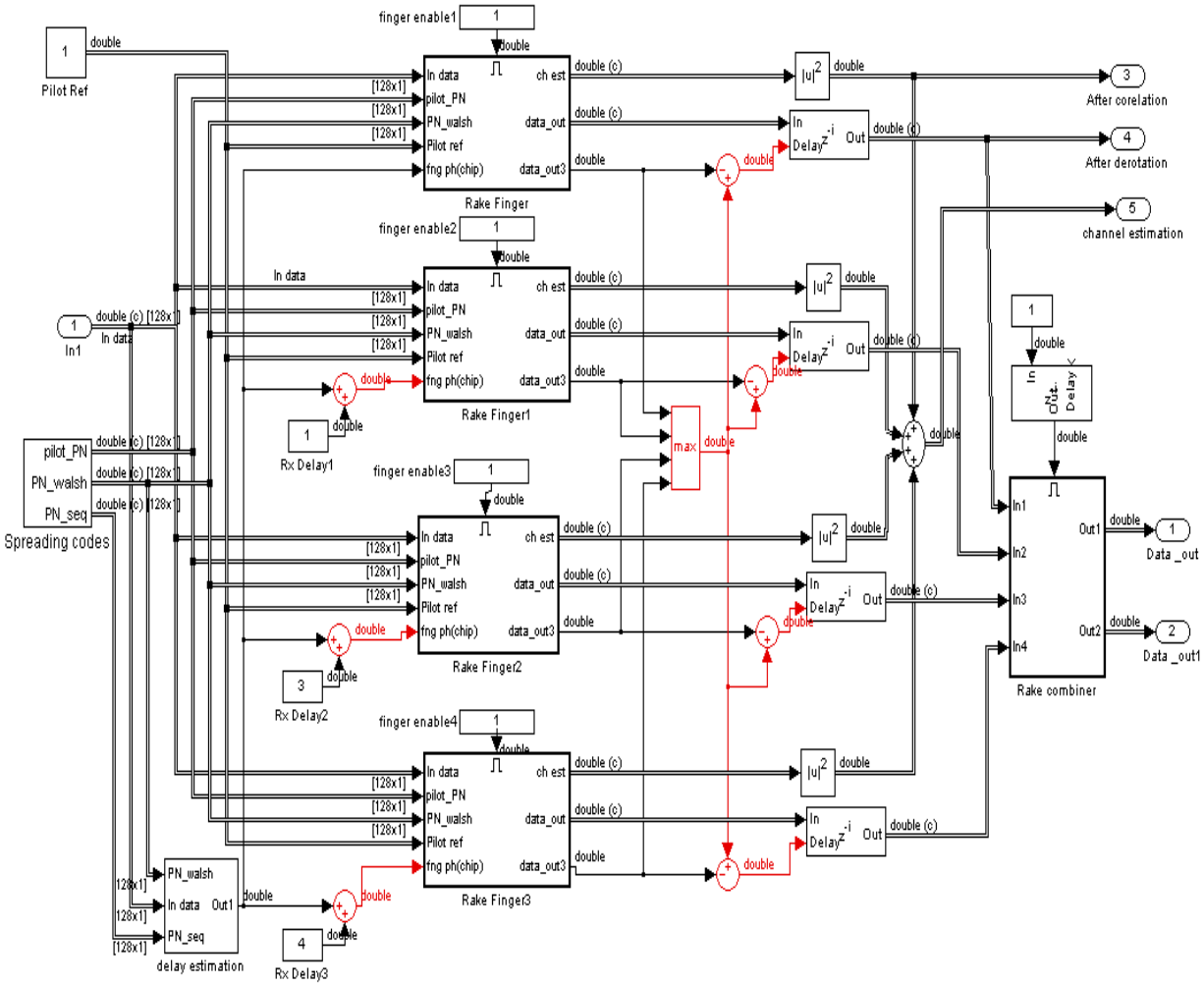

Figure 4.34: *Design of Rake Receiver*

The multipath channel through which radio wave transmits wirelessly can be viewed as the original transmitted wave plus many delayed copies of the original transmitted wave but with different magnitude and time-of-arrival at the receiver. Since each multipath component also contains the original information, so at the receiver, if the magnitude and time-of-arrival (phase) of each multipath component can be known (through a process

called channel estimation),then all the multipath components can be added coherently to bring up the information reliability.

The rake receiver is so named because of its analogous function to a garden rake, each finger collecting bit or symbol energy similarly to how tines on a rake collect leaves.

In particular, the rake receiver architecture allows an optimal combining of energy received over paths with different. It avoids wave cancellation (fades) if delayed paths arrive with phase differences and appropriately weighs signals coming in with different signal-to-noise ratios [36].

4.7.1.1 Spreading codes

Spreading codes are again generated in this block which works as reference signals for the estimation of delay in the channel and to estimate the behavior of channel.

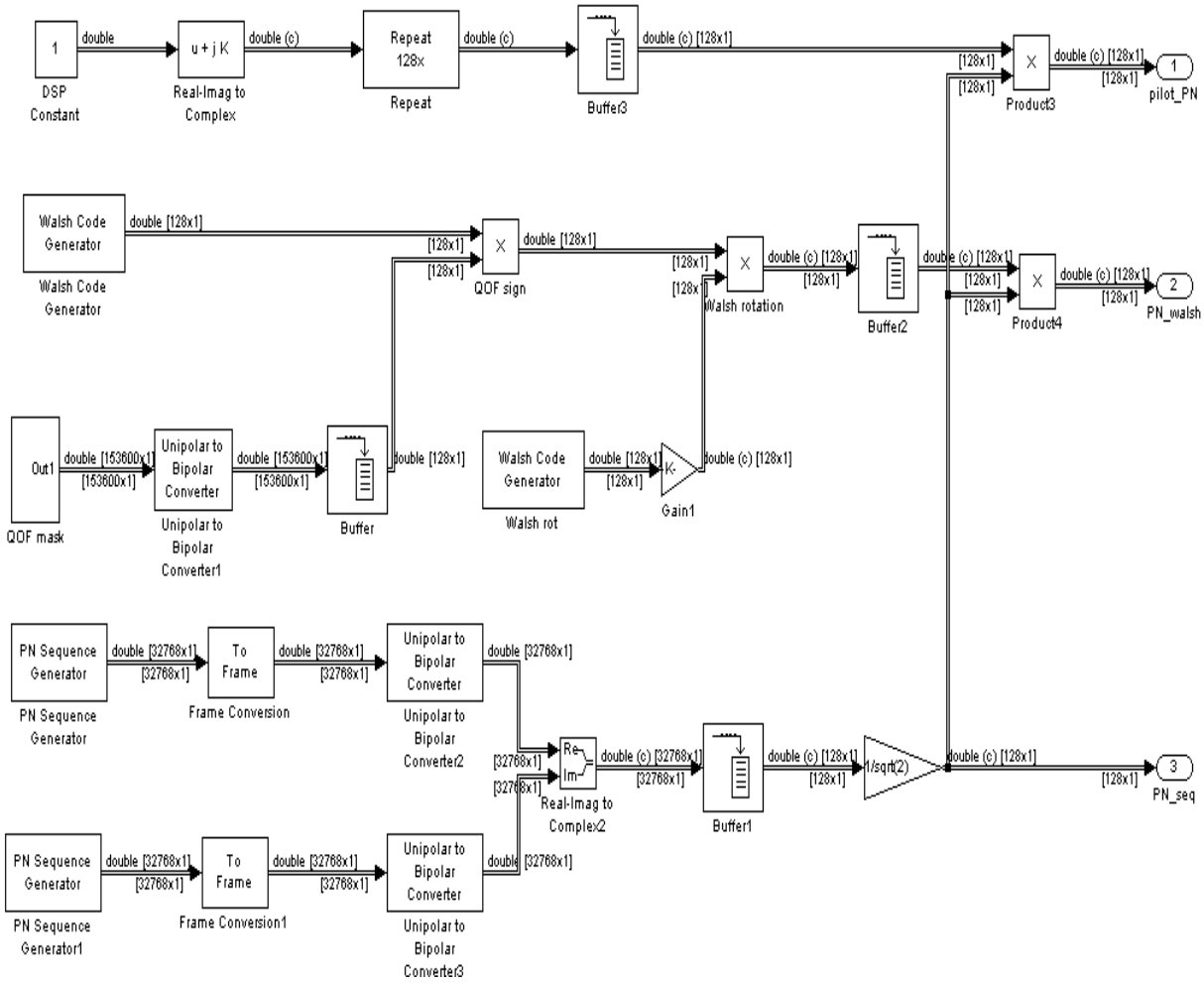

Figure 4.35: *Design of spreading code block*

In spreading codes, three coded output are generated:-

1. Pilot_PN :- It is the spreading of pilot signal by PN sequence

   Pilot_PN = Pilot x PN_seq

2. PN_walsh :- It is the code generated by using PN sequence, QOF sign and Walsh rot.

   PN_walsh = PN_seq x walsh

3. PN_seq:- It is PN sequence generated after applying orthogonal modulation over PN-I and PN-Q sequence as shown in figure 4.35.

The parameters of all the blocks for spreading code block are same as that of the parameters of spreading block in transmission section.

Output:- Three output codes, each having chip rate of 1.228800 Mbps. Each output is in form of frame of size 128 chips per frame. Each frame is of duration 0.1042 ms.

4.7.1.2 Delay estimation

In delay estimation block, delay is estimated for every frame received at the receiver side. data received at receiver side is given by

Indata(receiver) = data x PN_seq x walsh + Pilot x PN_seq (with delay) (4.2)

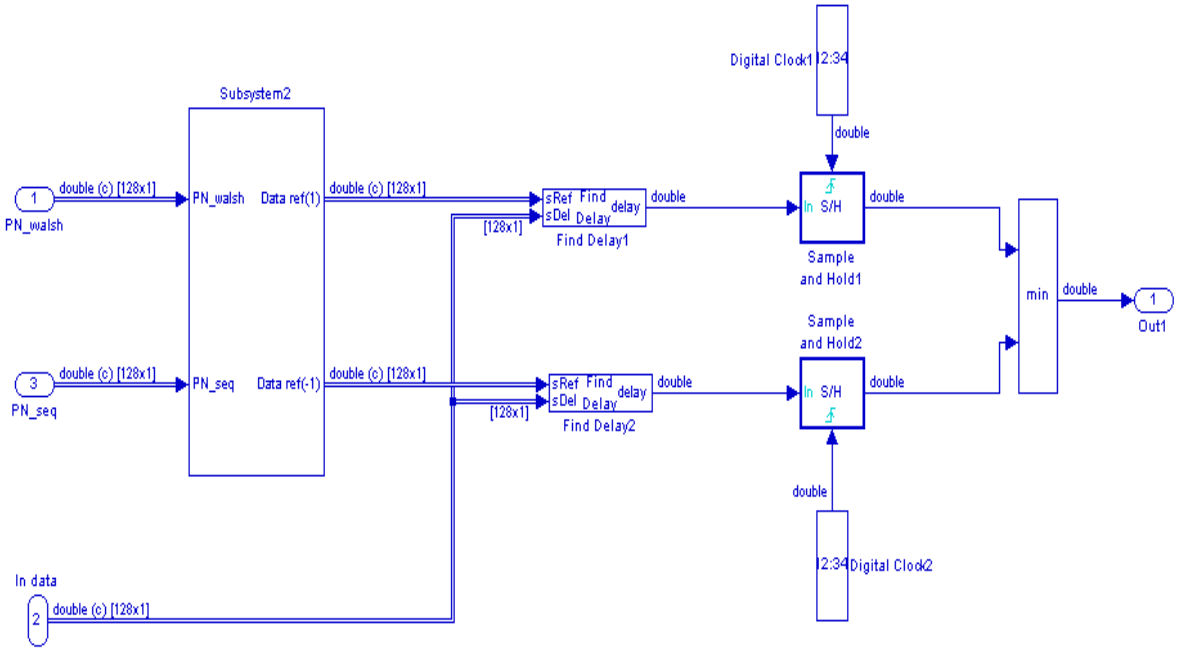

Figure 4.36: *Design of Delay estimation block*

Now for a frame of 128 chips, data value is constant (either 1 or -1) as it undergoes repetitions on transmitter side. Also pilot is constant as its value is set to 1. So, The In data comes out to be

Indata(receiver) = (1,-1) x PN_seq x walsh + PN_seq (4.3)

This means the two possible In data at receiver side for a frame are given by

Indata(1) = (1) x PN_seq x walsh + PN_seq(with delay) (4.4)

Indata(-1) =(-1) x PN_seq x walsh + PN_seq(with delay) (4.5)

Now, to estimate the delay same sequence is generated at receiver side by using PN_seq and PN_walsh outputs of spreading code block.

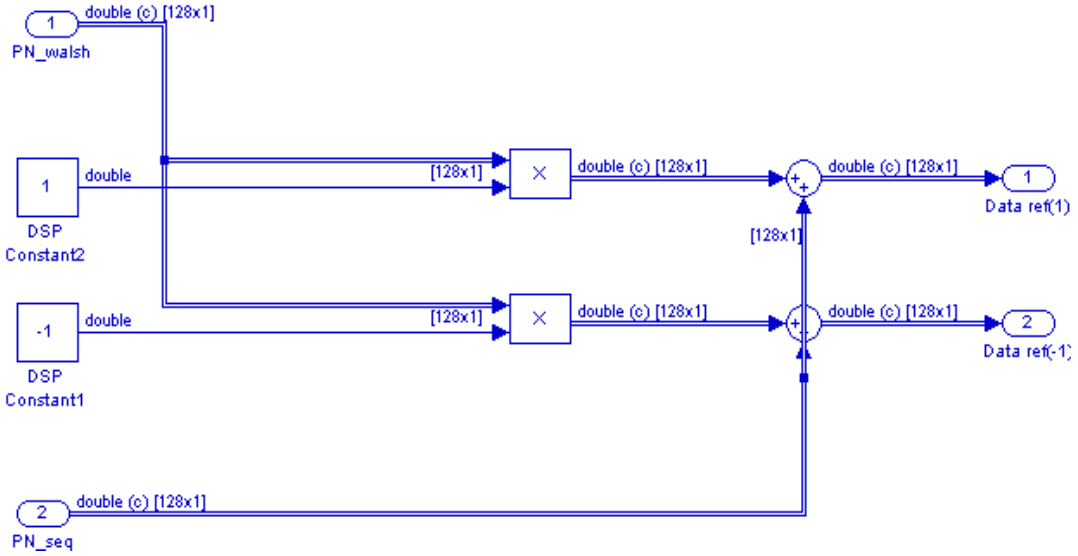

Figure 4.37: *Design of Subblock2*

Subsystem2 block perform the function of generation of reference In data without any delay as shown in figure 4.37 .

Where

Dataref(1) = (1) x PN_seq x walsh + PN_seq(without delay) (4.6)

Dataref(-1) =(-1) x PN_seq x walsh + PN_seq(without delay) (4.7)

Now, the Indata and Dataref (1,-1) are compared in find delay block. The outputs of find delay block are the delay between Indata and Dataref(1,-1). Then these outputs are sampled at a rate of 0.1042 ms (128/1228800) so that it provides one delay for each

frame. These sampled delays are passed through minimum block, which produces the smaller delay at the output.

Output:- This output gives the value of delay for each frame of the received data at a duration of .1042 ms.

4.7.1.3 Rake fingers

This block correlates the input signal over each Walsh code interval with the supplied PN and Walsh code sequences to estimate the channel and the data from the received signal. Using the known Walsh sequence for pilot symbols, this block estimates the in-phase and quadrature components of the channel. The input Walsh sequence, used to encode the data symbols, is used to estimate the in-phase and quadrature components of the received data[33].

Four rake fingers are used with different delay value so as to compensate for the delay due to any other channel distortion.

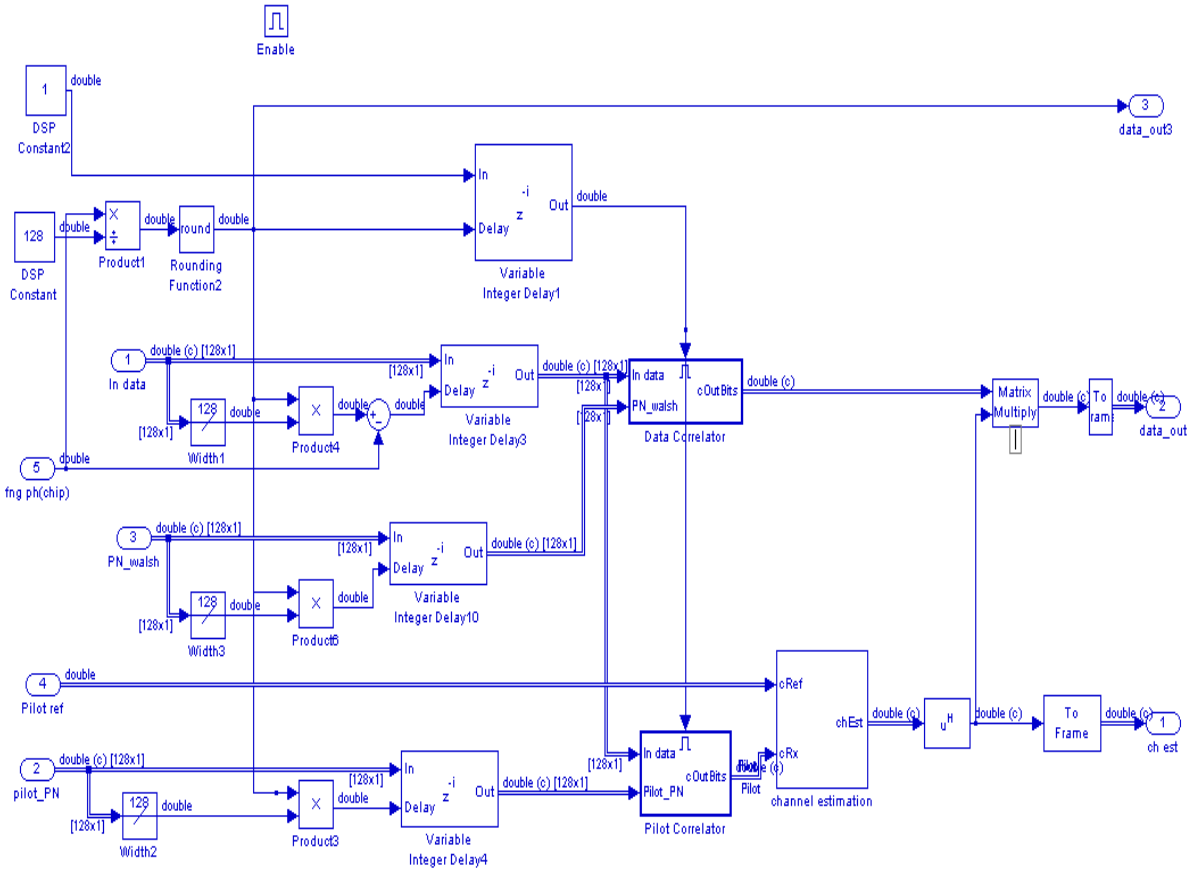

Figure 4.38: *Design of Rake Finger*

4.7.1.3.1 Delayed code

First PN_walsh code and Pilot_PN codes generated by spreading code block are delayed by the value specified by delay estimation block as shown in figure 4.38. This is done to bring the codes in synchronization with the Indata.

4.7.3.4.2 Data correlator

In this section distorted data is extracted from Indata. Distorted data has noise added to data due to rayleigh fading.

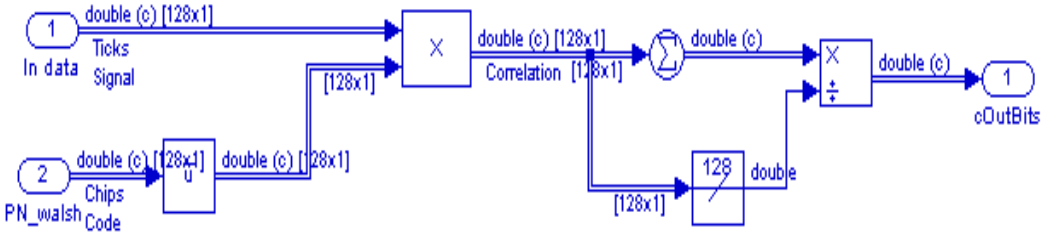

Figure 4.39: *Design of Data Correlator*

The operation performed in this block can be summed as

$$\text{Outbits} = \frac{1}{128}\sum_{n=1}^{128}[In\,data(n) \times \overline{PN\_walsh(n)}]$$

$$In\,data \times \overline{PN\_walsh} = [\text{data(distorted) x PN\_walsh + Pilot x PN\_seq}] \text{ x } \overline{PN\_walsh}$$

$$= \text{data(distorted)} + \text{cons.}$$

$$\text{So, Outbits} = \frac{1}{128}\sum_{n=1}^{128}\{[data(distorted)](n) + cons.\}$$

$$= \frac{1}{128}\sum_{n=1}^{128}\{[data(distorted)](n)\} + \text{cons.}$$

Constant=1

$$\text{So, Outbits} = \frac{1}{128}\sum_{n=1}^{128}\{[data(distorted)](n)\}$$

4.7.3.4.3 Pilot correlator

In this, Indata is correlated to Pilot_PN sequence.

The operation performed in this block can be summed as

$$\text{Outbits} = \frac{1}{128}\sum_{n=1}^{128}[In\,data(n) \times \overline{Pilot\_PN(n)}]$$

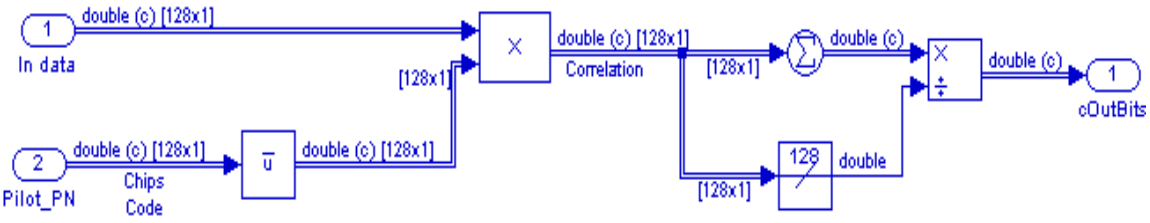

Figure 4.40: *Design of Pilot Correlator*

$$In\,data \times \overline{Pilot\_PN} = [\text{data(distorted) x PN\_walsh + Pilot x PN\_seq}] \text{ x } \overline{Pilot\_PN}$$

$$= \text{data(distorted) x } \overline{Pilot} + 1$$

$$\text{So, Outbits} = \frac{1}{128}\sum_{n=1}^{128}[\text{data(distorted) x } \overline{\text{Pilot}}](n) + 1$$

4.7.3.4.4 Channel estimation

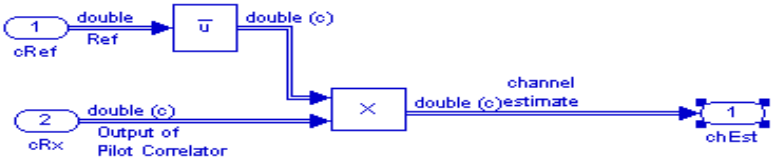

Figure 4.41: *Design of Channel estimator*

The operation performed in this block can be summed as

$$\text{Outbits} = [data(n) \times \overline{Pilot(n)}]$$

$$data \times \overline{Pilot} = \{\frac{1}{128}\sum_{n=1}^{128}[\text{data(distorted) x } \overline{\text{Pilot}}](n) + 1\} \text{ x } \overline{Pilot}$$

$$= \frac{1}{128}\sum_{n=1}^{128}[\text{ data(distorted)(n) x } \overline{Pilot}^2 + \overline{Pilot}\ ]$$

As pilot is 1, so $\overline{Pilot} = -\,j$ and $\overline{Pilot}^2 = (-\,j)\,(-\,j) = 1$

$$\text{So, } data \times \overline{Pilot} = \frac{1}{128}\sum_{n=1}^{128}[\text{data(distorted)(n)} - j]$$

As data is constant for a frame o128 chips, so the resultant signal is only distortion or rayleigh fading channel function .

$$\text{So, } data \times \overline{Pilot} = \frac{1}{128}\sum_{n=1}^{128}[\text{channel(n)} - j]$$

4.7.3.4.5 Rayleigh faded signal

The output of channel estimation block is applied to transpose function.

So, the output is given by

$$\text{Out} = -j\frac{1}{128}\sum_{n=1}^{128}[\text{channel}(n) - j] \quad = \quad -\frac{1}{128}\sum_{n=1}^{128}[\, j \text{ channel}(n)\,] - 1$$

$$= -\frac{1}{128}\sum_{n=1}^{128}[\, j \text{ channel}'(n)\,]$$

This output undergoes matrix multiplication with output of data correlator and the output is given by

$$\text{Output} = [\frac{1}{128}\sum_{n=1}^{128}\{[data(distorted)](n)\}\,] \text{ x } j\,\{\frac{1}{128}\sum_{n=1}^{128}[\, j \text{ channel}(n)\,] + 1\}$$

As data(distorted) = data x channel

$$\text{So, Output} = [\frac{1}{128}\sum_{n=1}^{128}\{data(n)\times channel(n)\}\,] \text{ x } j\,(-1)\{\frac{1}{128}\sum_{n=1}^{128}[\, j \text{ channel}'(n)\,]$$

$$\text{Output} = [\frac{1}{128}\sum_{n=1}^{128}\{data(n)\}$$

Output:- Output of rake receiver is undistorted data with 1 symbol per frame. The total data rate of the output is 9600 bps (1228800/128).

4.7.3.5 Rake combiner

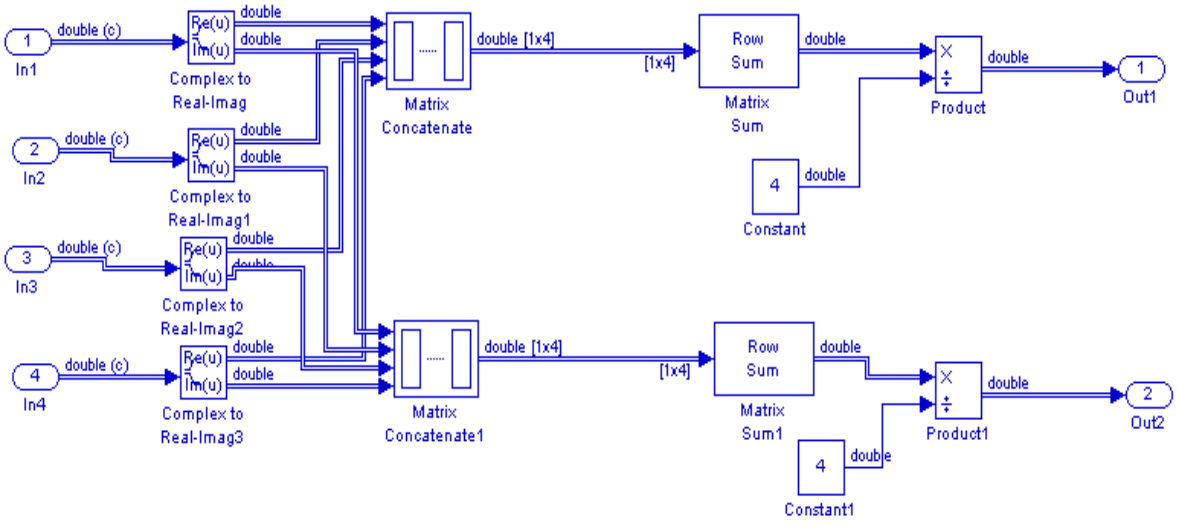

Figure 4.42: *Design of Rake Combiner*

The outputs of four rake receiver are combined in this block as shown in figure 4.42. Data is also separated into real and imaginary part and two outputs are there [36].

Output:- Output of receiver block has two output having 1 bit per frame. The output data rate is 9600 bps.

4.7.4 Symbol Demapping

In this section, orthogonal demapping is done by combining the two inputs (real and imaginary part of the symbol).

Figure 4.43: *Design of Symbol Demapping*

Output:- Output of symbol demapping block has 2 bits per frame. As interlacing is done, so the output data rate is double as that of the input i.e. 19200 bps (9600 x 2).

4.7.5 Long Code Descrambling and Power Control bit Extraction

In this section, power control bit is extracted and then descrambling of the data is carried out.

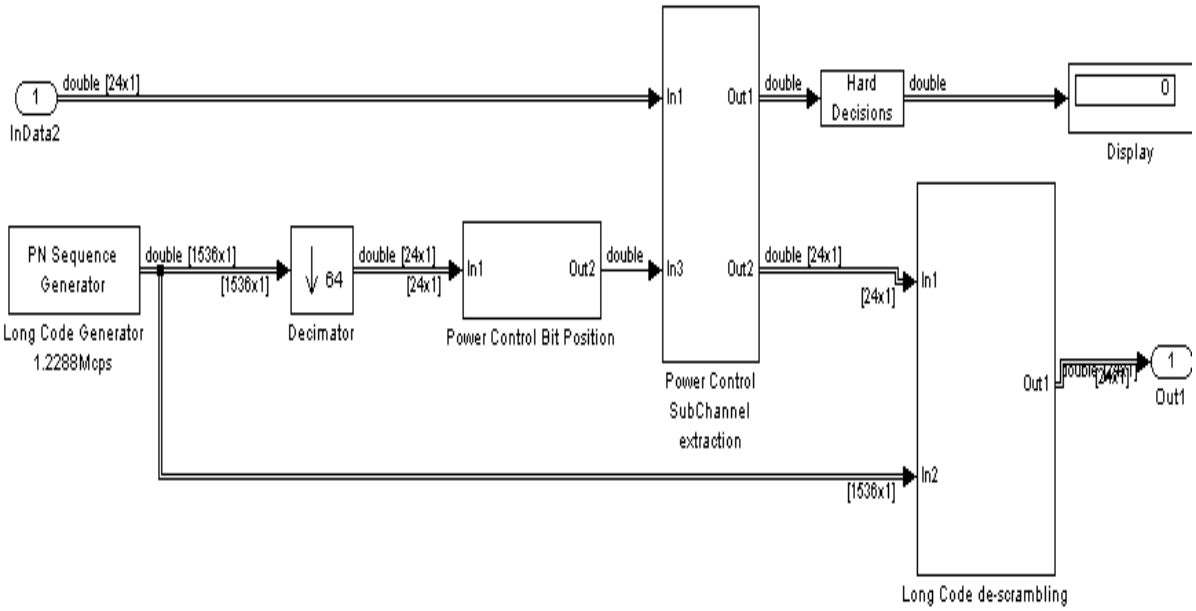

Figure 4.44: *Design of Long Code Descrambling and Power Control bit Extraction block*

4.7.3.1 PN sequence generator

Same as that on transmitter side

4.7.3.2 Power control bit position

Same as that on transmitter side

4.7.5.3 Power control subchannel extraction

It is basically an assigning block operating in matrix mode. In this, output is assigned the value of U2 when row and column at the enable input line occurs; otherwise output is assigned the value of U1 [35].

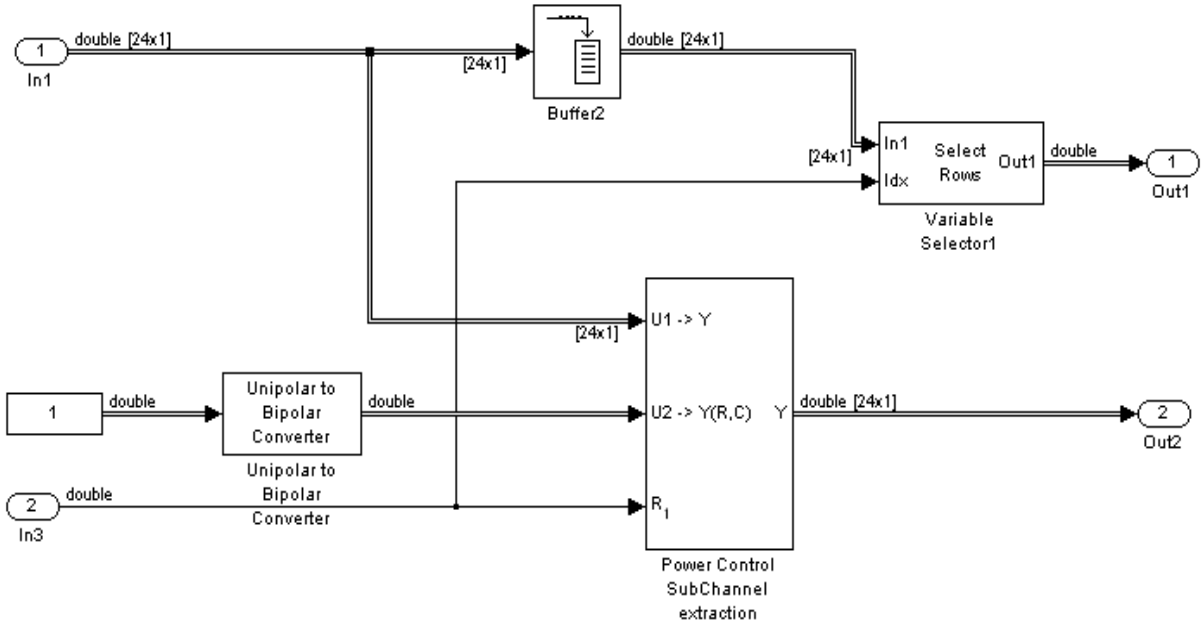

Figure 4.45: *Design of Power Control Subchannel Extraction block*

Operation:- At U1 input data at the rate 24 bits per frame of duration 1.25 ms is applied, at U2, binary data source is applied at the rate 1 bit during 1.25 ms duration and output of power control bit position is applied at enable input line. Column selection is made default to 1 and row is selected by power bit control bit position output. On reaching the selected row, power control subchannel is replaced by binary data source else output is same as data input.

One more output which display the position of power control bit in the frame.

Output:- Output is data bits with power bit extraction having data rate 24 bits per frame of duration of 1.25 ms.

4.7.5.4 Long code descrambling

Long code de-scrambling consists of modulo-2 addition (exclusive 'OR' circuit) of the input data and a binary value determined by the long code generator after decimation (one decimated LC chip out of every 64 chips) [38].

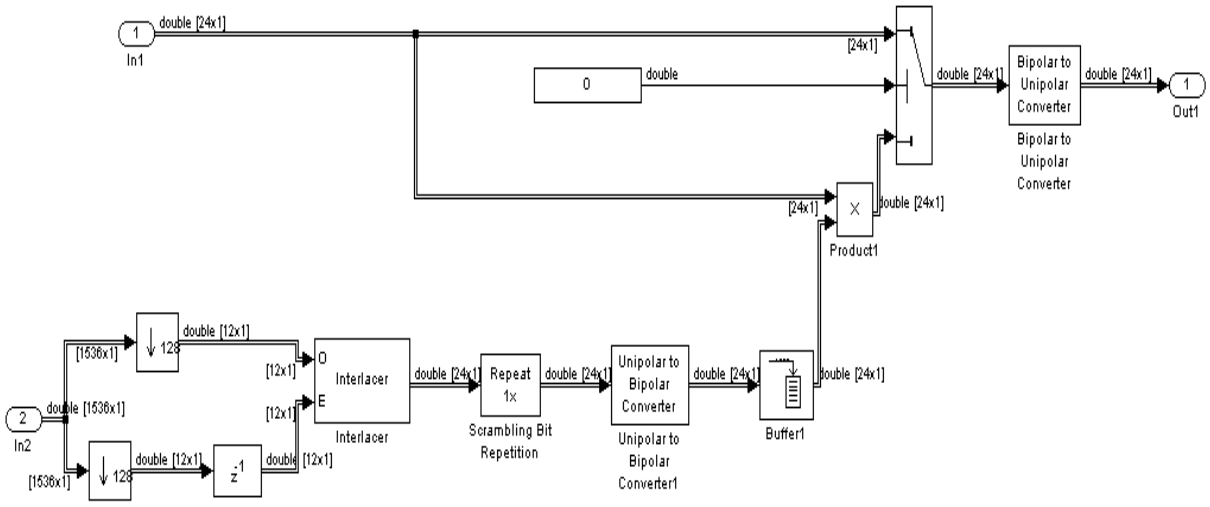

Figure 4.46: *Design of Long Code Descrambling*

4.7.3.4.1 Operation of long code descrambling

In Long code descrambling, first PN sequence is decimated by 128 bits resulting in output of rate 9600bps (12 bits per frame). This output is applied over two paths and interlaced with one path having one chip delay. The Interlacer block accepts two inputs that have the same vector size, complexity, and sample time. It produces one output vector by alternating elements from the first input (labeled O for odd) and from the

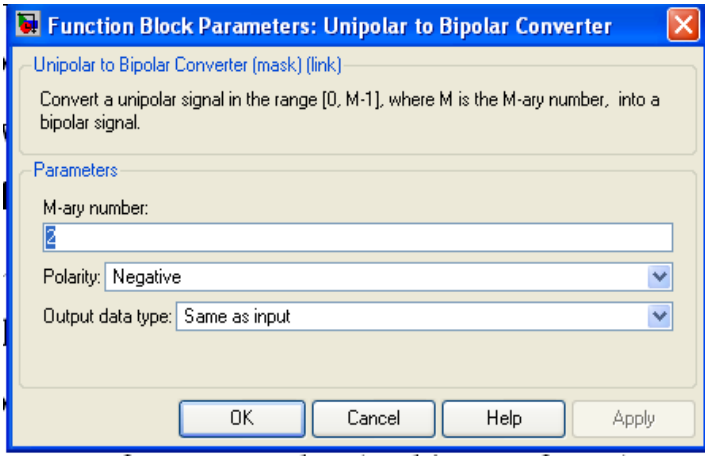

Figure 4.47*: Function block parameters of unipolar and bipolar converter*

second input (labeled E for even) . As a result, the output vector size is twice that of either input. The output vector has the same complexity and sample time of the inputs. This results in an output of rate 19200bps (24 bits per frame). Each frame is of duration 1.25ms (24/19200) .

The output of interlacer is passed through a unipolar to bipolar conversion block with negative polarity as shown in figure 4.47. In negative polarity, '0' bit is converted to 1 and '1' bit is converted to -1. This is done to carry out the modulo-2 addition of the data. Finally the data is passed through a buffer which generate a frame of size 24 bits. This data constitute the PN code sequence which is used to descramble the data input by mulplying the input data and PN sequence.

After this the input data without descrambling or the descrambled data is being mapped to the output by using a switch. If enable input of switch is 1, then input data without any descrambling is transferred to output; otherwise output is descrambled data. Output data is passed through a bipolar to unipolar conversion block with negative polarity set in function block parameters of bipolar to unipolar conversion block as shown in figure 4.48. .

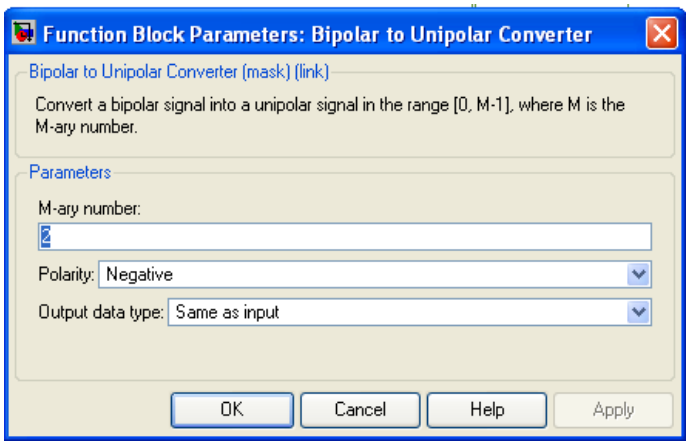

***Figure 4.48**: Function block parameters of bipolar to unipolar converter*

Output:- Output data is descrambled data having a data rate of 24 bits per frame i.e. a frame of 1.25ms duration. Total data rate is 19200bps.

4.8 DECODER

The next block is decoder. It performs various operations on the input data for error correction and for reducing bit error rate. Figure 4.49 shows the design of decoder.

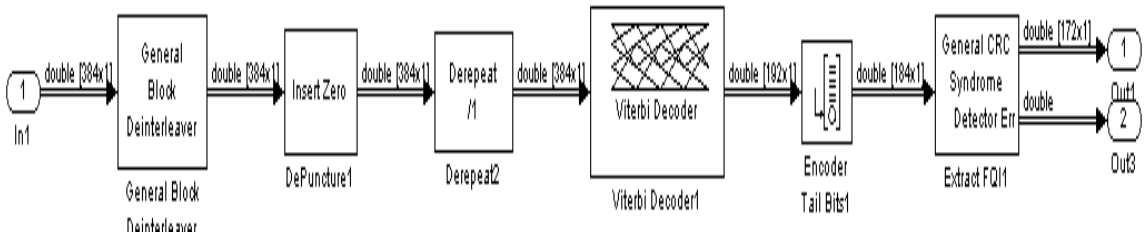

Figure 4.49: *Design of Decoder*

4.8.4 General Block Deinterleaver

The General Block Deinterleaver block rearranges the elements of its input vector without repeating or omitting any elements. The input can be real or complex. If the input contains N elements, then the Elements parameter is a vector of length N that indicates the indices, in order, of the output elements that came from the input vector. That is, for each integer k between 1 and N,

Output(Elements(k)) = Input(k)

The Elements parameter must contain unique integers between 1 and N.

If the input is frame-based, then both it and the Elements parameter must be column vectors.

To use this block as an inverse of the General Block Interleaver block, same Elements parameter are set in both blocks. In that case, the two blocks are inverses in the sense that applying the General Block Interleaver block followed by the General Block Deinterleaver block leaves data unchanged [37].

Output:- The element set in function block reverse the order of occurrence of the bits in the frame. So, the final output data rate of the encoder is 384 bits per frame or 19200 bps.

4.8.5 Depuncture

Same as puncture used on transmitter side

Output:-As depuncture vector is set to 1 so no removal or addition of bits is done, so output is same as that of the input.

4.8.6 Derepeat

The Derepeat block resamples the discrete input at a rate 1/N times the input sample rate by averaging N consecutive samples. This is one possible inverse of the Repeat block

(Signal Processing Blockset). The positive integer N is the Derepeat factor parameter in the Derepeat dialog.

The Initial condition parameter prescribes elements of the output when it is still too early for the input data to show up in the output. If the dimensions of the Initial condition parameter match the output dimensions, then the parameter represents the initial output value. If Initial condition is a scalar, then it represents the initial value of each element in the output[40].

Operation

If the input is frame-based, then the block derepeats each frame, treating distinct channels independently. Each element of the output is the average of N consecutive elements along a column of the input matrix. The Derepeat factor must be less than the frame size.

The Framing parameter determines how the block adjusts the rate at the output to accommodate the reduced number of samples. It is set to Maintain input frame rate. This means the block reduces the sampling rate by using a proportionally smaller frame size than the input. For derepetition by a factor of N, the output frame size is 1/N times the input frame size, but the input and output frame rates are equal. When you use this option, the Initial condition parameter does not apply and the block incurs no delay, because the input data immediately shows up in the output. For example, if a single-channel input with 64 elements is derepeated by a factor of 4, then the output contains 16 elements. The input and output frame periods are equal.

Output:- As the repetition count is 1 so the output is same as that of the input maintaining its input frame rate i.e. number of frame of output should be same as that of input which is 50 in count.

4.8.4 Viterbi Decoder

This block uses the Viterbi algorithm to optimally decode a frame of convolutionally encoded information. The Viterbi algorithm searches through the trellis, as defined by the encoder, for the most probable sequence and outputs the decoded data along with the metric for the final detected path. The decoder operates in continuous and noncontinuous operation modes.

Continuous operation mode applies to the Sync and Paging channels. In this mode, the decoder will not be initialized to an all-zero state between frames of input data. This operation mode will not introduce any processing delay whenever the frame length is a multiple of the decode length. Otherwise, there will be a processing delay of one frame.

Noncontinuous operation mode applies to the Traffic channel. In this mode, the decoder initializes to an all-zero state value prior to processing each input frame. As a result, this operation mode does not introduce any processing delay. Note that in the noncontinuous operation mode, the decoder starts the traceback in the zero state. This means that the last 8 bits of the sequence being decoded must be 0 [35].

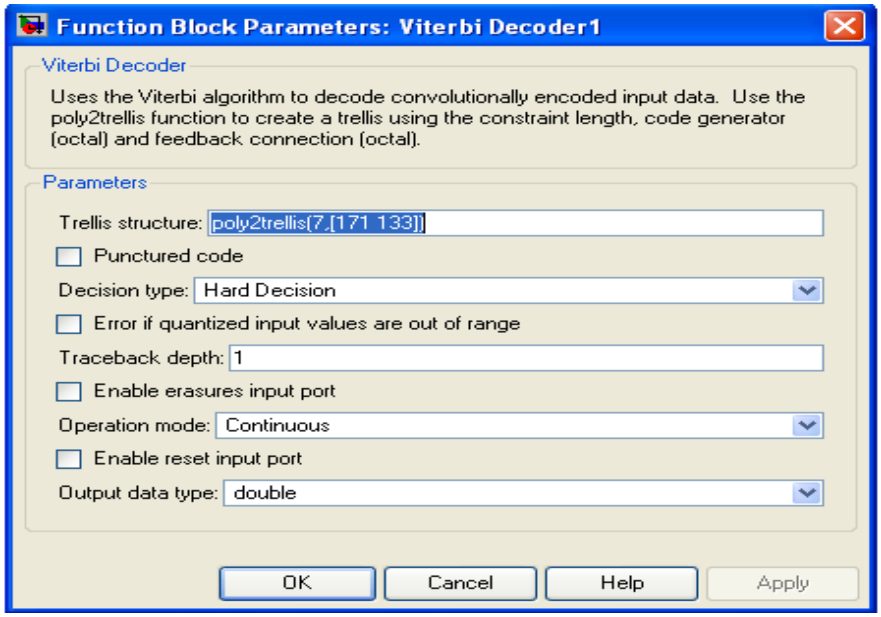

Figure 4.50: *Function block parameters for Viterbi Decoder*

Output:- The Viterbi decoder is of order 7 and has two feedback paths having feedback connection polynomials 171 and 133, so it has output having rate half that of the input rate. As the input data rate is 384 bits per frame, so output rate of Viterbi decoder is 192(384/2) bits per frame. The total data rate is 9600 bps (19200/ 2).

4.8.7 Decoder Tail Bits

Decoder tail bits remove tail bits from the end of every frame according to the parameters set in the source block parameter.

Output:- As the row size is set to 184(172+12), so total of 8 tail bits are removed at the end of every frame. The total data rate now becomes 9200 bps (184 X 50).

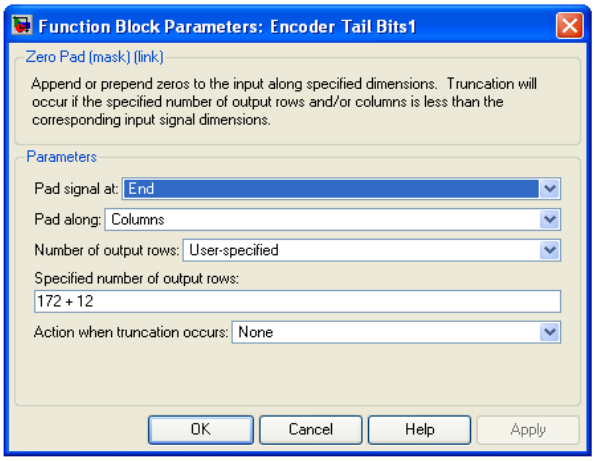

Figure 4.51: *Function block parameters of Encoder tail bits*

4.8.8 General CRC syndrome detector

The General CRC Syndrome Detector block computes checksums for its entire input frame. The block's second output is a vector whose size is the number of checksums, and whose entries are 0 if the checksum computation yields a zero value, and 1 otherwise. The block's first output is the set of message words with the checksums removed.

The block's parameter settings should agree with those in the General CRC Generator block.

The number of checksums the block calculates for each frame is specified by the Checksums per frame parameter. If the Checksums per frame value is k, the size of the input frame is n, and the degree of the generator polynomial is r, then k must divide n - k*r, which is the size of the message word [38].

Example:- Suppose the received codeword has size 16, the generator polynomial has degree 3, Initial states is [0], and Checksums per frame is 2. The block computes the two checksums of size 3, one from the first half of the received codeword, and the other from the second half of the received codeword, as shown in the figure 4.52. The initial states are not shown in this example, because an initial state of [0] does not affect the output of the CRC algorithm. The block concatenates the two halves of the message word as a single vector of size 10 and outputs this vector through the first output port. The block outputs a 2-by-1 binary frame vector whose entries depend on whether the computed checksums are zero. The figure 4.52 shows an example in which the first checksum is

nonzero and the second checksum is zero. This indicates that an error occurred in transmitting the first half of the codeword [36].

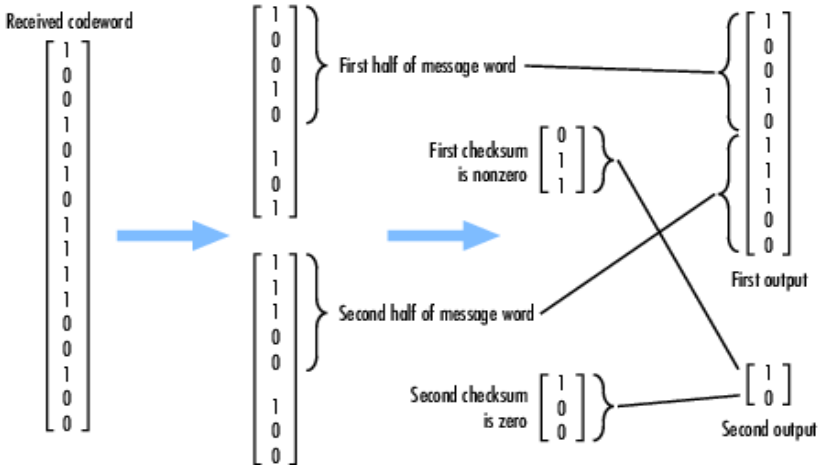

Figure 4.52: *Checksum calculation[36]*

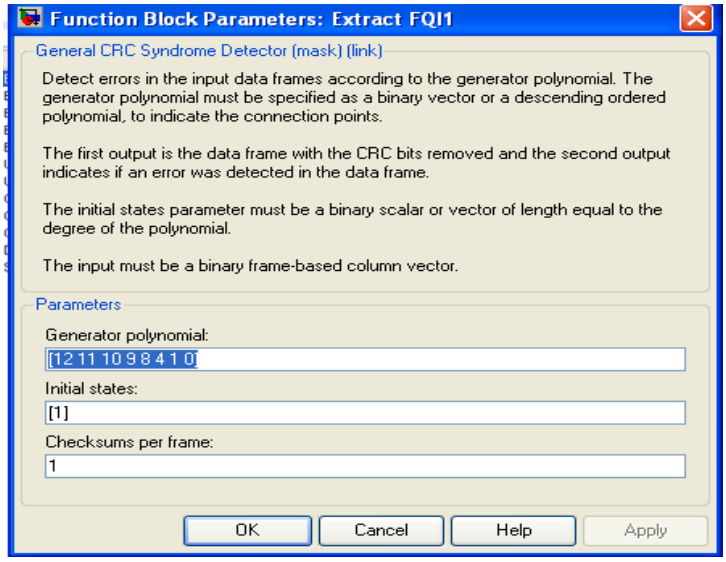

Figure 4.53: *Function Block Parameters for CRC Syndrome Detector*

The parameters are same as that for CRC generator on transmitter side

Output:-As the degree of generator polynomial is 12, so 12 bits are removed at the end of every frame. The total size of the frame becomes 172and the total data rate becomes 8600 bps (172 X 50).

This is all about the design of underwater CDMA2000 system. This chapter completely covers the implementation of underwater CDMA2000 system using MATLAB Simulink

Tools. The function of every block is covered in detail along with the output data rate after every block is also discussed. Along with this function block parameters are also shown. Now, in the next chapter, the performance of this system is evaluated by carrying out comparisons.

CHAPTER 5

CONCLUSION AND FUTURE SCOPE

In this chapter, the simulation performance of the underwater communication using CDMA technology, introduced in chapter 3, are presented. In the Performance evaluation, main focus is on the delay varying nature of the channel and secondly on the channel estimation. The model of underwater CDMA2000 has included the solution for both these problems as discussed in chapter 1. The performance of underwater CDMA2000 system is judged on the basis of the bit error rate at the different stages of the system. This is done by comparing the signal on the transmitter side to the receiver side.

5.1 BER after Receiver Section

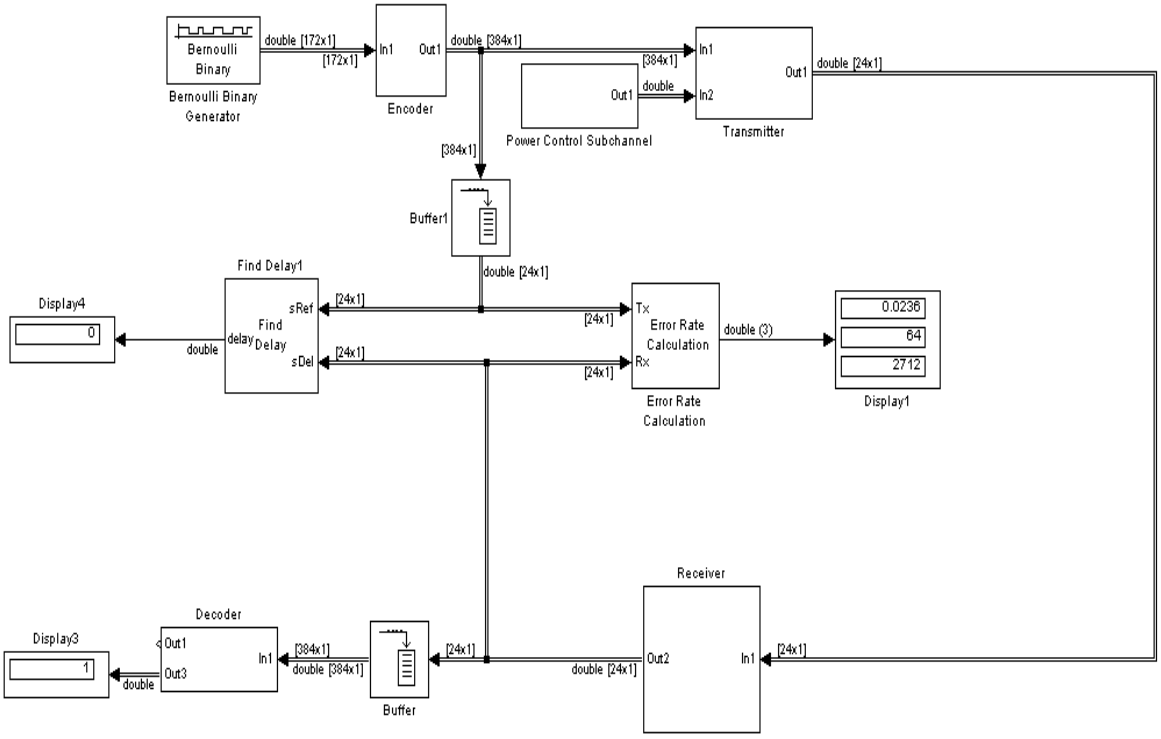

Figure 5.1: *Design of UWCDMA2000 with BER after Receiver section*

Figure 5.1 is showing the bit error rate after the receiver stage. It is calculated by comparing the signal before transmitter section on transmission side with the signal after the receiver section on the receiver side as shown in figure 5.1.

Error rate calculate block shows three outputs. The first output shows the bit error rate having a value of 0.0236. Second output shows the total number of error samples i.e.64. Third output is the total number of samples i.e. 2712. Thus, the conclusion is that among 2712 samples, 64 samples have error having a total bit error rate of 0.0236. The error in the sample is due to the power control bit addition on the transmitter side and extraction of the power control bit on the receiver side. While extracting the power bit, it is being replaced by '1' bit which may be '0' or '1' on transmitter side before placing power control bit. As in a frame of 1.25 ms, one symbol among 24 symbols in frame is replaced by power control bit so maximum bit error rate can be up to 0.0417(1/24).

One more block is used which is find delay block. This block calculates the delay between the two signals. The output delay between the two signals is zero.

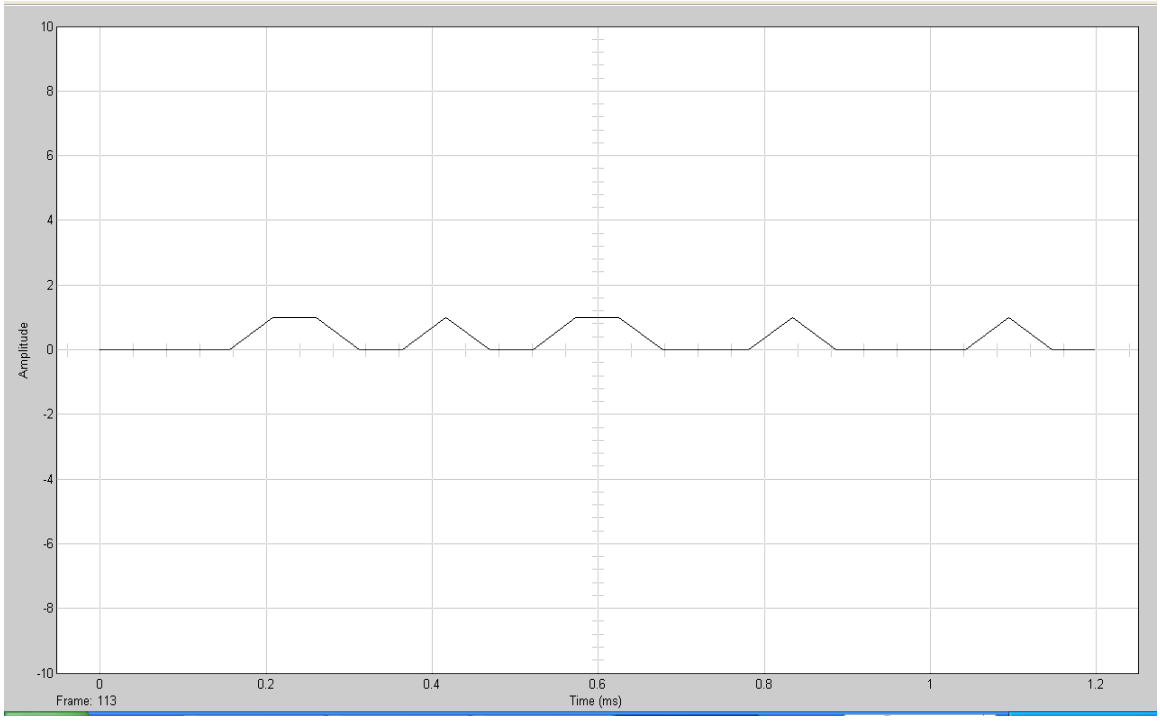

Figure 5.2: *Signal before transmitter section in time domain*

Figure 5.2 and 5.3 shows the signal before transmitter section and after receiver section in time domain for frame of size 24 bits and having a duration of 1.25 ms(24/19200).

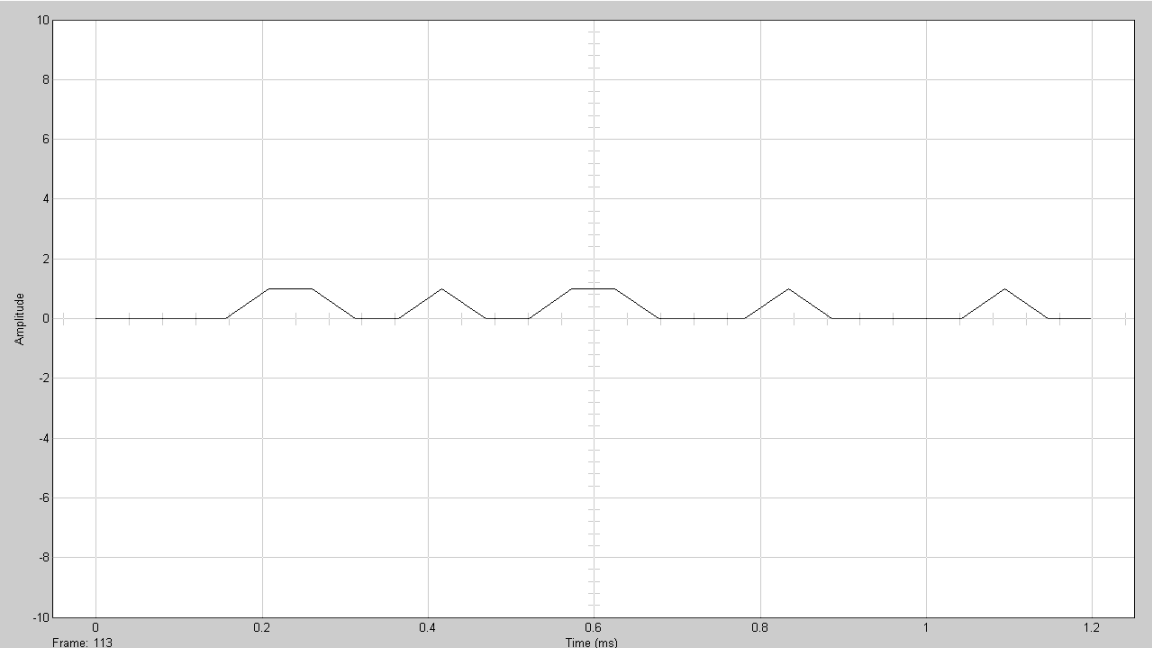

Figure 5.3: *Signal after receiver section*

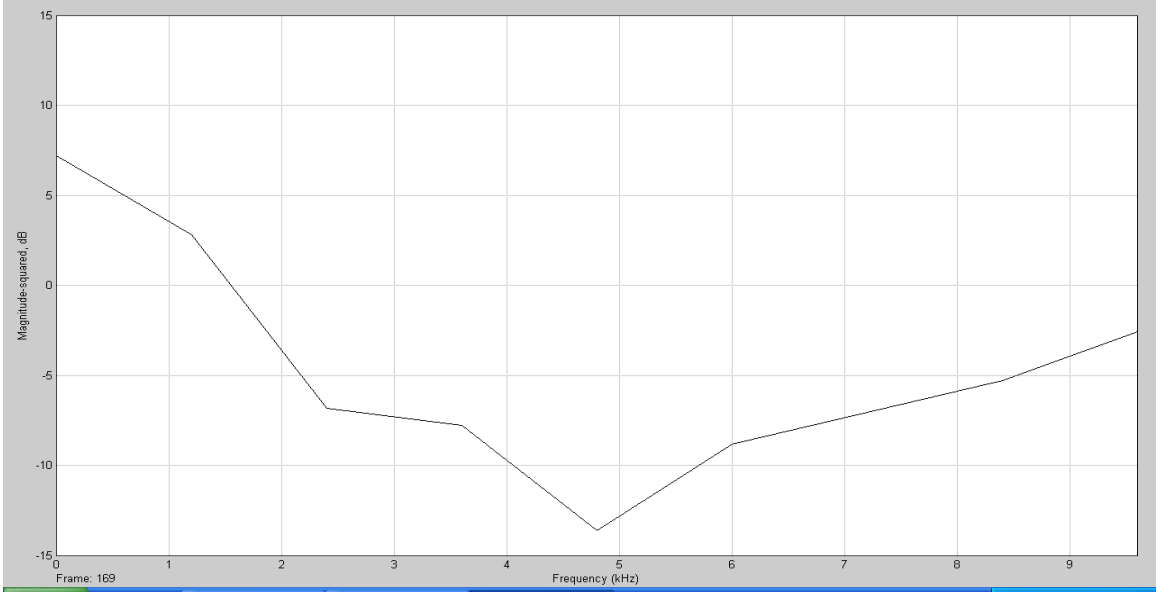

Figure 5.4: *Signal before transmission section in frequency domain*

Figure 5.4 and 5.5 shows the signal before transmitter section and after receiver section in frequency domain for frame of size 16 bits as FFT and IFFT is calculated only for powers of 2. The frequency range is set from 0 to $f_s/2$ and the sampling frequency is 19200 Hz. So, frequency ranges from 0 to 9.6 kHz(19200/2) as shown in figure 5.4 and 5.5.

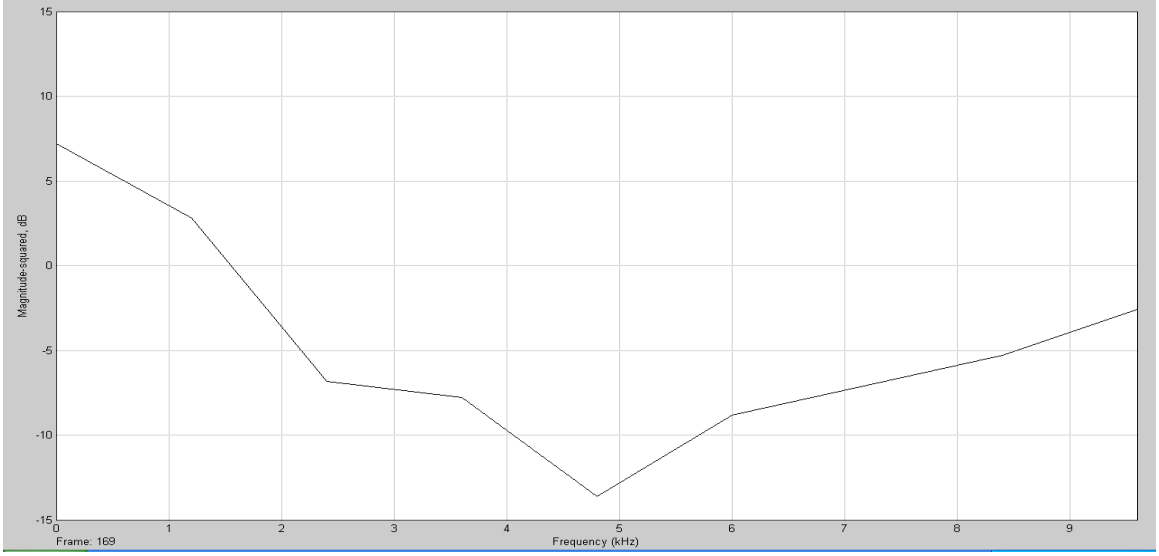

Figure 5.5: *Signal after receiver section in frequency domain*

5.2 BER of Underwater CDMA2000 System

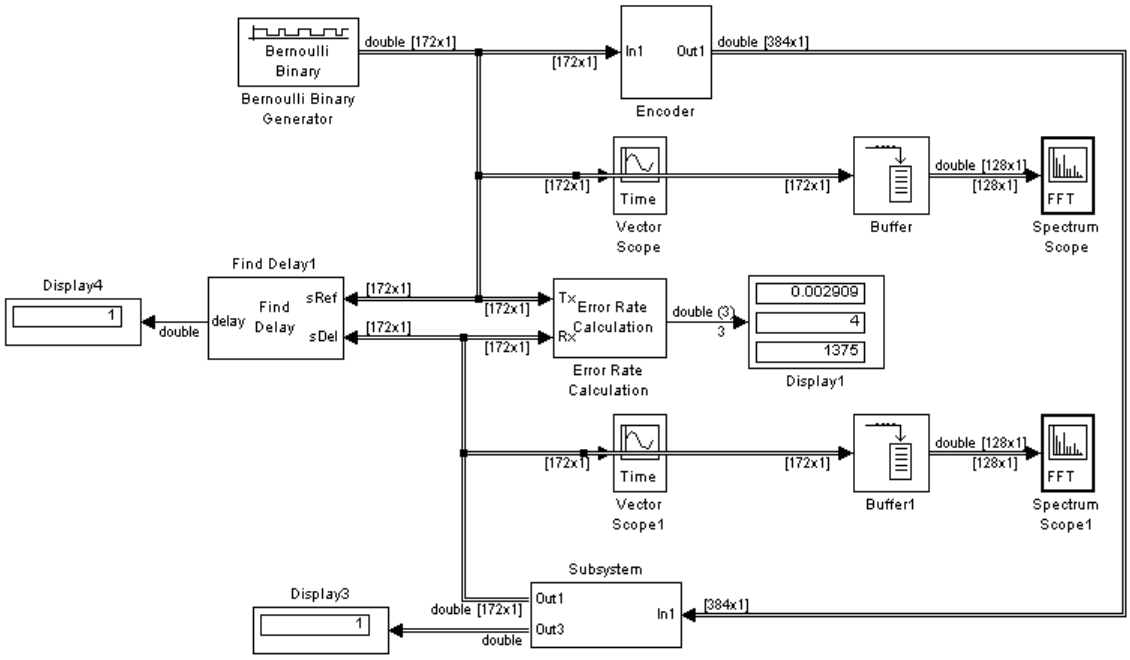

Figure 5.6: *Design of UWCDMA2000 with BER after Receiver section*

Figure 5.6 is showing the bit error rate at the output of the Underwater CDMA2000 System. It is calculated by comparing the signal generated by Bernoulli's binary generator on transmission side with the signal After the decoder section on the receiver side as shown in figure 5.6.

Error rate calculate block shows three outputs. The first output shows the bit error rate having a value of 0.002909. Second output shows the total number of error samples i.e.4. Third output is the total number of samples i.e. 1375. Thus, the conclusion is that among 1375 samples, 4 samples have error having a total bit error rate of 0.002909.

One more block is used which is find delay block. This block calculate the delay between the two signals. The output delay between the two signals is one.

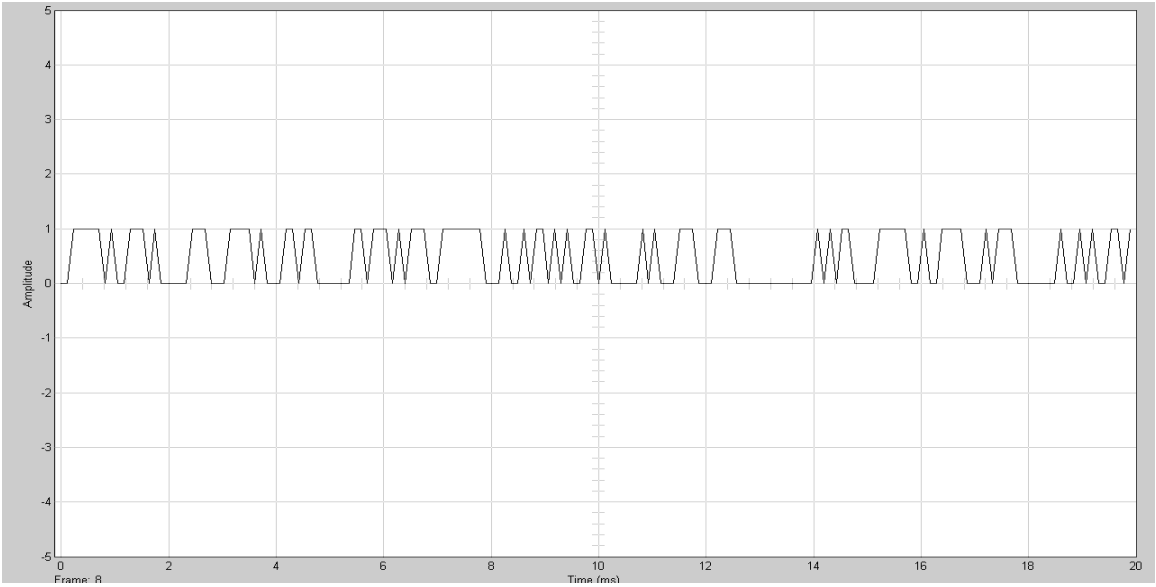

Figure 5.7: *Signal generated by bernoulli's generator in time domain*

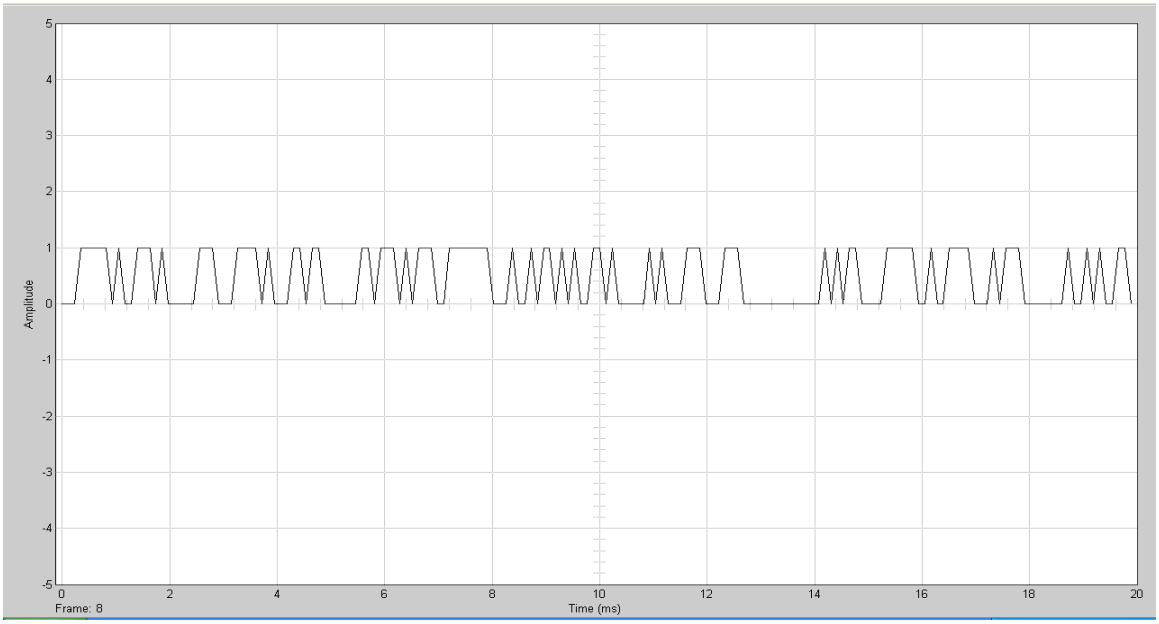

Figure 5.8: *Signal retrieved on receiver side in time domain*

Figure 5.7 and 5.8 shows the signal generated by bernoulli's generator on transmitter side and signal retrieved on receiver side in time domain for frame of size 172 bits and having a duration of 20 ms. Total number of 50 frames are transmitted in 1 sec. This results in a total data rate of 8600 bits per sec (172 x 50).

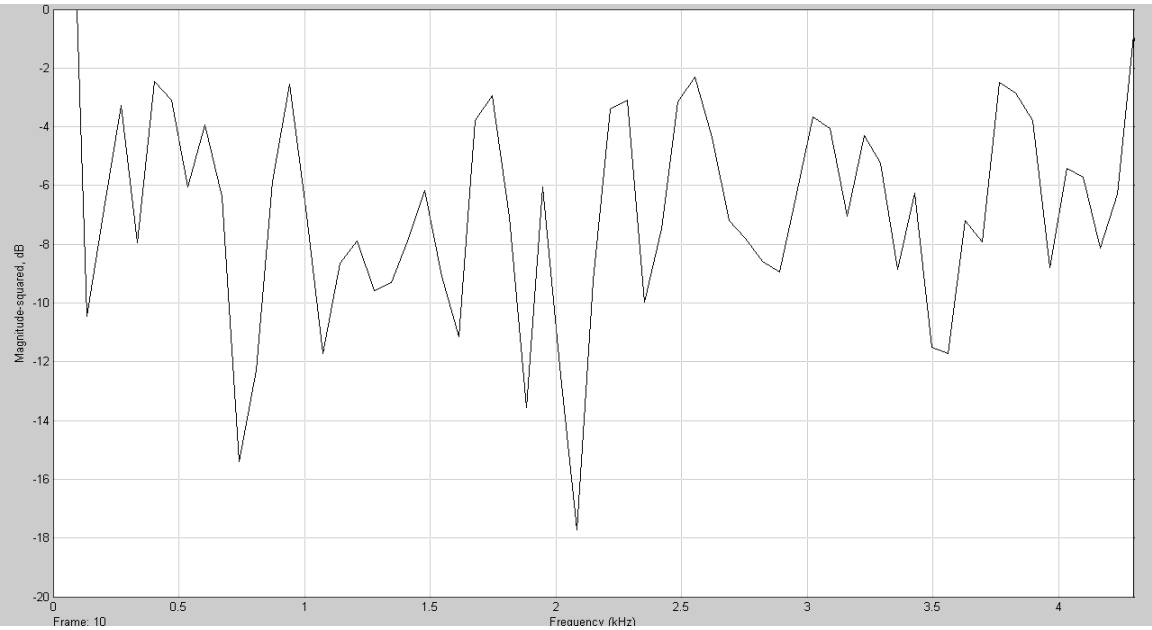

Figure 5.9: *Signal generated by bernoulli's generator in frequency domain*

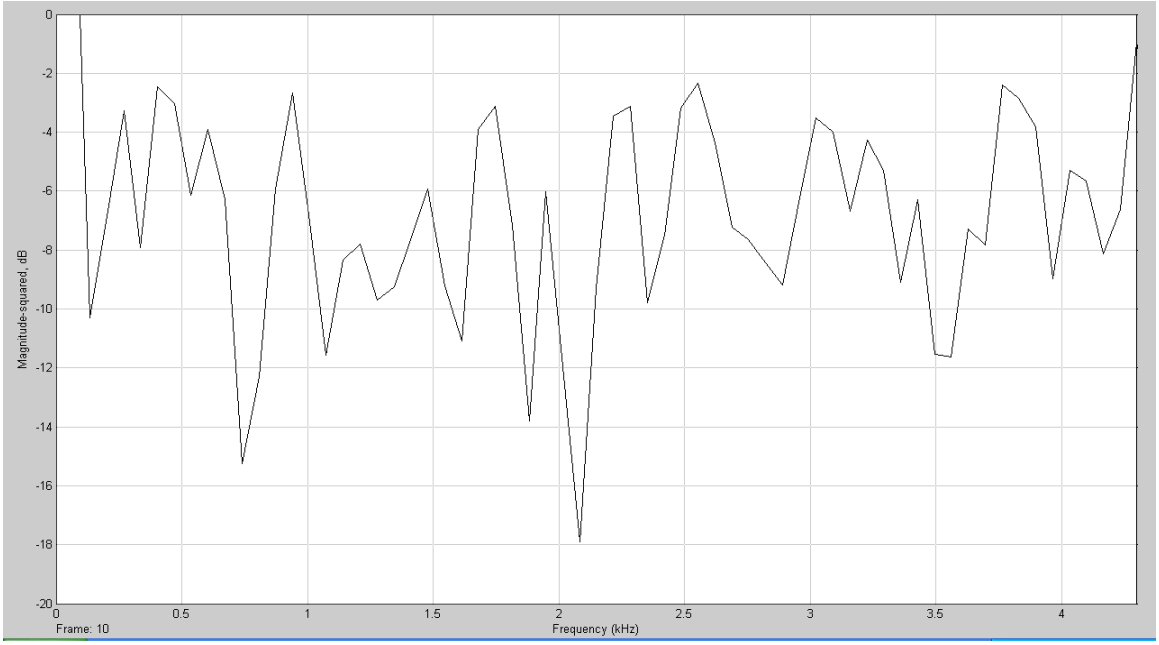

Figure 5.10: *Signal retrieved on receiver side in frequency domain*

Figure 5.9 and 5.10 shows the signal generated by bernoulli's generator on transmitter side and signal retrieved on receiver side in frequency domain for frame of size 128 bits as FFT and IFFT is calculated only for powers of 2. The frequency range is set from 0 to $f_s/2$ and the sampling frequency is 8600 Hz(172 x 50). So, frequency ranges from 0 to 4.3 kHz(8600/2) as shown in figure 5.9 and 5.10.

5.5 Comparison of signal with and without channel estimation

The signals before and after channel correlation are shown below. This is done by placing Discrete time scatter plot scope block after the data correlator block whose output is a faded signal and second discrete time scatter plot scope block is placed at the position when channel effect is being removed from the signal. Both the positions are shown in figure 5.11.

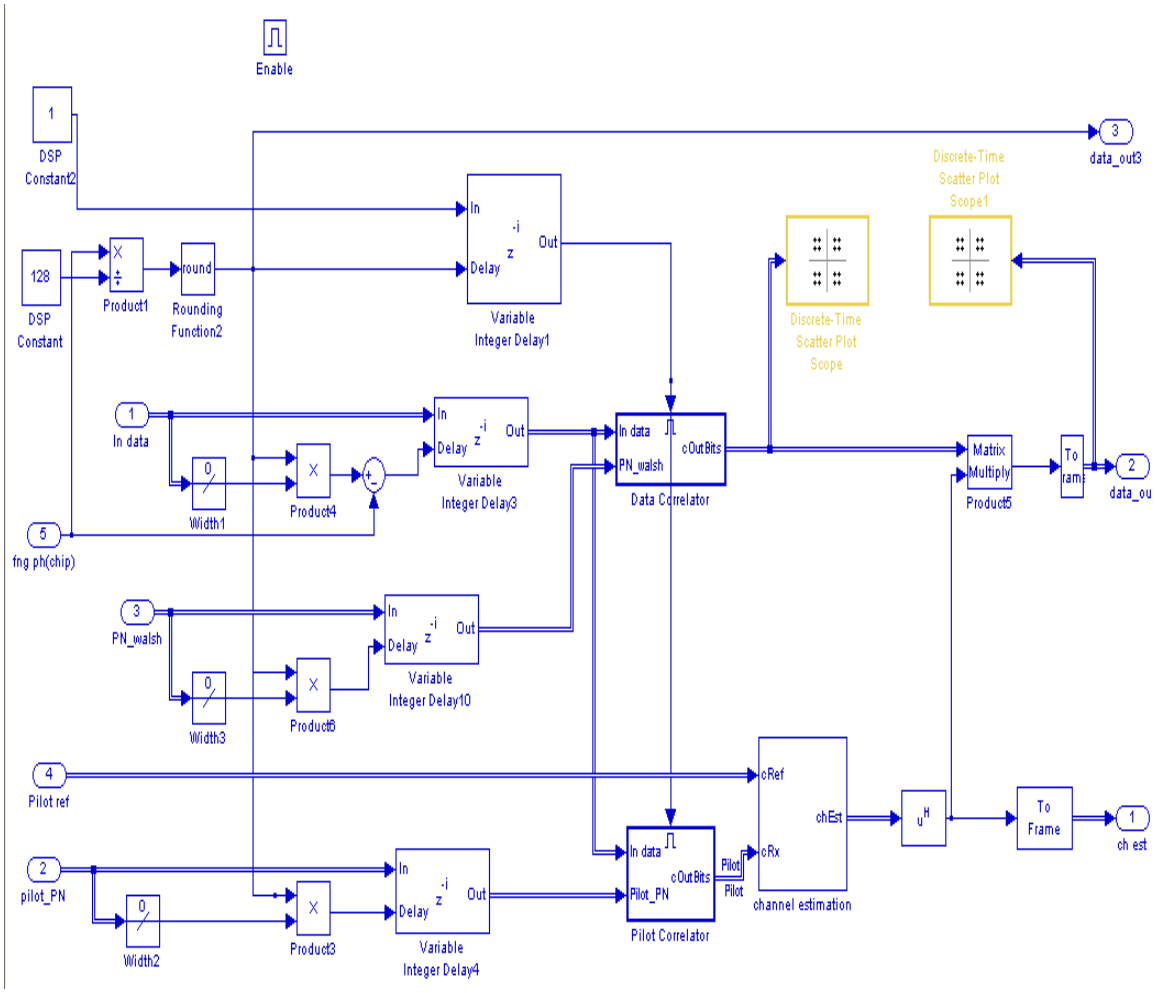

Figure 5.11: *Design of rake finger*

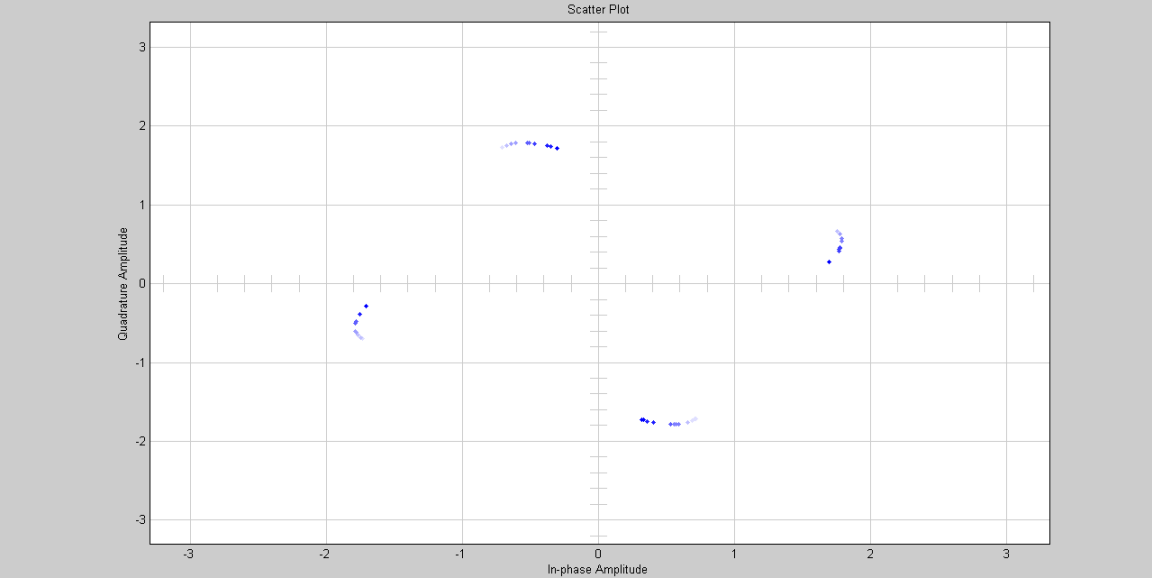

Figure 5.12: *Constellation diagram of faded signal*

Figure 5.12 shows the distorted signal. As is shown in constellation diagram, different points are no longer showing quadrature phase shift modulation. So, the signal is distorted by channel.

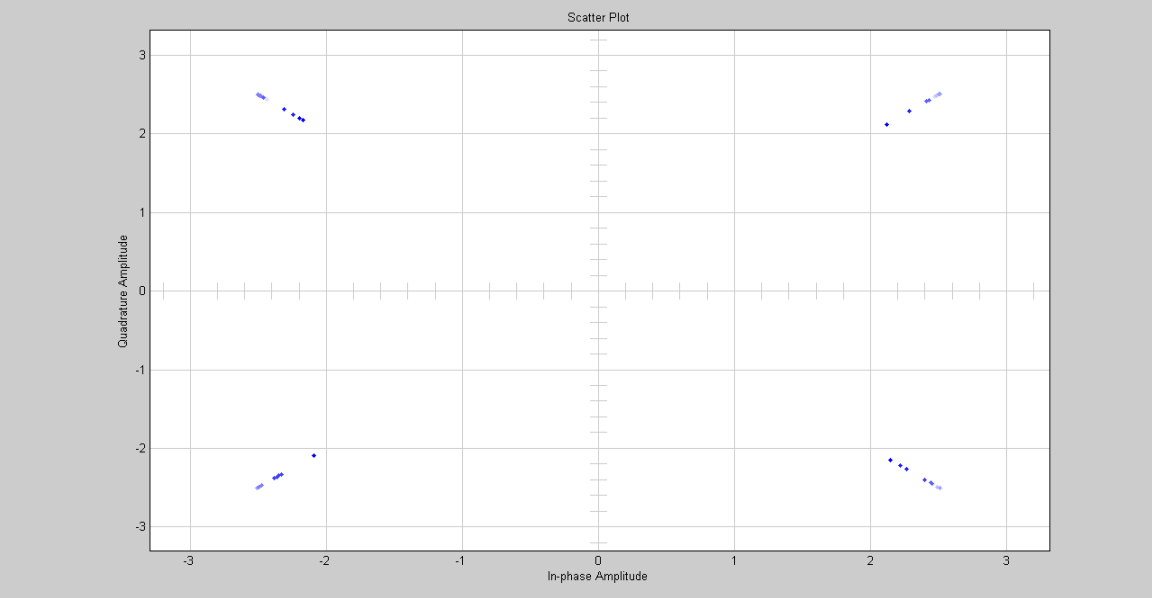

Figure 5.13: *Constellation diagram of signal after channel correlation*

Figure 5.13 shows the signal after channel compensation i.e. effect of channel on the signal is being removed. This can be easily verified from the constellation diagram shown in figure as the different points are showing quadrature phase shift modulation.

5.4 Channel Estimation

The channel behavior with time is shown in this section. This is shown by attaching a time vector scope block on the channel estimation output of rake receiver block as shown in the figure 5.14.

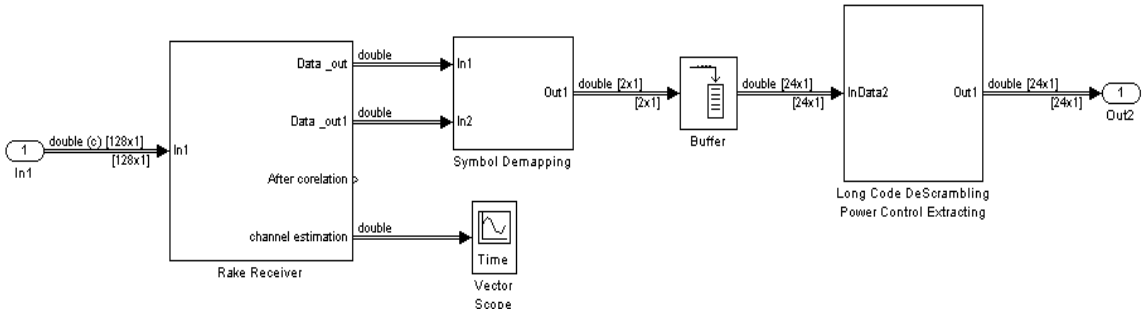

Figure 5.14: *design of receiver section*

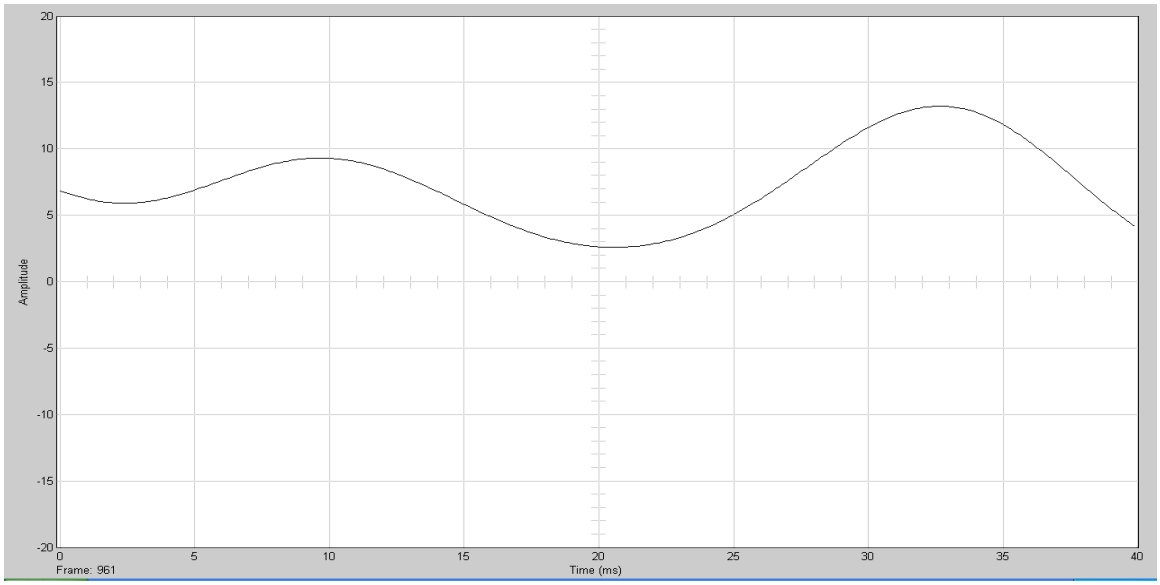

Figure 5.15: *Impulse response of channel in time domain*

Figure 5.15 shows the output of channel estimation on the receiver side.

5.5 Position of power control bit

Figure 5.16 include a display block which shows the position where power control bit is inserted in the frame.

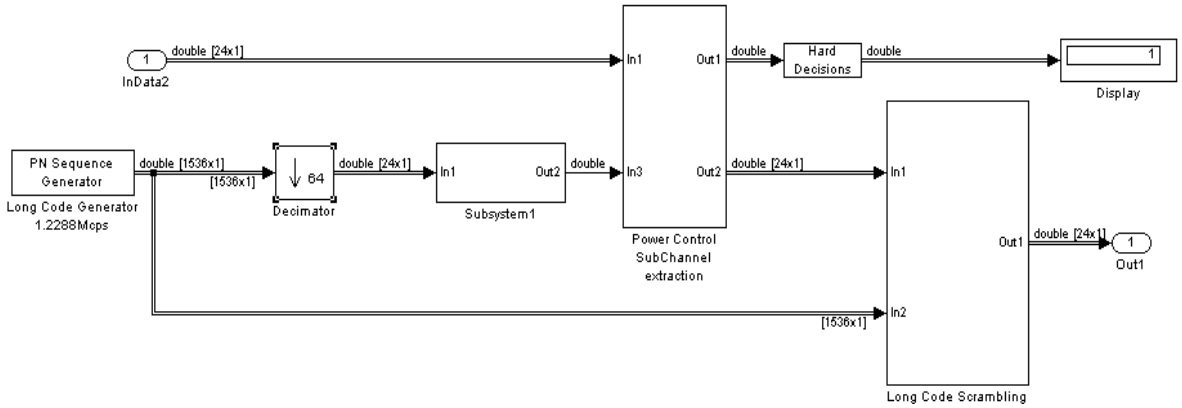

Figure 5.16: P*ower Control Bit Position display*

5.6 Comparison of signal retrieved with and without channel fading

This comparison will show whether correct data is obtained at the output after channel estimation. Signals at the rake combiner output without including any channel in the system are shown in figure 5.18 and 5.19. Signal at the rake combiner output including channel in the system are shown in figure 5.20 and figure 5.21. The similarity between the figures shows that data is correctly retrieved after channel estimation.

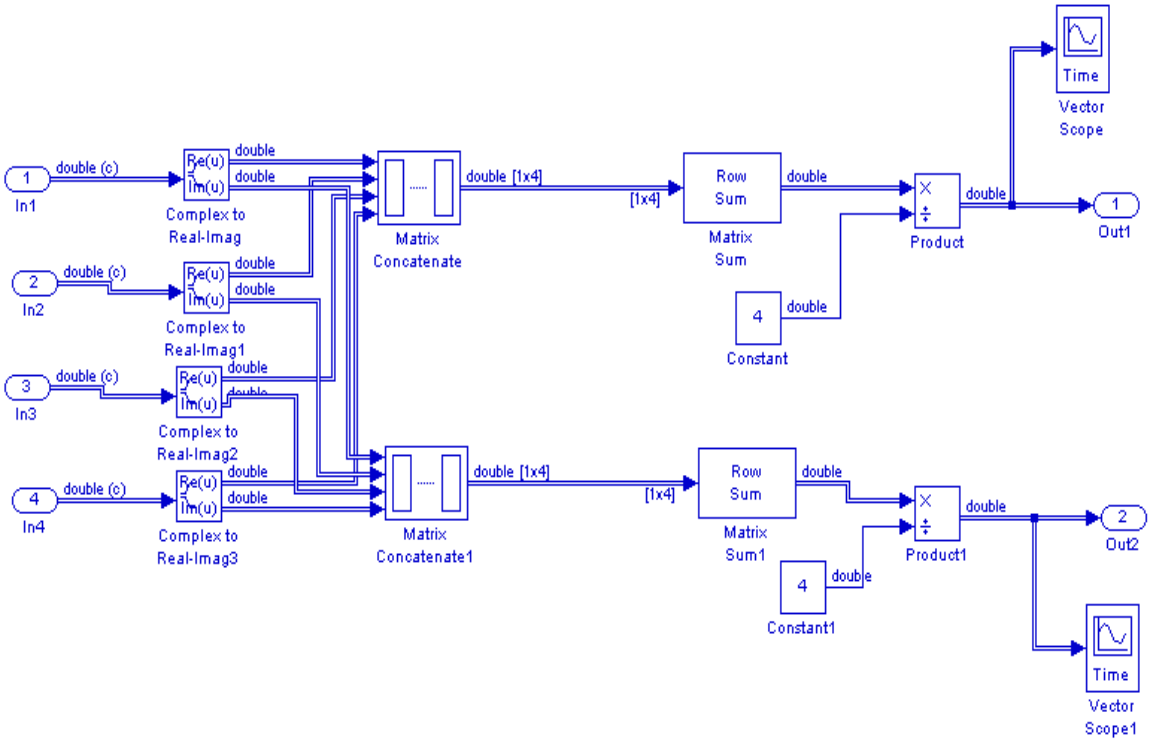

Figure 5.17: *Design of rake receiver*

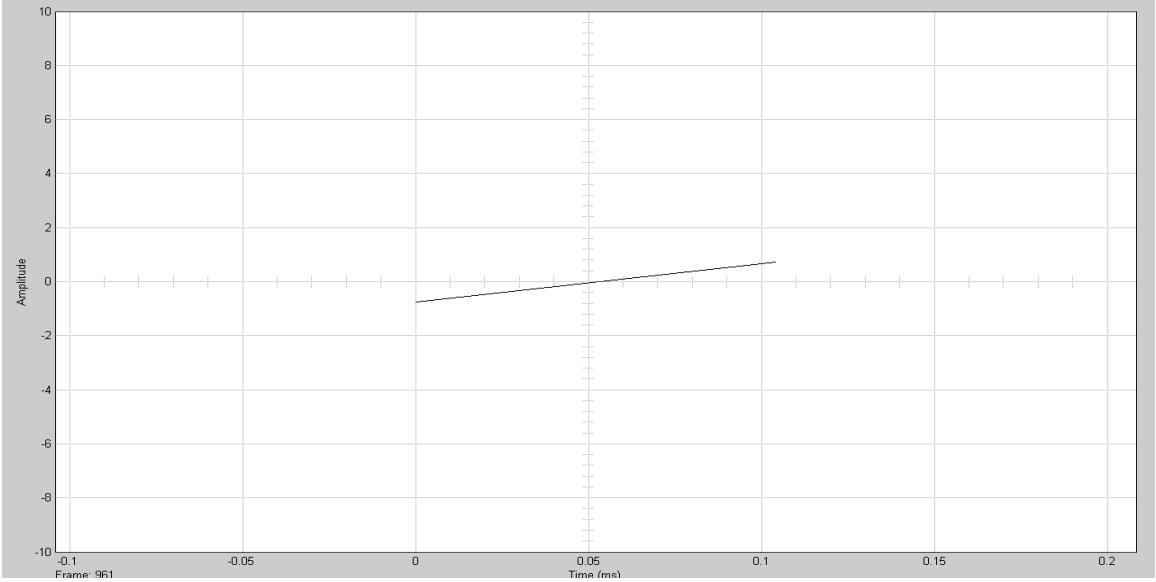

Figure 5.18: *Rake combiner first output without including channel in system*

Figure no. 5.18, 5.19 and Figure 5.20, 5.21 shows the output of rake combiner without and with channel in the system respectively. These figures shows the signal for the period of 0.1042msec(128/1228800) which is the time period of one symbol. As the Quadrature phase shift modulation is done, so one symbol will carry two bits as shown in figures with a data rate of 19200 bps. The time period of one bit is 0.1042/2 i.e. 0.0521msec (1/19200).

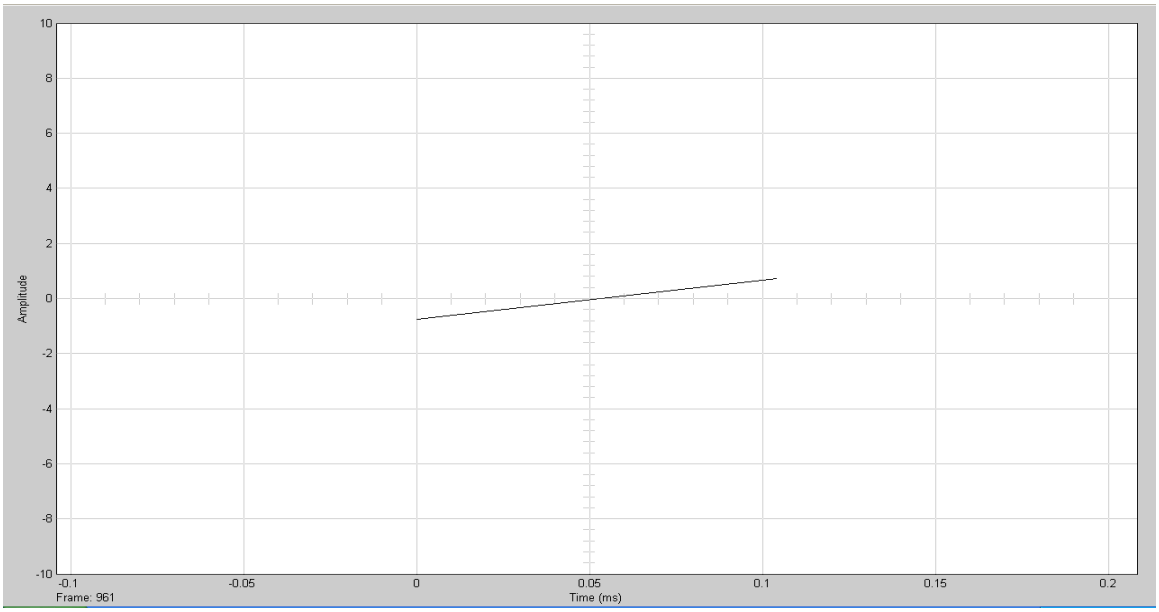

Figure 5.19: *Rake combiner Second output without including channel in system*

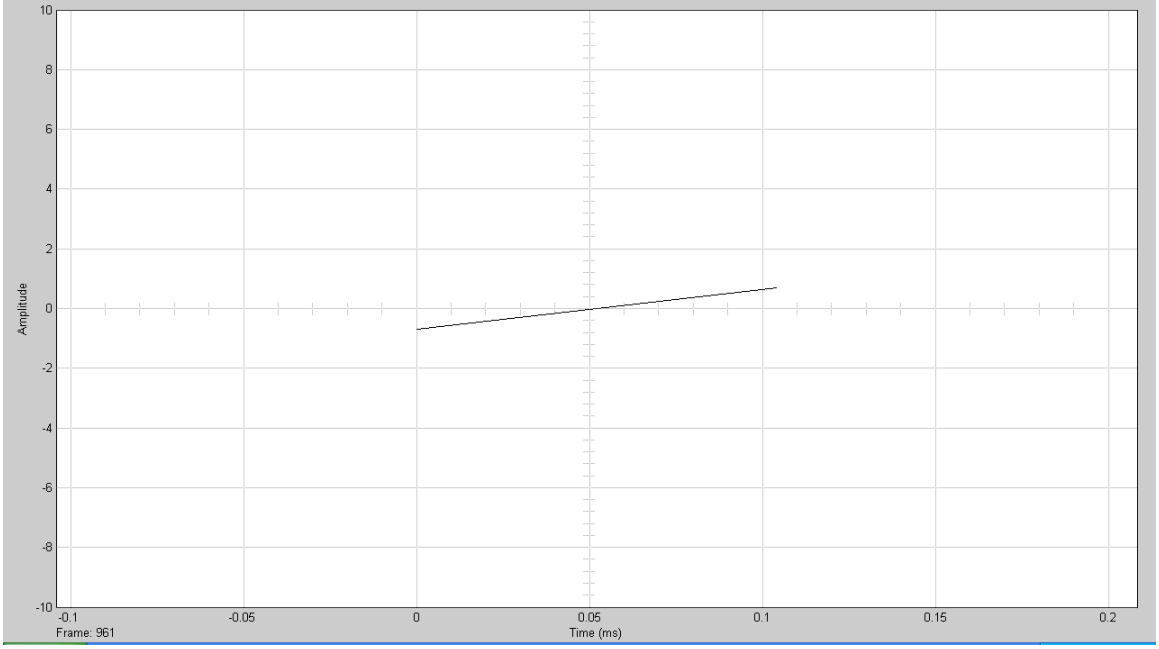

Figure 5.20: *Rake combiner first output including channel in system*

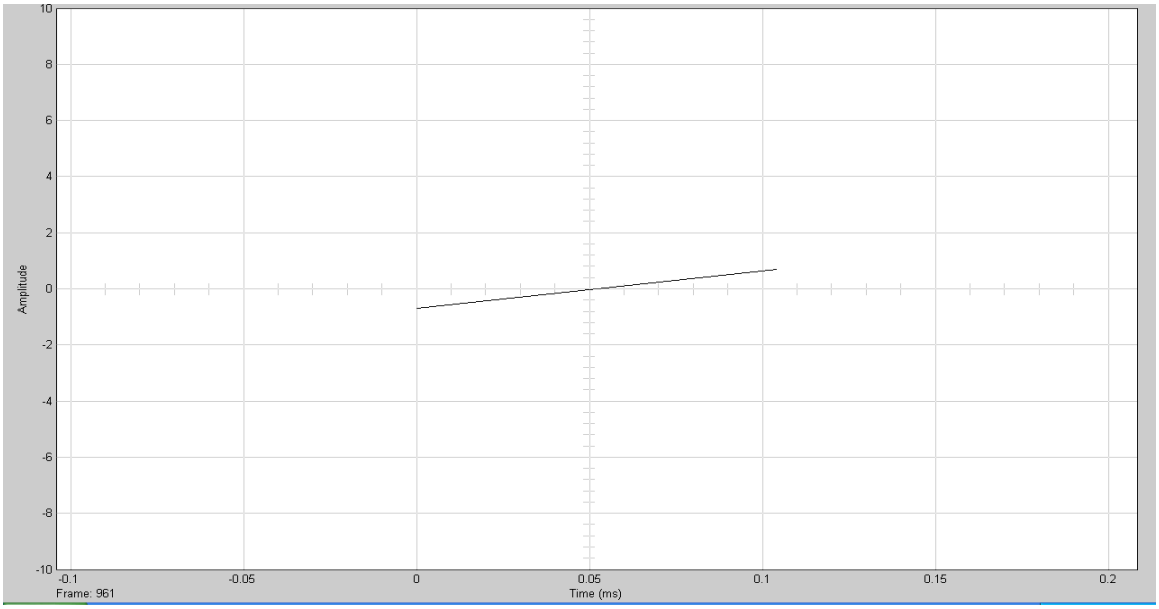

Figure 5.21: *Rake combiner second output including channel in system*

5.7 Transmitted signal with and without fading

Figure 5.22 shows the transmitted signal and Figure 5.23 shows the transmitted signal after rayleigh fading in frequency domain.

Figure 5.24 shows the constellation diagram of the transmitted signal and Figure 5.25 shows the constellation diagram of transmitted signal after rayleigh fading.

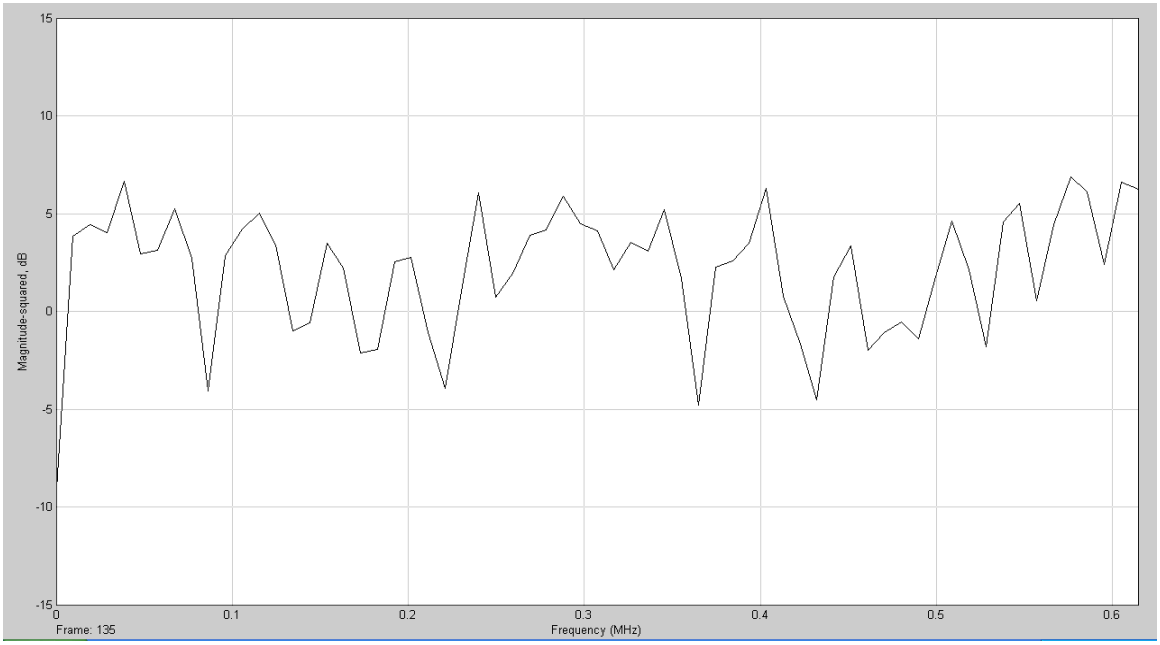

Figure 5.22: *Transmitted signal before fading in frequency domain*

As frequency range is set from 0 to $f_s/2$, so the graph has a frequency range of 0 to 0.6144MHz(1228800/2).

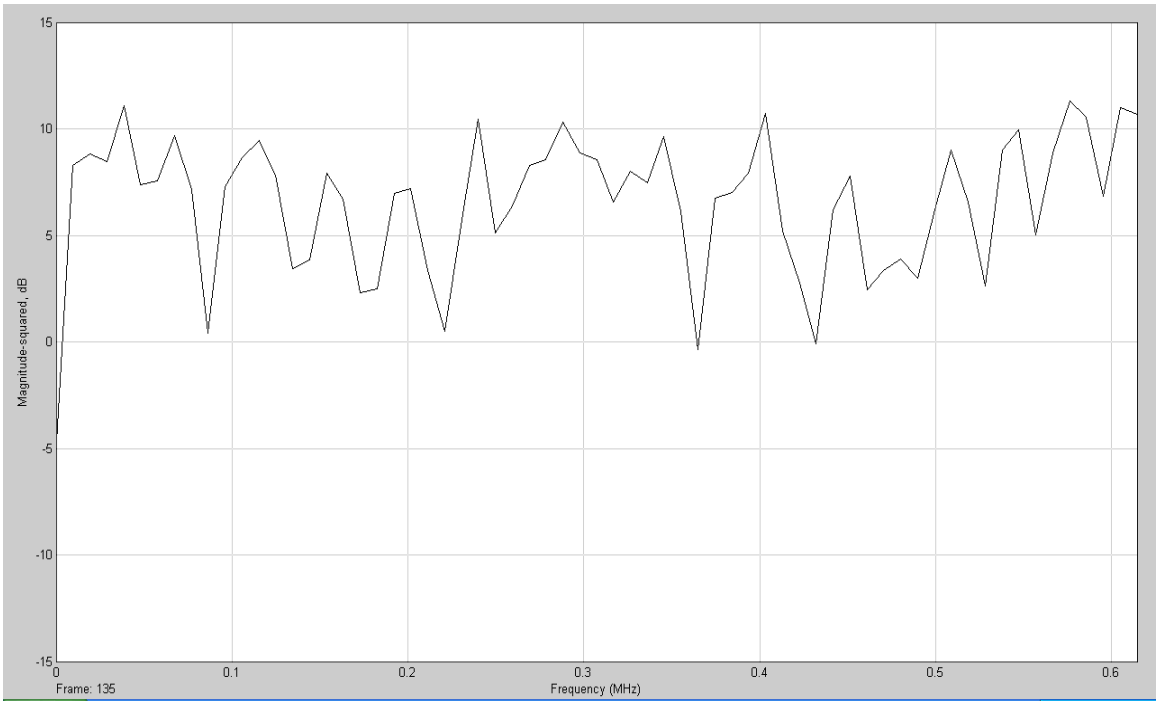

Figure 5.23*: Signal after fading in frequency domain*

On comparing Figure 5.22 and 5.23, it is clear that channel varies the amplitude of the signal.

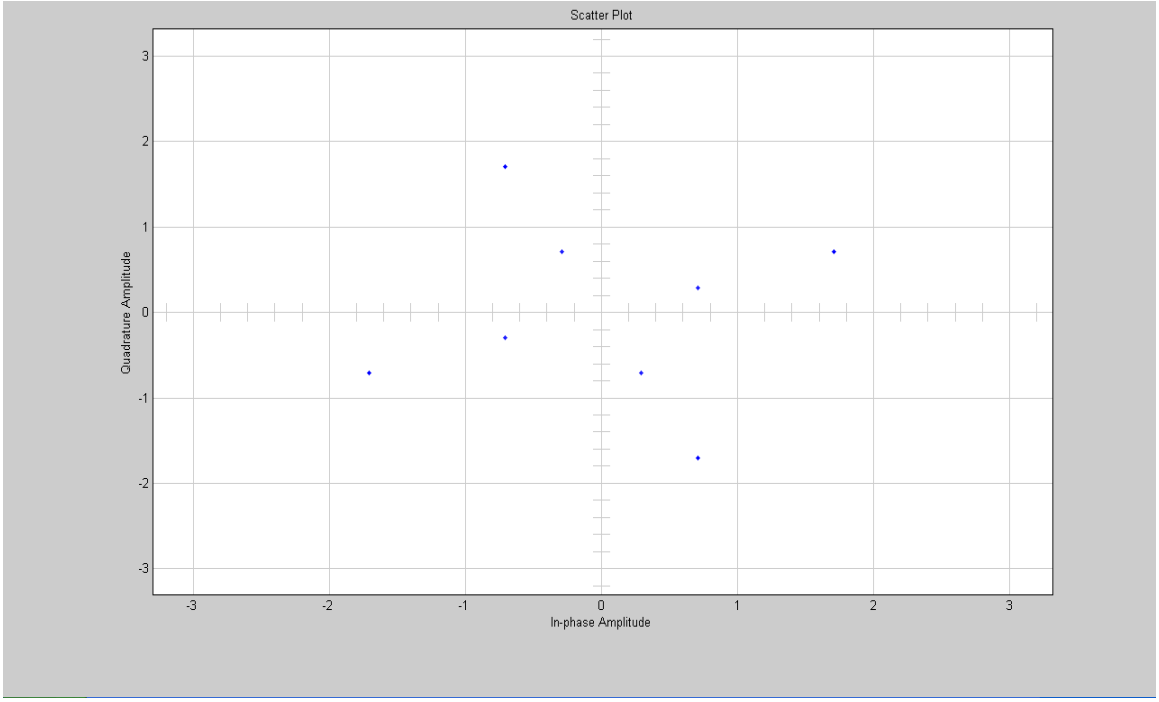

Figure 5.24: *Constellation diagram of transmitted signal before fading*

Figure 5.24 shows the constellation diagram of transmitted signal before fading for Quadrature phase shift modulation. So, the points on the constellation diagram are at four phase angles depending on the amplitude of real and imaginary parts. From figure 5.24, it can be seen that the amplitude of the signals is either $0.7071(1/\sqrt{2})$ or 1.7071. This is more clear from the figure 5.25 and figure 5.26 which shows the real and imaginary part of the signal shown in constellation diagram. Either the amplitude is 0.7071 or 1.7071. Amplitude equal to 0.7071 and 1.7071 are due to orthogonal spreading and quadrature spreading in spreading code block on transmitter side.

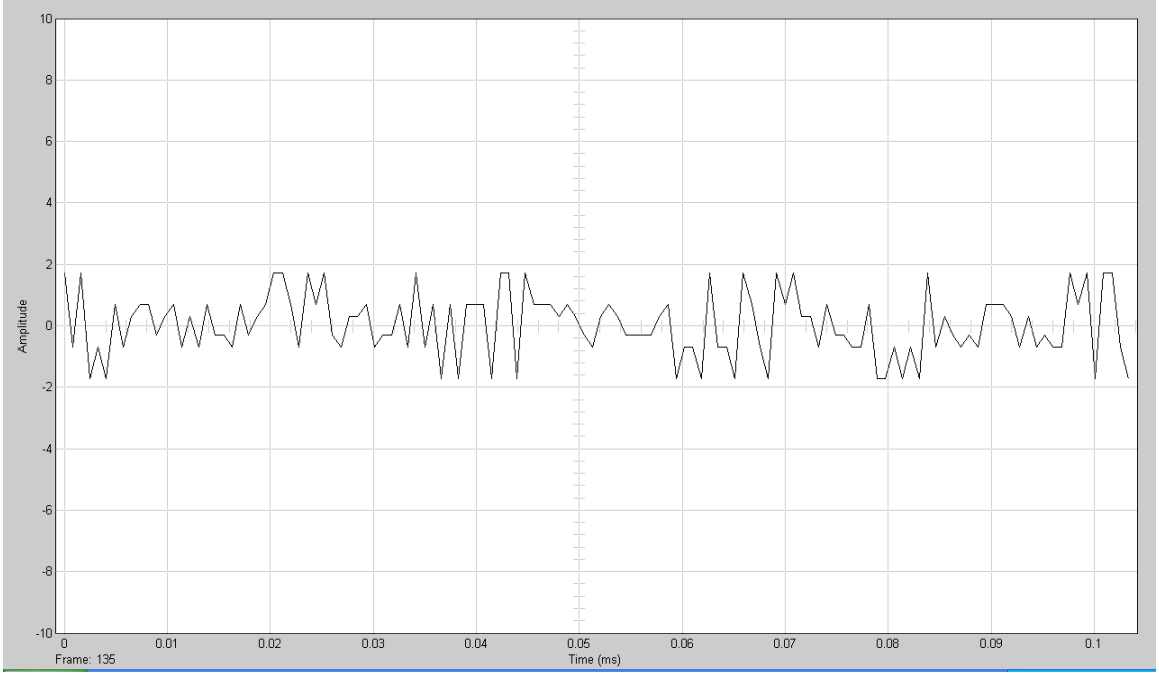

Figure 5.25: *Real part of the transmitted signal before fading*

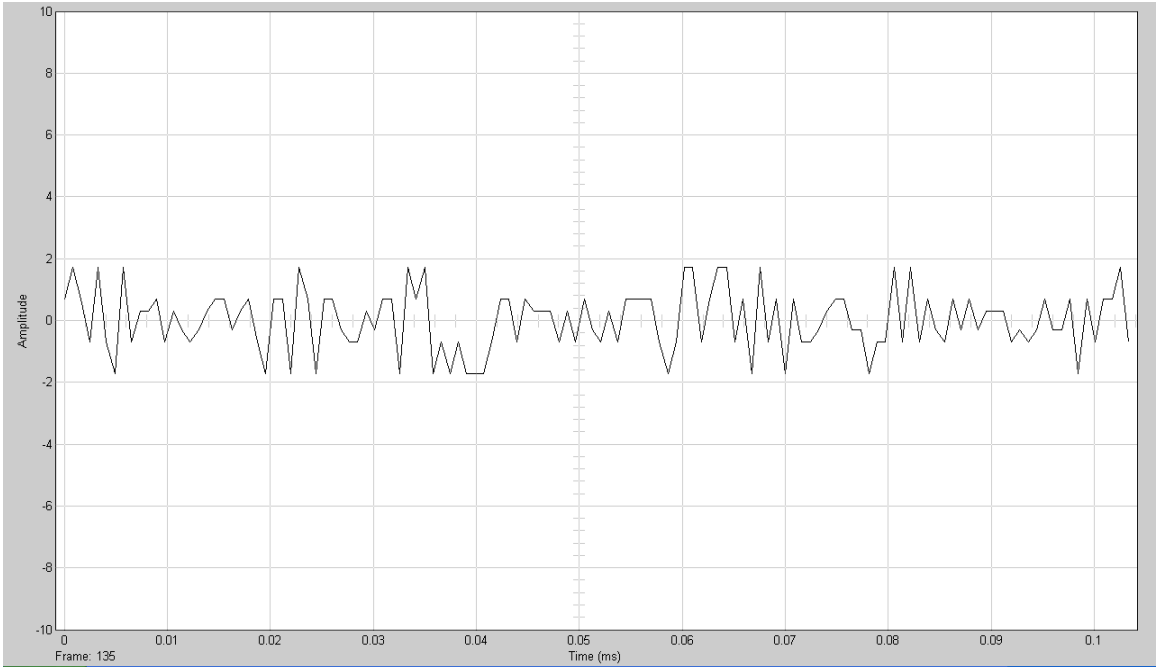

Figure 5.26: *Imaginary part of transmitted signal before fading*

Figure 5.25 and Figure 5.26 shows the frame of size 128 bits. The total data rate is 1.2288Mbps. The time period of one frame is 0.1042msec (128/1228800) as is clear from figure 5.25 and 5.26.

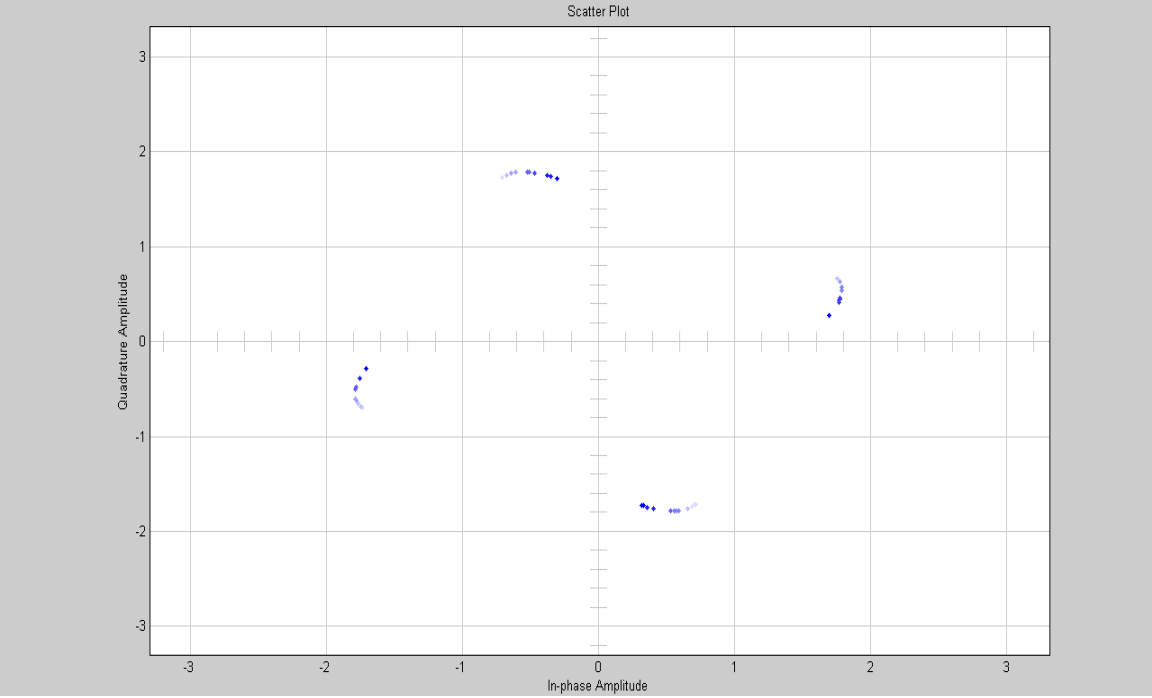

Figure 5.27: *Constellation diagram of signal after fading*

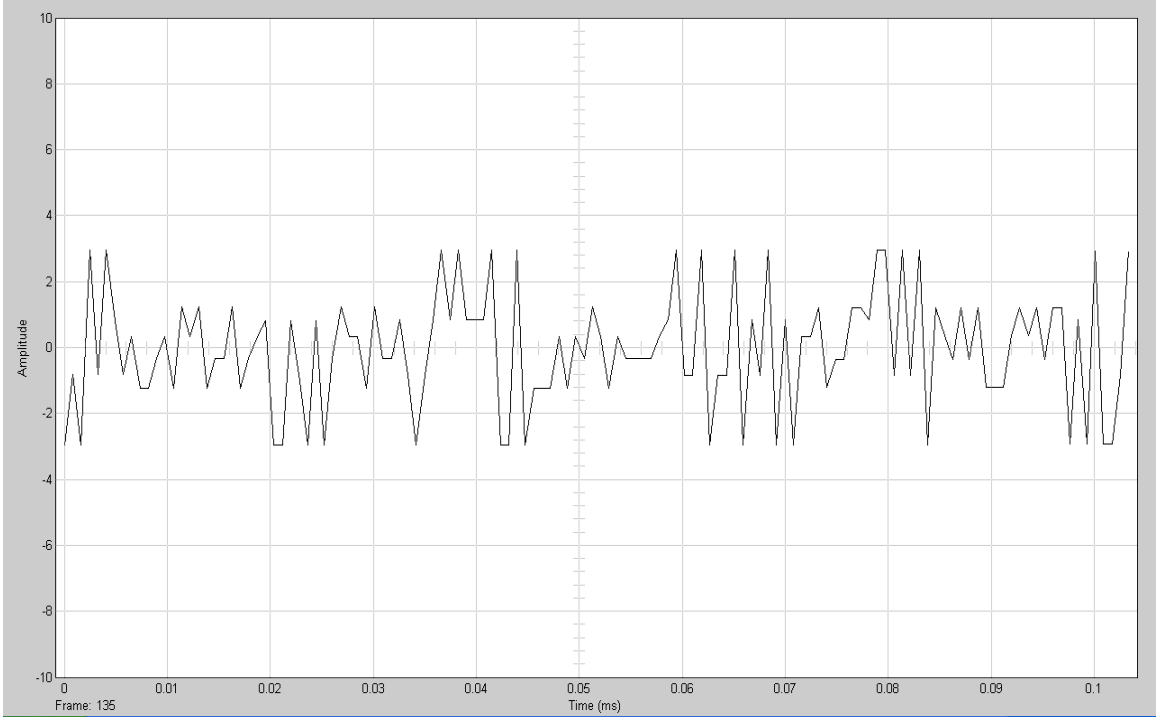

Figure 5.28: *Real part of transmitted signal after fading*

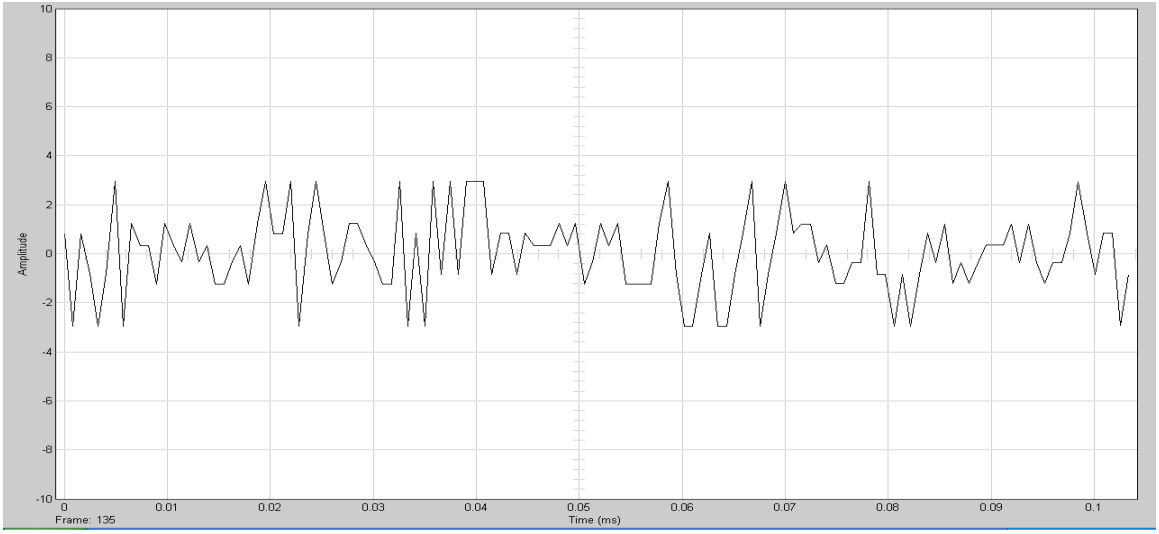

Figure 5.29: *Imaginary part of transmitted signal after fading*

Figure 5.28 and Figure 5.29 shows the frame of size 128 bits. The total data rate is 1.2288Mbps. The time period of one frame is 0.1042msec (128/1228800) as is clear from figure 5.28 and 5.29.

5.8 Comparison of signals at different stages on transmitter and receiver side

In this section, signals at different stages on transmitter and receiver side of underwater CDMA2000 system are shown. The comparison of the signal shows the accuracy level of the system.

Three comparisons are shown between the signals obtained after CRC generator, encoder tail bit block and Convolutional encoder on transmitter side and the signals before CRC detector, tail bit block and viterbi decoder on receiver side respectively. For carrying out the comparison, three vector scope blocks are placed after CRC generator, encoder tail bit block and Convolutional encoder in encoder block as shown in figure 5.30 and three vector scope blocks are placed before CRC detector, tail bit block and viterbi decoder in decoder block as shown in figure 5.31.

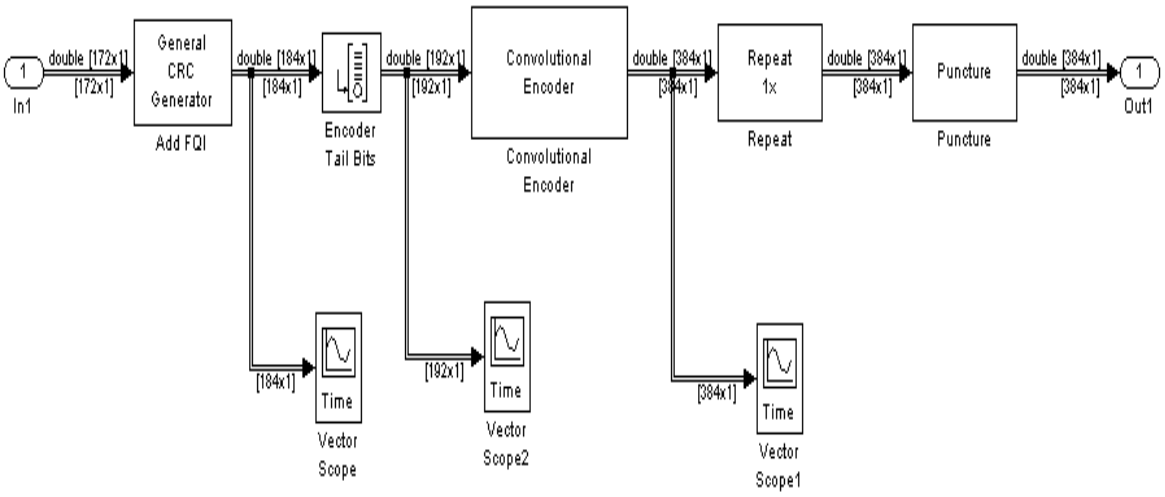

Figure 5.30: *Design of encoder*

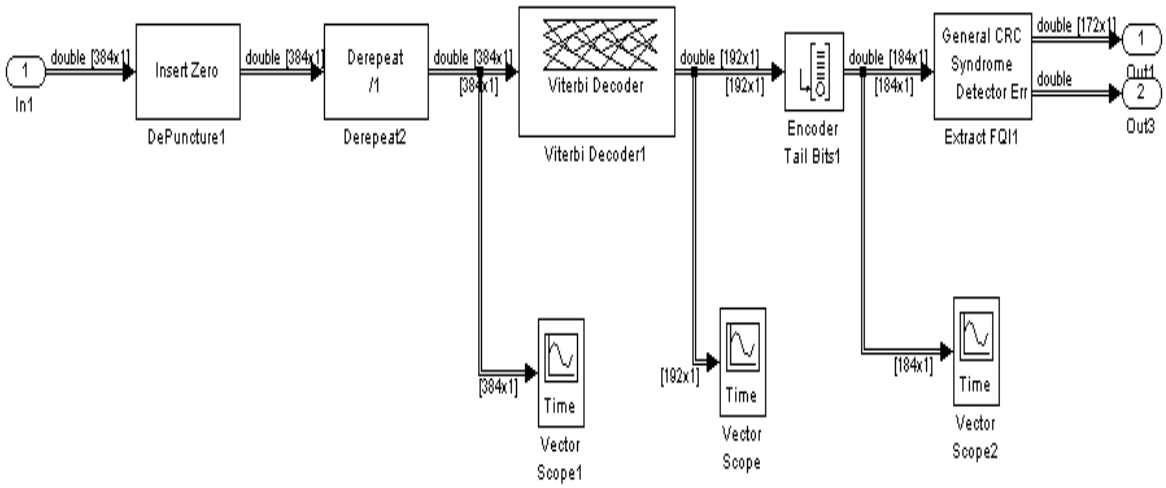

Figure 5.31: *Design of decoder*

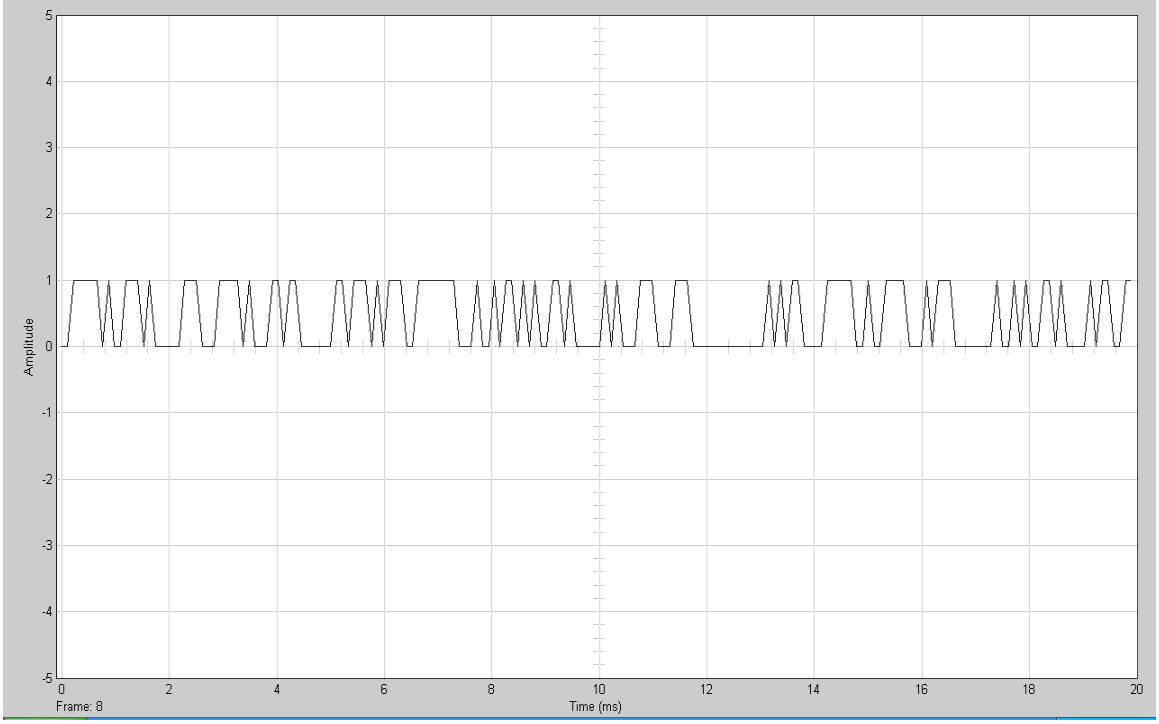

***Figure 5.32**: Signal after CRC generator*

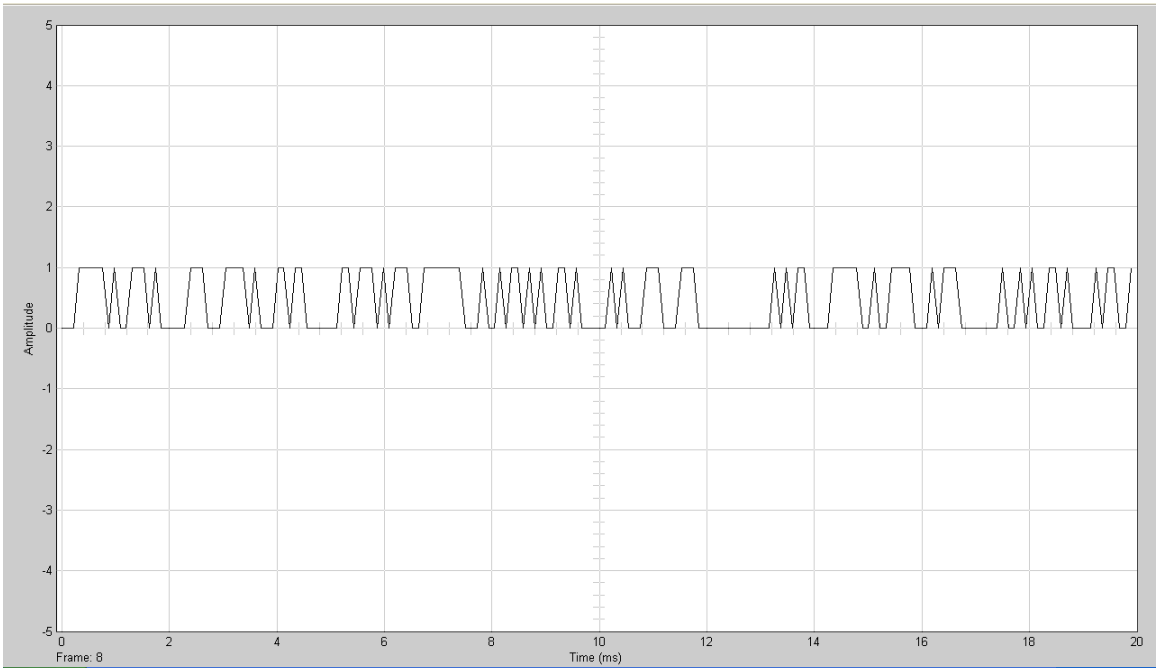

***Figure 5.33:** Signal before CRC detector on receiver side*

Figure 5.32 and figure 5.33 show the signals after CRC generator on transmitter side and before CRC detector on receiver side respectively. On comparing two signals, both are

same with a delay of 1 bit. The signal shows a frame of size 184 bits(172 data bits and 12 CRC bits). The total data rate is 9200bps with total of 50 frames transmitted per second. So, the time period of one frame is 20msec(184/9200) as is clear from figure 5.32 and figure 5.33.

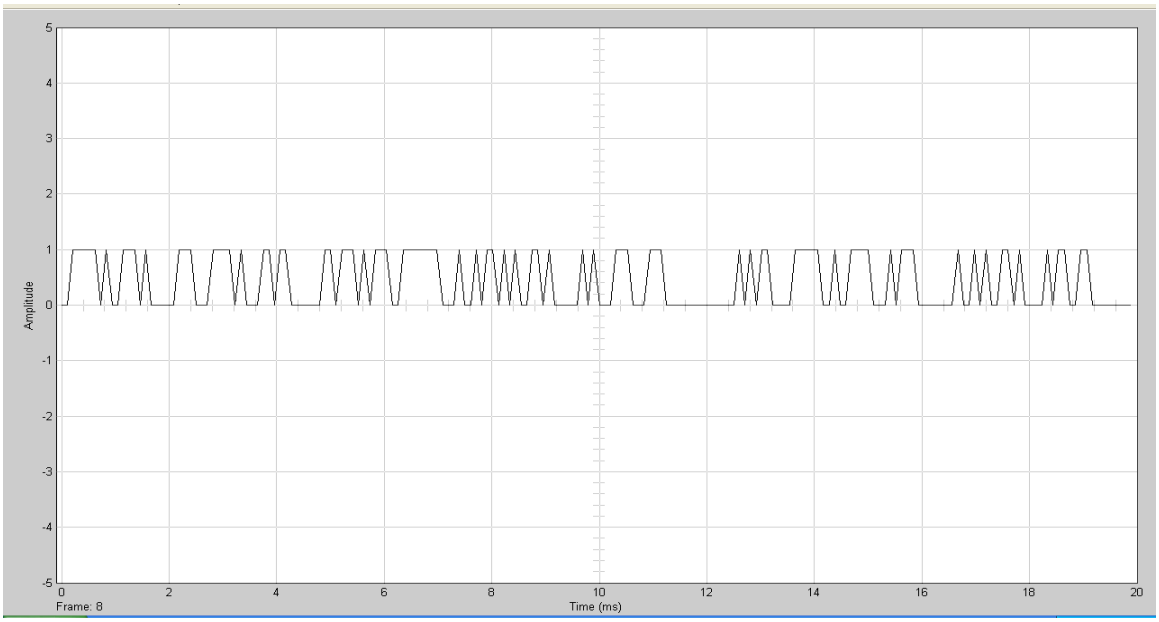

Figure 5.34*: Signal after tail bit addition on transmitter side*

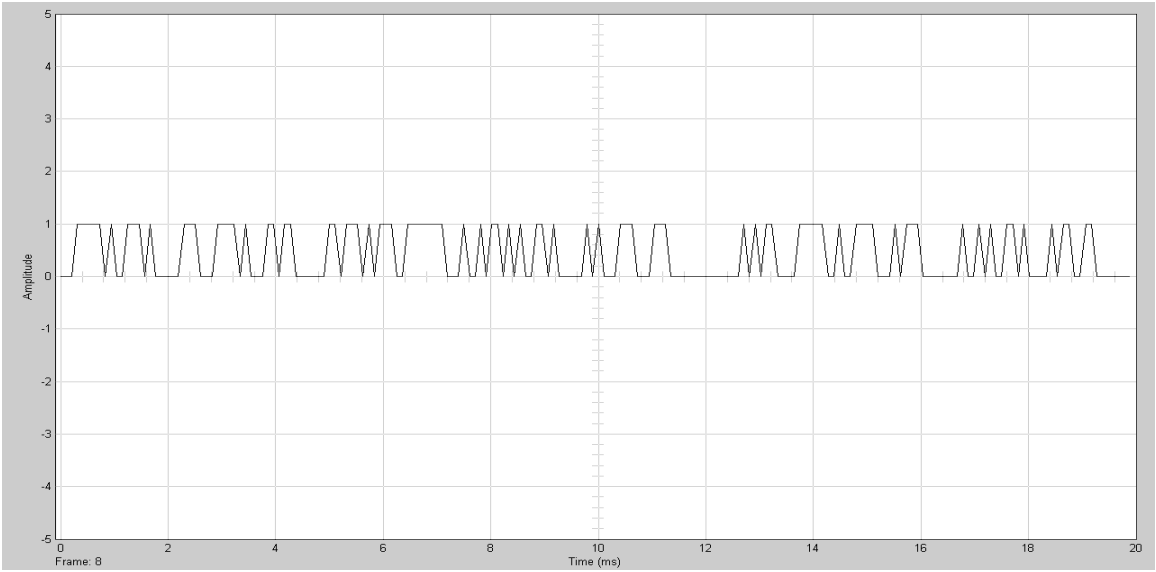

Figure 5.35: *Signal before tail bit removal on receiver side*

Figure 5.34 and figure 5.35 show the signals after tail bit addition on transmitter side and before tail bit removal on receiver side respectively. On comparing two signals, both are

same with a delay of 1 bit. The signal shows a frame of size 192 bits(172 data bits, 12 CRC bits and 8 tail bits). The total data rate is 9600bps with total of 50 frames transmitted per second. So, the time period of one frame is 20msec(192/9600) as is clear from figure 5.34 and figure 5.35.

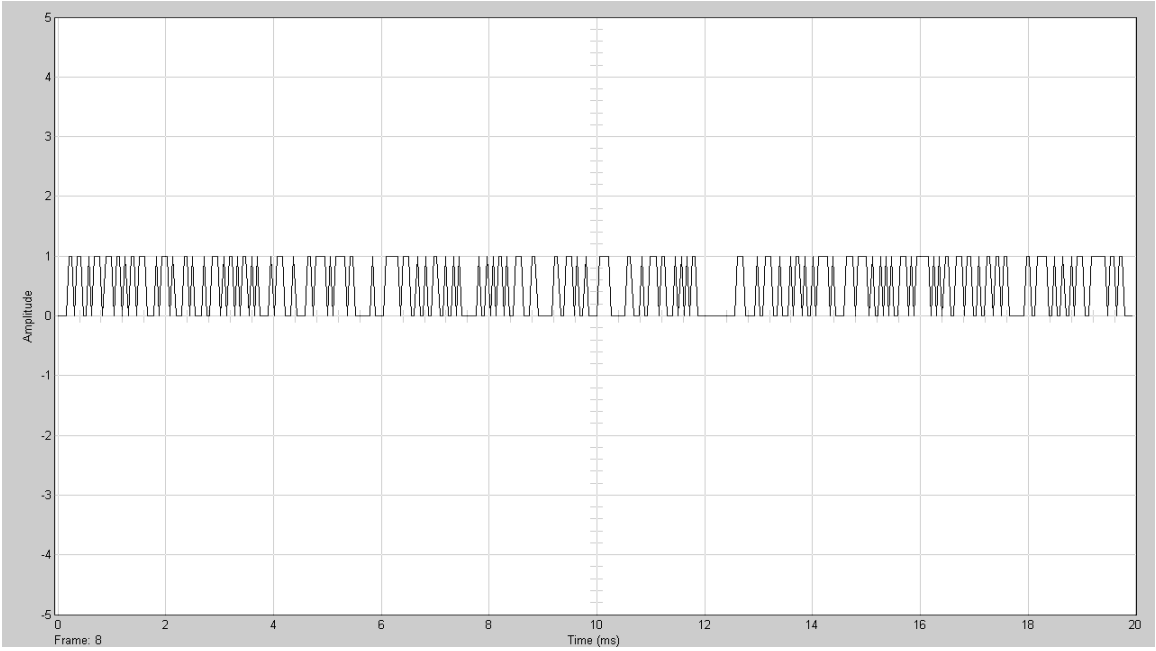

Figure 5.36: *Signal after convolutional encoder on transmitter side*

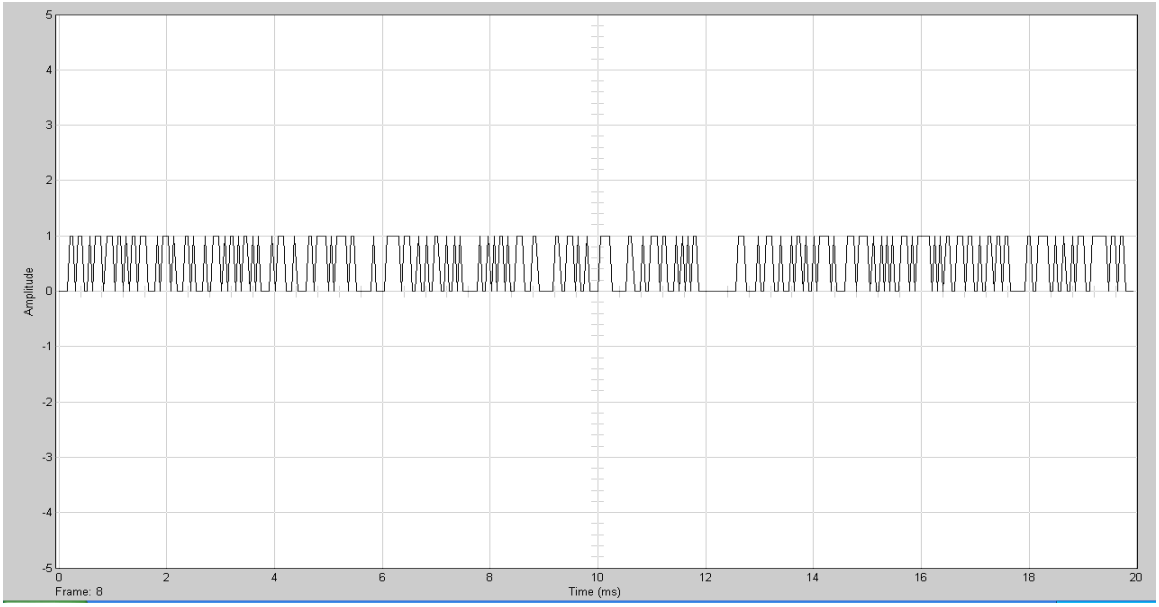

Figure 5.37: *Signal before viterbi decoder on receiver side*

Figure 5.36 and figure 5.37 show the signals after tail bit addition on transmitter side and before tail bit removal on receiver side respectively. On comparing two signals, both are same with a delay of 1 bit. The signal shows a frame of size 384 bits(192 x 2). The total data rate is 19200bps with total of 50 frames transmitted per second. So, the time period of one frame is 20msec(384/19200) as is clear from figure 5.36 and figure 5.37.

Two comparisons are shown between the signals obtained after Long code scrambling and power control subchannel insertion on transmitter side and the signals before Long code descrambling and power bit subchannel extraction on receiver side respectively. For carrying out the comparison, two vector scope blocks are placed after Long code scrambling and power control subchannel insertion in Long code scrambling and power control mapping block as shown in figure 5.38 and two vector scope blocks are placed before Long code descrambling and power subchannel extraction in Long code descrambling and power control bit extraction block as shown in figure 5.39.

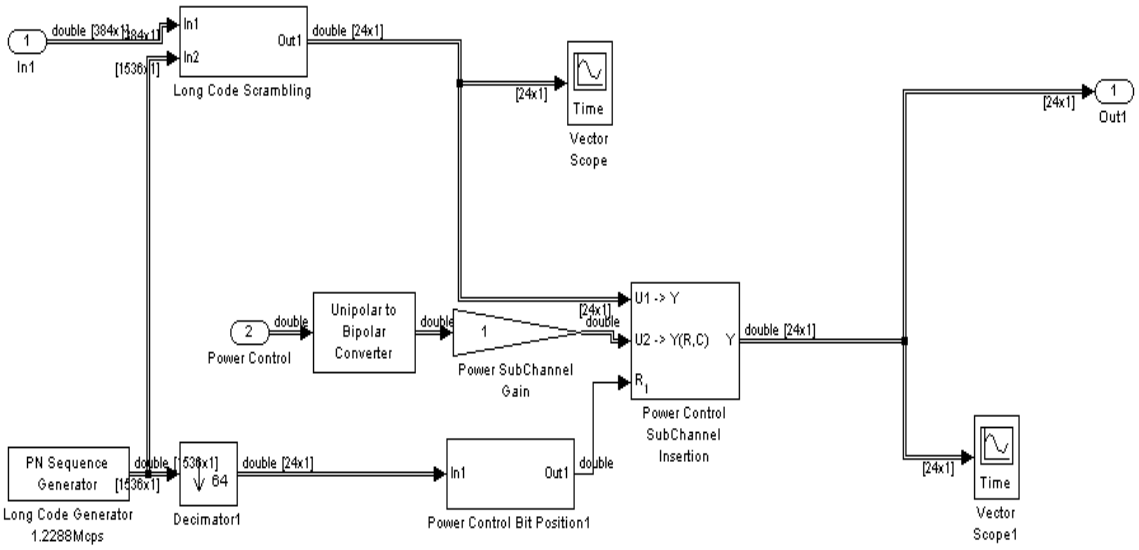

Figure 5.38: *Design of long code scrambling power control mapping*

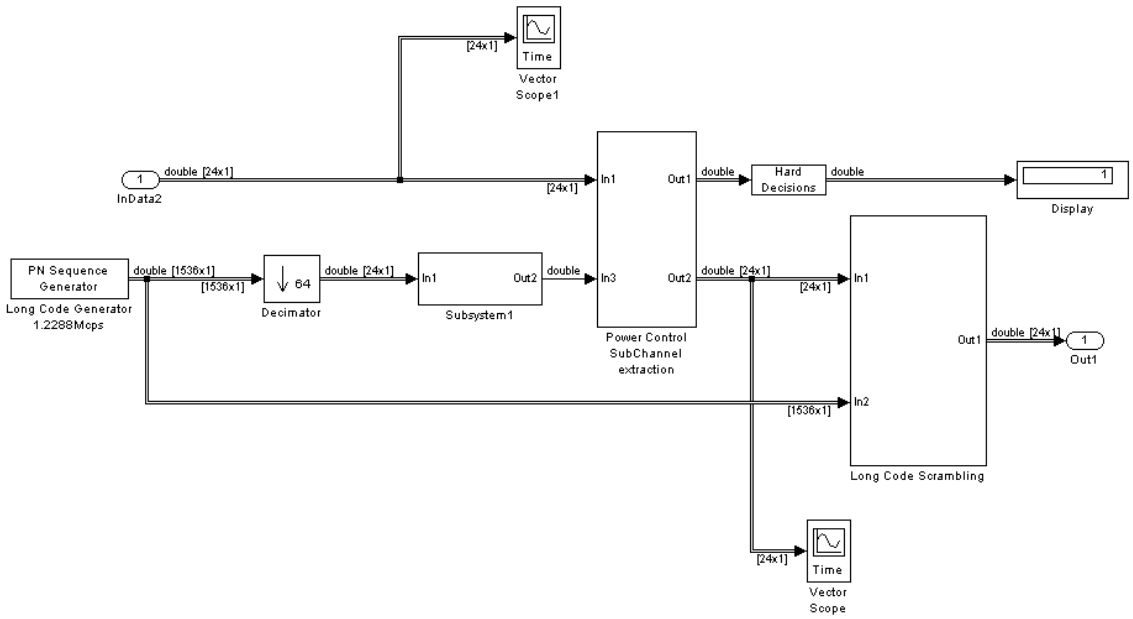

Figure 5.39: *Design of long code descrambling power control subchannel extraction block*

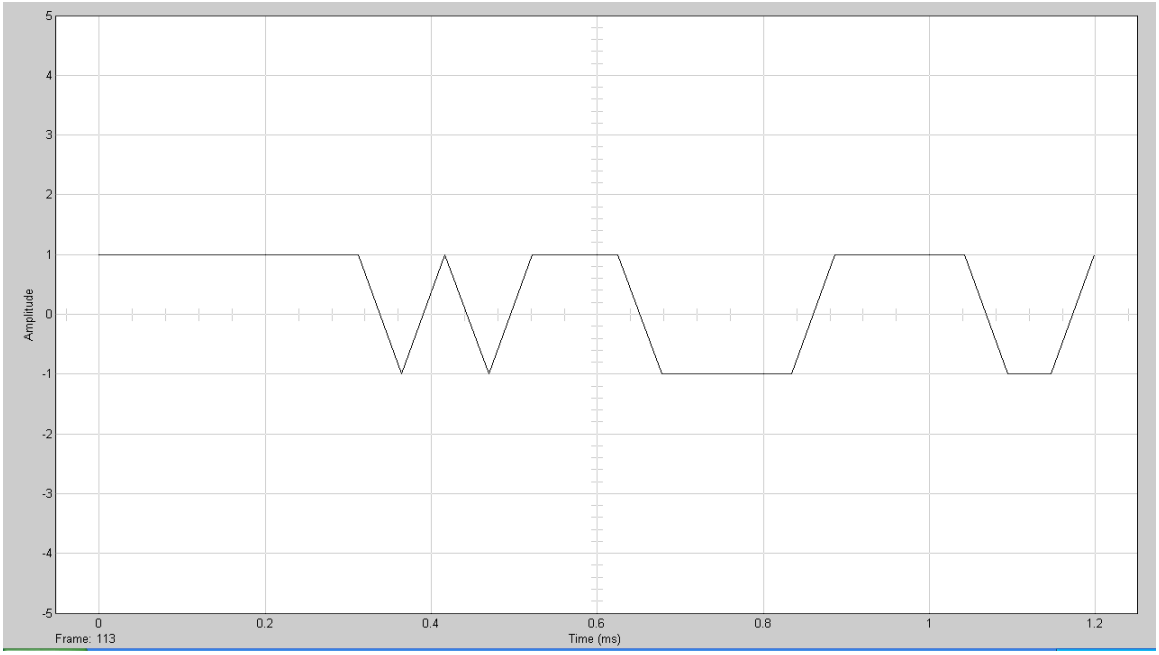

Figure 5.40*: Signal after Long code scrambling on transmitter side*

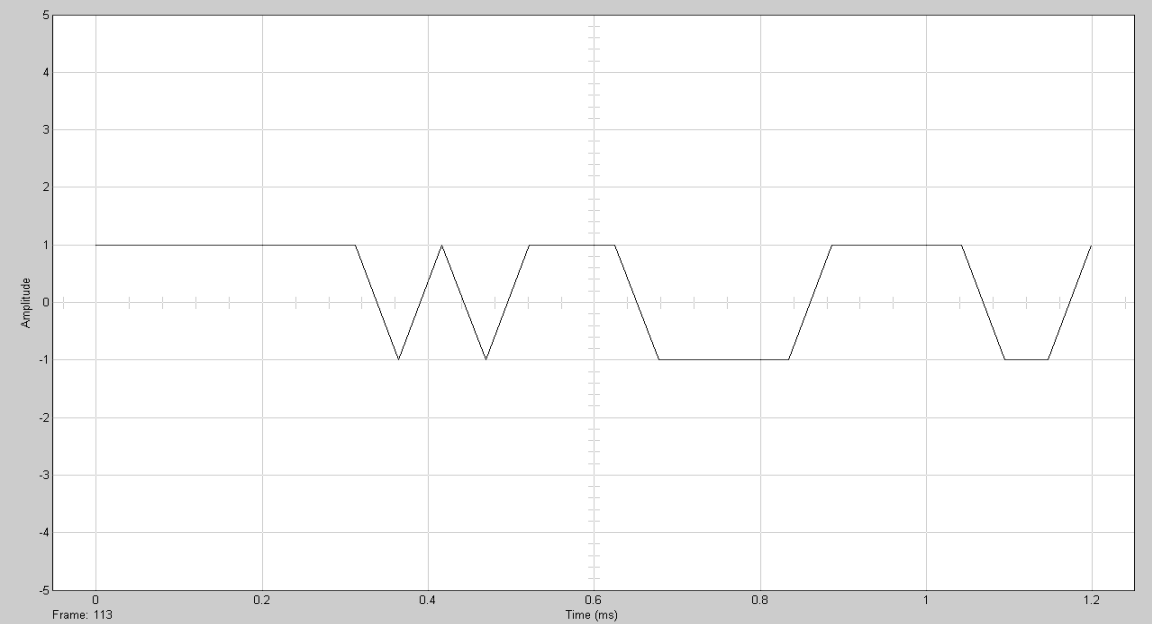

Figure 5.41:*Signal before Long code scrambling on receiver side*

Figure 5.40 and figure 5.41 show the signals after long code scrambling on transmitter side and before long code descrambling on receiver side respectively. On comparing two signals, both are same. The signal shows a frame of size 24 bits. The total data rate is 19200bps with total of 800 power control group frames transmitted per second. So, the time period of one frame is 1.25msec(24/19200) as is clear from figure 5.40 and figure 5.41.

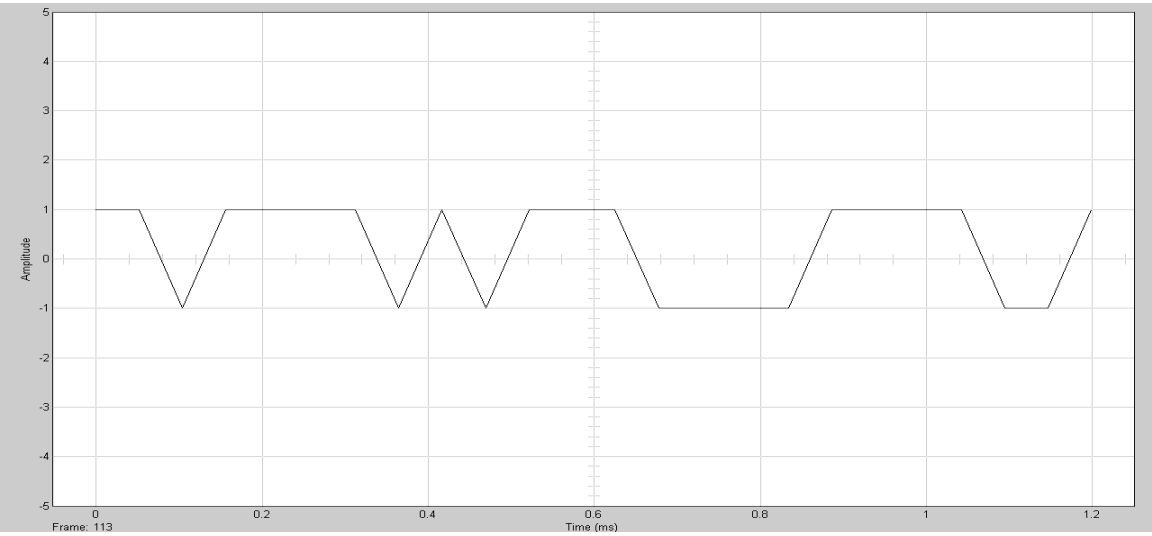

Figure 5.42:*Signal after power control sub channel insertion on transmitter side*

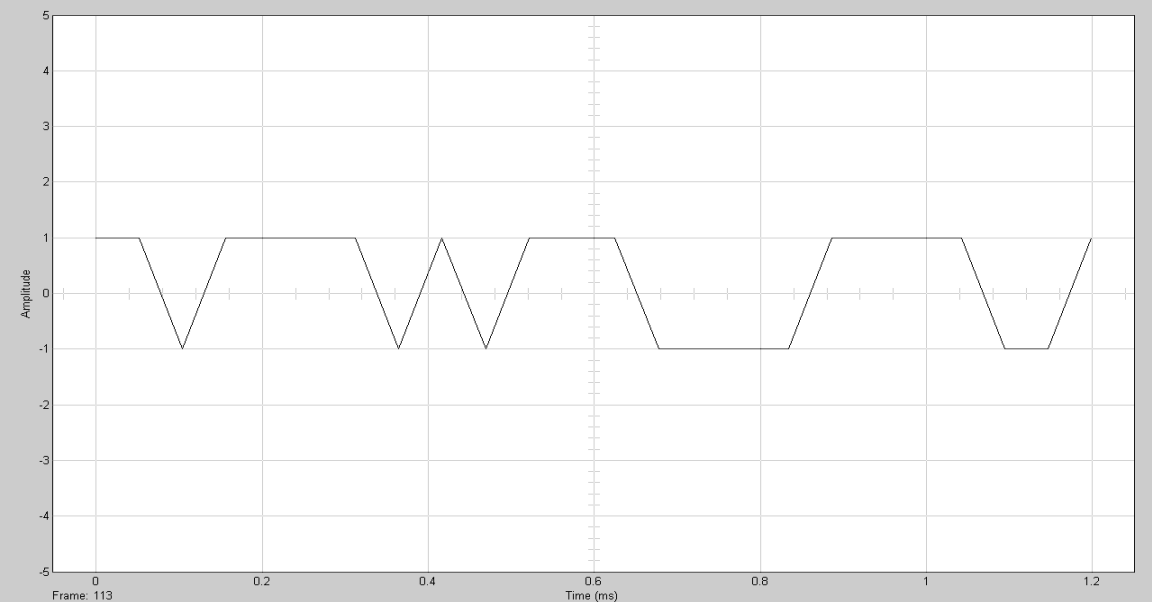

Figure 5.43:*Signal before Power control sub channel extraction on receiver side*

Figure 5.42 and figure 5.43 show the signals after power control subchannel insertion on transmitter side and before power control subchannel extraction on receiver side respectively. On comparing two signals, both are same. The signal shows a frame of size 24 bits. The total data rate is 19200bps with total of 800 power control group frames transmitted per second. So, the time period of one frame is 1.25msec (24/19200) as is clear from figure 5.42 and figure 5.43.

5.9 Conclusions

- Underwater CDMA2000 system has a bit error rate of 0.0236 after the receiver section because of extraction of power control bit and replacing it by '1' bit. As 1 bit is added in 1.25 msec, so probability of maximum bit error rate can be upto 0.0417(1/24).
- Synchronization between the signal at transmitter and receiver side shows that delay estimation is performed accurately.
- Underwater CDMA2000 system has a bit error rate of 0.002809 at the output of the system.
- Signals taken before and after channel compensation shows that channel estimation technique is implemented correctly.

- Display block shows the position of the power control bit so that it can be used to set the power level of the retransmitted signal.
- Comparison of signal taken with and without channel fading shows that data is retrieved correctly after channel and delay estimation in the rake receiver block.
- Signals before and after channel fading are shown in time, frequency and constellation formats. They show the effect of channel on the signal in all the three formats.

5.9 Future Scope

To enable more compatible CDMA system specifically tailored for underwater acoustic sensor networks,the following open research issues need to be addressed:

- In case CDMA is adopted, which we strongly advocate, it is necessary to design access codes with high auto-correlation and low cross-correlation properties to achieve minimum interference among users. This needs to be achieved even when the transmitting and receiving nodes are not synchronized.
- Research on optimal data packet length is needed to maximize the network efficiency.
- It is necessary to design low-complexity encoders and decoders to limit the processing power required to implement FEC functionalities. The feasibility and the energy-efficiency of non-convolutional error control coding schemes should be evaluated
- Distributed protocols should be devised to reduce the activity of a device when its battery is depleting without compromising network operation.

REFERENCES

[1] SOREIDE, N., WOODY, C., and HOLT, S., "Overview of Ocean Based Buoys and Drifters: Present Applications and Future Needs," in International Conference on Interactive Information and Processing Systems for Meteorology, Oceanography, and Hydrology (IIPS), Jan.2004.

[2] YANG, X., ONG, K. G., DRESCHEL, W. R., ZENG, K., MUNGLE, C. S., and GRIMES,C. A., "Design of a Wireless Sensor Network for Long-term, In-situ Monitoring of an Aqueous Environment," Sensors, vol. 2, pp. 455–472, 2002.

[3] YU, W., SAHINOGLU, Z., and VETRO, A., "Energy-Efficient JPEG 2000 Image Transmission over Wireless Sensor Networks," in Proc. of IEEE Global Communications Conference (GLOBECOM), (Dallas, TX, USA), pp. 2738–2743, January 2004.

[4] STOJANOVIC, M., CATIPOVIC, J., and PROAKIS, J., "Phase Coherent Digital Communications for Underwater Acoustic Channels," IEEE Journal of Oceanic Engineering, vol. 19, pp. 100–111, Jan. 1994.

[5] FREITAG, L., STOJANOVIC, M., SINGH, S., and JOHNSON, M., "Analysis of Channel Effects on Direct-sequence and Frequency-hopped Spread-spectrum Acoustic Communication," IEEE Journal of Oceanic Engineering, vol. 26, pp. 586–593, Oct. 2001.

[6] KILFOYLE, D. and BAGGEROER, A., "The State of the Art in Underwater Acoustic Telemetry," IEEE Journal of Oceanic Engineering, vol. 25, pp. 4–27, Jan. 2000.

[7] URICK, R. J. Principles of Underwater Sound. McGraw-Hill, 1983.

[8] STOJANOVIC, M., PROAKIS, J., and CATIPOVIC, J., "Analysis of the Impact of Channel Estimation Errors on the Performance of a Decision Feedback Equalizer in Multipath Fading Channels," IEEE Transactions on Communications, vol. 43, pp. 877–886, Feb./Mar./Apr. 1995.

[9] KALOFONOS, D., STOJANOVIC, M., and PROAKIS, J., “Performance of Adaptive MCCDMA Detectors in Rapidly Fading Rayleigh Channels,” IEEE Transactions on Wireless Communications, vol. 2, pp. 229–239, Mar. 2003.

[10] STOJANOVIC, M., PROAKIS, J., and CATIPOVIC, J., “Performance of High-rate Adaptive Equalization on a Shallow Water Acoustic Channel,” Journal of the Acoustical Society of America, vol. 100, pp. 2213–2219, Oct. 1996.

[11] STOJANOVIC, M., “Acoustic (Underwater) Communications,” in Encyclopedia of Telecommunications(PROAKIS, J. G., ed.), John Wiley and Sons, 2003.

[12] DAVIS, R., ERIKSEN, C., and JONES, C., “Autonomous Buoyancy-driven Underwater Gliders,” in The Technology and Applications of Autonomous Underwater Vehicles (GRIFFITHS, G., ed.), Taylor and Francis, London, 2002.

[13] HOWE, B., MCGINNIS, T., and KIRKHAM, H., “Sensor Networks for Cabled Ocean Observatories,” in Geophysical Research Abstracts, vol. 5, 2003.

[14] JALBERT, J., BLIDBERG, D., and AGEEV, M., “Some Design Considerations for a Solar Powered AUV: Energy Management and its Impact on Operational Characteristics,” Unmanned Systems, vol. 15, pp. 26–31, Fall 1997.

[15] RAVELOMANANA, V., “Extremal Properties of Three-dimensional Sensor Networks with Applications,” IEEE Transactions on Mobile Computing, vol. 3, pp. 246–257, July/Sept. 2004.

[16] FREITAG, L. and STOJANOVIC, M., “Acoustic Communications for Regional Undersea Observatories,” in Proc. of Oceanology International, (London, UK), Mar. 2002.

[17] HINCHEY, M., “Development of a Small Autonomous Underwater Drifter,” in Proc. of IEEE Newfoundland Electrical and Computer Engineering Conference (NECEC), (Chicago, IL, USA), Nov. 2004.

[18] SOZER, E., STOJANOVIC, M., and PROAKIS, J., “Underwater Acoustic Networks,” IEEE Journal of Oceanic Engineering, vol. 25, pp. 72–83, Jan. 2000.

[19] “CDMA Systems Engineering Handbook”by JhongSam Lee and Leonard E. Miller, 1998

[20] "CDMA: Principles of Spread Spectrum Communication" by Andrew J. Viterbi. 245 p. Addison-Wesley 1995.

[21] Basics of Code Division Multiple Access (CDMA) - Page 81 by Raghuveer M. Rao, Sohail A. Dianat - Technology & Engineering - 2005

[22] IEEE Personal Communications: A Publication of the IEEE Communications ... - Page 65 by Institute of Electrical and Electronics Engineers, IEEE Communications Society, IEEE Computer Society, Vehicular Technology Society - Microcomputers - 1994

[23] Single and Multi-Carrier DS-CDMA: Multi-User Detection, Space-Time Spreading ... - Page 9 by Lajos Hanzo, L-L. Yang, John Wiley & Sons, E-L. Kuan, Kai Yen - Technology & Engineering – 2003

[24] Spread Spectrum and CDMA: Principles and Applications - Page 369 by Valery P. Ipatov - Technology & Engineering - 2005

[25] 3G Wireless Networks - Page 489 by Clint Smith, Daniel Collins, Inc NetLibrary

[26] 3G CDMA2000 Wireless System Engineering by Samuel C. Yang - Technology & Engineering - 2004

[27] Introduction to 3G Mobile Communications - Page 21 by Juha Korhonen - Technology & Engineering – 2003

[28] Next Generation Mobile Systems: 3G and Beyond - Page 36 by Minoru Etoh - Technology & Engineering – 2005

[29] CDMA2000 Evolution: System Concepts and Design Principles by Kamran Etemad - Computers – 2004

[30] Designing Cdma2000 Systems by Leonhard Korowajczuk, Bruno de Souza Abreu Xavier, John Wiley & Sons, Arlindo Moreira Fartes Filho, Leila Zurba Ribeiro, Cristine Korowajczuk, Luiz A Dasilva - Technology & Engineering

[31] Introduction to CDMA Wireless Communications by Mosa Ali Abu-Rgheff - Technology & Engineering – 2007

[32] Channel coding performance in cdma2000 systems paper appears in: Emerging Technologies Symposium: Broadband, Wireless Internet Access, 2000 IEEE by Li, Q. Ramesh, N.S. Wireless Technol. Lab., Lucent Technol., Whippany, NJ;

[33] 2003 IEEE International Conference on Communications - Page 396 by Institute of Electrical and Electronics Engineers, IEEE Communications Society, IEEE

Communications Society, ICC Globecom., ICC Globecom - Technology & Engineering – 2003

[34] Third generation mobile telecommunication systems: UMTS and IMT-2000 - Page 81 by Peter Stavroulakis - Technology & Engineering – 2001

[35] Getting Started with MATLAB 7: A Quick Introduction for Scientists and Engineers (The Oxford Series in Electrical and Computer Engineering) by Rudra Pratap (Paperback - Aug 4, 2005)

[36] Student Edition of MATLAB Version 5 for Windows by Mathworks, Mathworks Staff, and MathWorks Inc. (Textbook Binding - April 28, 1997)

[37] MATLAB SIMULINK TOOL 7.2 help

[38] The Student Edition of Matlab Version 5 User's Guide by Duane Hanselman, Bruce Littlefield, MathWorks Inc., and Mathworks (Paperback - Jan 15, 1997)

[39] Essential MATLAB for Engineers and Scientists, Third Edition by Brian Hahn and Dan Valentine (Paperback - Mar 8, 2007)

[40] MATLAB: An Introduction with Applications by Amos Gilat (Paperback - Jan 2, 2008)

[41] MATLAB Guide by Desmond J. Higham and Nicholas J. Higham (Hardcover - Mar 2005)

[42] Numerical Analysis Using MATLAB and Spreadsheets by Steven Karris